The Dissertation Committee for Jayson Walter Jay Certifies that this is the

approved version of the following dissertation:

Mast Cell Influence in the Progression of Post-burn Hypertrophic Scar Pathophysiology

Committee:

_____
Celeste C. Finnerty, PhD, Supervisor

_____
David N. Herndon, MD, Co-Chair

_____
Hal K. Hawkins, MD, PhD

_____
Michael G. Wilkerson, MD

_____
Edward E. Tredget, MD

_____
Dean, Graduate School

Mast Cell Influence in the Progression of Post-burn Hypertrophic Scar Pathophysiology

by

Jayson Walter Jay, BS, MS

Dissertation

Presented to the Faculty of the Graduate School of

The University of Texas Medical Branch

in Partial Fulfillment

of the Requirements

for the Degree of

Doctor of Philosophy

The University of Texas Medical Branch
November 2018

Dedication

To my beautiful, understanding, and loving wife Jessica and my son Andrew (and coming very soon, my new daughter), this dissertation is dedicated to you - I will love you to the end of time! To my wonderful extended family, Polly Lee, Billy Lee, Rebecca Lee, Lacy Lee and Tony Huynh, thank you as well. Mom, you've been gone for a while now, but I know you have never left my side; thank you for raising me to be the man I am today and for watching over us all. I would also like to dedicate this dissertation to all burn survivors; your perseverance to overcome injury inspires the world.

Acknowledgements

Most importantly, I would like to acknowledge and thank my mentor Dr. Celeste C. Finnerty for her unwavering support, scientific teaching, and guidance throughout this research journey. I would also like to thank Dr. Amina El Ayadi, Dr. Anesh Prasai, Ye Wang, and Dr. Michael Wetzel, my extended lab family. Without their expertise, professional input, and friendship, this dissertation would not be possible. I thank my graduate program faculty and staff for their leadership and guidance: Dr. Mark Hellmich, Dr. Celia Chao, Dr. Judy Aronson, and Donna Adams. I sincerely thank the members of my supervisory committee as well. Dr. David Herndon is a pioneer and world-recognized leader in pediatric burn care and has been instrumental through pre-clinical aspects of this work. Dr. Hal Hawkins is an exceptional histopathologist whose expertise was integral while guiding me through the many histological aspects of these studies. Dr. Wilkerson advanced my understanding of dermatopathology and constantly pushed me to analyze fibrotic pathologies in new ways. Dr. Edward Tredget is a global leader in burn care and recognized hypertrophic scar expert whose knowledge and constant support guided this research.

I thank Dr. Robert Cox and Sam Jacob from the Shriners Hospitals for Children – Galveston Histopathology Core. Their expert assistance and fruitful scientific discussions were instrumental to this project. I thank Dr. Patrick Clayton, whose friendship was invaluable over the years, and remains so. I also thank Sharon Best for her assistance and friendship, and for always providing helpful advice. I sincerely appreciate the countless number of professionals at Shriners Hospitals for Children in Galveston, including Chris Nieten, the clinical and support staffs, and the metabolism faculty for their assistance in acquiring samples, along with their overall generosity and kindness. As the axiom states, it truly does 'take a village'; I sincerely thank everyone for their contribution to this research, it simply would not have been possible without you.

Mast Cell Influence in the Progression of Post-burn Hypertrophic Scar Pathophysiology

Publication No._____

Jayson Walter Jay, PhD

The University of Texas Medical Branch, 2018

Supervisor: Celeste C. Finnerty

Abstract

Painful, motion-limiting hypertrophic scars (HTS) form after protracted wound healing in patients with severe full-thickness burns and pose difficult treatment challenges. Despite substantial reduction in post-burn mortality, long-term outcomes of HTS are the most serious therapeutic challenge following severe burn injury. Investigations into cellular influences in post-burn scar pathophysiology are constrained to dermal fibroblast activity in the wound and signaling among inflammatory cell populations such as neutrophils, macrophages, and T-lymphocytes. However, mast cells are known to initiate fibroproliferative signaling in other fibrotic pathologies and, their influence in burn wounds is poorly understood. In the present investigation, we show increased mast cell density and dissemination throughout post-burn scars concomitant with elevated serum tryptase concentrations over time in pediatric burn survivors.

Using *in vitro* approaches, we demonstrate tryptase's ability to activate proliferation in primary post-burn HTS fibroblasts compared to that of non-burned skin fibroblasts. Tryptase, an abundant mast cell protease, directly cleaves and activates the protease-activator receptor-2 (PAR2) and activation has proliferative and fibrotic consequences. We demonstrate that PAR2 is highly expressed in post-burn HTSs and, activation sustains fibroproliferative signaling. Co-culture with post-burn HTS fibroblasts and human mast cells elevated expression of collagen-1 and α-smooth muscle actin, facilitating a myofibrotic shift. Most importantly, PAR2 blockade or PAR2 mRNA knockdown significantly attenuated mast cell-induced fibrotic phenotype in post-burn HTS fibroblasts.

We also demonstrate that mast cell stabilization minimizes HTS formation in a post-burn *in vivo* model. Cromolyn sodium (CS) is an FDA-approved mast cell stabilizer that significantly inhibits degranulation and has been used to successfully relieve detrimental symptoms of mast cell activation. Here, we applied a 4% topical emulsification of CS to post-burn HTSs of red Duroc pigs. CS significantly reduced mast cell density and scar severity over time. Scar height, volume, and collagen deposition were all lessened considerably compared to vehicle treatment alone or autologous split-thickness skin grafts. Additionally, we show that mast cell stabilization decreases fibroproliferation by impeding tryptase-induced PAR2 signaling. Together, this evidence suggests that localized mast cell stabilization, in combination with current therapies, may be an effective approach to reduce pathologic scarring following a severe burn.

TABLE OF CONTENTS

List of Tables

List of Figures

List of Abbreviations

α-SMA	alpha smooth muscle actin
ANOVA	Analysis of variance
APC	Antigen presenting cell
BSA	Bovine serum albumin
CD	Cluster of differentiation
CS	Cromolyn sodium
CTTF	Corrected total tissue fluorescence
ELISA	Enzyme-linked immunosorbent assay
ETI	Epidermal thickness index
FcεRI	High affinity IgE receptor
FDA	United States Food and Drug Administration
GPCR	G-protein-coupled receptor
H&E	Hematoxylin and eosin
HTS	Hypertrophic scar
IACUC	Institutional Animal Care and Use Committee
IF	Infantile hemangioma
IHC	Immunohistochemistry
IL	Interleukin
IOD	Integrated optical density
MCP	Mouse mast cell protease
MCP-1	Monocyte chemoattractant protein-1

MIP-1	Macrophage inflammatory protein-1
MMP	Matrix metalloproteinase
NBS	Non-burned skin
PAR2	Protease-activated receptor-2
PBS	Phosphate-buffered saline
PBST	Phosphate-buffered saline with Tween 20
rh	Recombinant, human
SCF	Stem cell factor
STSG	Split-thickness skin graft
TBSA	Total body surface area
TBST	Tris-buffered saline with Tween 20
TGF-β1	Transforming growth factor-beta 1
UTMB	University of Texas Medical Branch

CHAPTER 1 - INTRODUCTION: NEGLECTED CELL POPULATION IN THE HEALING BURN WOUND: EVIDENCE FOR MAST CELL INVOLVEMENT IN POST-BURN SCARRING

BURN INJURY PATHOPHYSIOLOGY

Burns directly cause approximately 200,000 deaths each year and are a major global health problem accounting for over 11 million injuries annually that require medical attention.[1] However, with the incorporation of better strategies for burn wound closure, decreasing the hypermetabolic response, and supporting inhalation injury, survival has increased significantly[2] leading to more long-term problems such as scarring and its negative effect on quality of life.[3] Suboptimal wound healing caused by inflammation, delayed wound closure, and infection contributes to the formation of hypertrophic scars (HTS) in 70-90% of patients with massive burns [4]. Histologically, HTS are devoid of adnexal structures and have thick, densely packed, and immature collagen fibers that often form nodules with sharp borders. These scars are pruritic, inflamed, painful and limit movement of the affected area. Studies of the underlying scar pathophysiology have typically focused on the dermal fibroblasts.[5]

Following a full-thickness burn, fibroblasts in the papillary dermis are destroyed, leaving only a subpopulation of deep dermal fibroblasts to occupy the burn wound. Several studies have demonstrated that these remaining fibroblasts express more collagen, upregulate greater ECM production, and are inherently more fibrogenic.[6,7] This evidence underscores the concept of a critical depth as hypothesized by Tredget *et al.* and Dunkin *et al.*[8-10] A distinct depth above which, fibroblast populations are regenerative and a wound

will heal without scarring, but below which, altered fibroblasts proliferate, produce excess collagen, and promote hypertrophic scar formation. However, fibrosis is an intricate and complex process that involves complicated interplay between wound fibroblasts, migrating cells and inflammatory signaling.[11]

Neutrophils, macrophages, and lymphocytes are other important cell populations that have critical roles during the inflammatory phase post-burn. These cells release an abundance of cytokines known to stimulate profibrotic signaling in wound fibroblasts, which contributes to scar pathogenesis and will be discussed in detail below. However, therapies such as interferon-alpha, transforming growth factor-β modulators, and intralesional corticosteroid injections, designed to target these immune cells, inflammatory cytokines, and fibrotic molecular mechanisms, have produced only moderate success.

Other therapy options exist to treat HTS only after scars have formed. Physical manipulations such as silicone sheeting, pressure garments, surgical resections, and even massage can improve aspects of HTS, but resolution is incomplete. Advanced therapies such as lasers are being utilized more regularly today. Lasers ablate fibrotic tissue and promote repopulation of normal tissue into the void, but long-term evidence for efficacy is lacking. These therapies offer promise, however, the majority of cellular, molecular, and physical manipulations to reduce scarring have been inadequate, and suggests other cell populations and unknown mechanisms may be involved in HTS pathogenesis. A range of cell populations during the wound healing cascade has been well described in the literature; however, the mast cell has often been overlooked and under reported in the context of post-burn wound healing. This review demonstrates that mast cells are a vital population in the

healing burn wound and reveals that they may be critical components that initiate and drive HTS progression.

IMMUNITY AND INFLAMMATION IN THE HEALING BURN WOUND

Cytokines produced by a variety of immune cell populations in the post-burn wound may change the healing environment to oscillate between pro- and anti-inflammatory states. However, protracted hypermetabolism favors extension of the initial inflammatory phase in wound healing, further perturbing cellular proliferation and wound remodeling. Of these immune cell populations, macrophages play important roles in wound healing to eliminate pathogens and produce cytokines that trigger additional immune responses. Macrophages may initiate the adaptive immune responses and are major sources for Interleukin (IL)-1 and IL-6 that stimulate T-cell and antigen-presenting cell (APC) activation as well as enhancing B-cell maturation. These other cells are recruited by the macrophages by production of cytokines and growth factors. Macrophages also produce IL-12 which promotes T_H1 cells while simultaneously suppressing T_H2 cells, further shifting the balance of the healing burn wound to a more pro-inflammatory landscape and possibly contributing to the pathogenesis of hypertrophic scar. Next, neutrophils migrate to the wound and are found to be consistently elevated and, as a result of persistently increased post-burn catecholamine levels, migration to the wound continues for weeks.[12] This sustained neutrophil presence significantly delays healing.[13] Despite the documented influence of these immune cell populations on the healing burn wound, mast cells are often overlooked in post-burn pathological scarring.

Growing evidence suggests mast cells within the healing burn wound may contribute more to damaging fibrosis than previously thought. As the major source of

histamine, which may have consequences in co-morbid post-burn itch and pain, mast cells are now being implicated in the pathogenesis and progression of post-burn hypertrophic scarring.[14,15] Mast cells also participate in other scarring pathologies by inducing cardiac hypertrophy and pulmonary and renal fibroses.[16-18] Early investigations in human burn survivors have shown increased mast cell density in both pediatric and adult hypertrophic scars[14,19,20] compared to mature scars from uninjured, non-burned patients. Studies with scald-injured mast cell-deficient mice show hallmarks of impaired wound healing including decreased angiogenesis, reduced fibroblast proliferation and significantly altered extracellular matrix.[21] Furthermore, several key chemotactic factors known to influence mast cell migration have been found in burn wounds. Mast cell presence in the healing burn wound may indicate a vital role in the pathogenesis of post-burn hypertrophic.

MAST CELL CHEMOTAXIS TO THE BURN WOUND

A host of chemoattractant and chemotactic factors that are upregulated following injury may enhance mast cell recruitment to areas of post-burn scarring. When compared to non-burned patients, serum concentrations of pro- and anti-inflammatory cytokines and chemokines remain significantly elevated in patients with large thermal burn injuries.[22,23] A number of these factors may serve to directly influence mast cell chemotaxis to the burn wound including transforming growth factor-beta (TGF-β), stem cell factor (SCF), monocyte chemoattractant protein -1 (MCP-1), and macrophage inflammatory protein-1 (MIP-1).

It is well-established that TGF-β is a powerful fibrogenic initiator. Many investigations over the last half-century have demonstrated TGF-β to induce pulmonary, cardiac, and hepatic fibrosis [24-26] through convergent cellular mechanisms activating

SMAD pathways; in turn, promoting the increased production of collagen. Furthermore, in burn injury, elevated serum levels of TGF-β are seen in patients with hypertrophic scars compared to uninjured healthy adults.[20] Animal studies utilizing neutralizing antibodies to TGF-β in several fibrotic pathologies have been shown to inhibit fibrotic advancement and TGF-β blockade has also been used to decrease dermal scarring in human *in vitro* models.[27] The abundance of TGF-β in the burn scar favors continued fibrotic progression, but it may also serve to aid in the migration of mast cells to the scar as well. Indeed, several lines of research indicate TGF-β to be a potent chemotactic factor for mast cells. Exposure to nominal concentrations of TGF-β induces rapid morphologic changes in mast cells [28] and TGF-β antagonism can mitigate mast cell migration by mechanism still not completely understood.[29] This evidence along with other soluble factors within the wound may account for significantly elevated mast cell numbers within burn scars over time.

Stem cell Factor (SCF), also known as c-kit ligand, is required for myeloid differentiation and essential for mast cell maturation. It is produced by cells at sites of active hematopoiesis such as bone marrow, the fetal liver and, in the skin, by fibroblasts and endothelial cells. Importantly, mast cells are the only hematopoietic progenitors to express the SCF receptor, c-kit (CD117), as terminally differentiated cells. SCF presence in wounds or ischemic areas is associated with increased mast cell accumulation and thought to occur through signaling activation of Ras and mTORC pathways, leading to actin rearrangement and subsequent chemotaxis. [30,31] Though limited evidence exists for its increased presence post-burn, further investigations are needed to establish this important factor's role following severe burn injuries. In addition to TGF-β and SCF,

expanding evidence now points to several members the CC Chemokine (CCL[X]) family as potential mediators to mast cell chemotaxis.

Both macrophage inflammatory protein-1β (MIP-1β) as well as monocyte MCP-1, CCL-4, and -2, respectively, are known to be elevated following burn injury [22]. Both of these secreted chemokines have been reported as powerful chemoattractants to mast cells in various pathologies and mast cells themselves may produce an abundance of CCL-2 to act in an autocrine fashion. [32,33]

A wide-ranging host of potential cytokines may induce mast cell migration and these diverse mast cell chemoattractants may provide prospective targets for future study in post-burn wound healing.[34] Although divergent differentiation mechanisms involving these cytokines and chemokines are responsible for mast cells destined for mucosal residence than those fated for connective tissue such as skin, once residing in tissue, mast cells exert their likely fibrotic effects through the process of degranulation which is discussed below.

MAST CELL DEGRANULATION IN THE BURN WOUND

Mast cells may induce or continue to influence a hypertrophic fibroblast phenotype in several ways through degranulation of preformed mediators. The process of degranulation is classically initiated and mediated by antigen cross-linked IgE. Cross-linked IgE activates the high affinity IgE receptor (FCεRI), abundant on mast cells, in turn increasing calcium signaling which leads to rapid vesicle exocytosis of both pre-formed and *de novo* mediators. IgE levels have been shown to increase significantly in burned adults compared to non-burned adults between days 14 and 22 post-burn and some studies have measured 20-fold increases in IgE in the post-burn acute stage.[35,36] This data suggests that mast cells

have more than sufficient levels of its primary degranulation agonist and further indicates active B-cell immunoglobulin synthesis. In addition to classical IgE mast cell activation, further evidence points to mast cell degranulation by non-canonical, FCεRi-independent means.

Other potentially important and somewhat surprising factors may impact mast cell degranulation. First among these is the neuropeptide Substance P. It is best known for its mediation of sensory pain signaling, but it may also play a role in inflammatory responses following cutaneous injury. Elevated levels of Substance P are reported in post-burn hypertrophic scars and it is has been demonstrated as well to enhance mast cell degranulation.[37-39] Consequently, in addition to histamine accounting for the induction of post-burn neurogenic itch, Substance P may provide a novel and intriguing target in post-burn hypertrophic scar pathophysiology in relation to mast cell activation.

Physical stretch or tissue distortion may also provide the means to directly activate mast cells in post-burn wounds. Transient receptor vanilloid receptors are activated by stretch such as during the physical trauma of burn injury or even subsequent post-burn anti scarring treatments. Studies in microdeformational wound therapy, negative pressure-stretched skin at the histological level, reported that mouse homologues MCP-4, -5, and -6 to the most abundant mast cell proteases (chymase, elastase, and tryptase, respectively) were significantly elevated following treatment suggesting that mast cells are still able to degranulate in the absence of other perturbing stimuli. [40]

Of further interest in alternate mast cell activation is the potential role for β-adrenergic receptor (β-AR) signaling. Although more investigations are needed to determine if adrenergic stimulation can indeed degranulate mast cells, fascinating new data

shows significantly increased expression of the β2-AR isoform in histological samples of severe infantile hemangiomas (IF) compared to control tissue. [41] IF has similar pathophysiological characteristics to those of post-burn hypertrophic scar and this line of research suggest β-AR antagonism can be used to ease mast cell degranulation in healing burn wounds. This is exceptionally relevant because of the considerably elevated catecholamines levels post-burn and will be of increasing importance as propranolol becomes the standard of care to reduce cardiac load and hypermetabolism following burn injury. Further study is needed to establish this potential link.

Consequently, the burn wound environment not only attracts an influx of mast cells to burn tissue through an excess of major chemoattractant molecules and peptides, but the milieu also provides the prime environment, which actively allows persistent degranulation of mast cells. However, the chief mast cell determinants to post-burn hypertrophy and hyperplasia are pre-formed and *de novo* mediators released in this hyperinflammatory setting as described below.

MAST CELL MEDIATORS AND THEIR POTENTIAL ROLE IN POST-BURN FIBROSIS

Potent pre-formed mast cell granules histamine, vascular endothelial growth factor, and fibroblast growth factor exert proangiogenic effects within the burn wound that induce vascular permeability.[42-45] Vessel leakage allows other immune cells to infiltrate the wound, which serves to increase and sustain pro-inflammatory paracrine signaling. This, together with concomitant increases in chemotactic factors, subsequently allows further mast cell migration to the wound in what can be described as a positive feedback loop. Mast cells are critical reservoirs for abundant pre-formed and *de novo* mediators that may

have profound consequences in post-burn fibrosis, summarized in Table 1. Several of the most important of these mediators are discussed below.

Pre-formed Mediators

Histamine

Histamine is a powerful vasoactive amine and is one of the most bountiful granules stored in mast cells. Histamine is rapidly released in response to IgE mast cell activation and is the main compound implicated in hypersensitivity reactions. However, a role for histamine has also been identified in fibrotic pathologies. Results from clinical samples of life-threatening biliary atresia in humans show significantly elevated histamine levels in the absence of other mast cell mediators and, in the resultant hepatic fibrosis, mast cell density was shown to be considerably increased.[46,47] Studies also show that histamine had significant potential to activate immortalized 3T3 mice fibroblasts to close artificial wounds *in vitro*. Investigators concluded that histamine, through the H2 histamine receptor, induced mitogenic signaling and subsequent fibroblast proliferation.[48] Blocking the H2 receptor in another study, investigators completely abrogated fibroproliferation in pulmonary fibroblasts, further confirming histamine's proliferative impact, although, exact mechanism have yet to be elucidated.

Importantly, Tredget *et al.* (1998) reported significantly elevated plasma N-methylhistamine, the major histamine metabolite, in nine adult burn survivors (mean TBSA = 49.7%) with severe hypertrophic scars approximately 1 year post-burn.[20] This was the first clinical evidence suggesting active mast cell degranulation following burn injury. A later study conducted by Johansson *et al.* (2012) in eight burned adults (mean TBSA = 24.0%) showed no significant increases in histamine or methylhistamine excretion up to

48 hours after burn injury compared with healthy adults, although they may be implicated in later inflammation.[49] Completed at two different time points however, these independent studies suggest that mast cells play a minimal role acutely following a burn, but may be integral to the pathogenesis and progression of hypertrophic scars, months and years following the initial burn injury.

Chymase

Chymase is a neutral serine protease and is found in moderate quantities in connective tissue resident mast cells; concentrations of the protease are minimal in mucosal mast cells.[50] Chymase has broad enzymatic activity targeting extracellular matrix components and has been shown to inactivate thrombin, which has major consequences in hemostasis and during the initial inflammatory phase of wound healing. By cleaving thrombin, mast cell chymase inhibits clot formation, thus promoting vascular permeability, which sustains protracted inflammation.[51] Mast cell chymase facilitates TGF-β activation in post-burn wound, further progression hypertrophic scar through activation of pro-fibrotic signaling in fibroblasts resulting in excess collagen deposition.[52,53] Additionally, chymase has been demonstrated to promote pro-inflammatory and profibrotic cytokine production in connective tissue fibroblasts[54,55] and has also been shown to remodel extracellular matrix post-burn.[56] Chymase may be responsible for cleaving a wide variety of extracellular targets and thus, indirectly be more permissive for fibroblast growth and proliferation. However, evidence for direct involvement in fibrotic pathogenies remains elusive.

Tryptase

Tryptase is the most plentiful serine protease contained within stored granules and accounts for over half of all factors produced by mast cells.[57] It is a tetrameric enzyme with four active sites that has specificity for several extracellular matrix targets. Following degranulation, tryptase has been demonstrated to cleave fibronectin and activate MMP-3, which has major implications in extracellular matrix remodeling.[58] Interestingly, tryptase release has been shown to activate surrounding mast cells, further amplifying the signal and leading to sustained inflammation.[59] However, its potential to act more as a growth factor than to modify extracellular matrix components has greater consequences in the context of fibrosis.

Elevated serum tryptase concentration is used to diagnose mast cell disorders such as mastocytosis and is a clinical indicator of mast cell activation. Investigations reveal that increased tryptase levels often accompany fibrotic disorders. Mentula *et al.* reported elevated serum tryptase in over 40 patients with acute pancreatitis compared to healthy patients and Klion *et al.* observed significantly increased serum tryptase in patients with confirmed endomyocardial fibrosis compared to healthy adult tryptase levels.[60,61] Studies conducted in animal models of ventilator-induced pulmonary fibrosis also report raised serum tryptase in lavage fluid during disease progression, which indicates that tryptase is required for fibrotic onset and further links mast cell activation to fibrogenesis.

Several investigations have proposed mechanisms to explain tryptase's fibrotic capacity. Studies show that tryptase has potent angiogenic potential by directly stimulating endothelial cell proliferation and tube formation.[62] Furthermore, tryptase has also been demonstrated to increase the expression and enhance the release of VEGF from

osteoarthritic chondrocytes *in vitro*. [63] Increased vasculature is beneficial during early wound healing in order to deliver nutrients and remove waste. However, sustained angiogenesis is pathological and harmful in HTS progression as it provides excess substrates for increased metabolism, which upregulates wound fibroblast proliferation. In addition to enzymatically cleaving extracellular matrix targets and inducing enhanced angiogenesis, tryptase is recognized to activate the protease-activated receptor-2 (PAR2). Tryptase cleaves this unique G-protein coupled receptor, which initiates mitogenic signaling. PAR2 signaling results in cellular proliferation and increased collagen output[64] and sustained activation is implicated in several fibrotic conditions including pulmonary, pancreatic, and hepatic fibrosis.[65-67] However, this important pathway has not been studied in HTS pathophysiology and more investigations are required to elucidate the tryptase-PAR2 signaling axis post-burn.

Other pre-formed mast cell mediators including fibroblast growth factor, tumor necrosis factor, and platelet-derived growth factor have been implicated as fibrogenic. Relative abundance is minimal in mast cells, and evidence detecting appreciable concentrations at any time following major burn injury is lacking. However, *de novo* mediators, rapidly synthesized upon mast cell activation, may also have an important role in fibrotic pathogenesis.

De novo Mediators

Upon fulminate activation, mast cells rapidly degranulate releasing the contents of stored granules. However, signaling also induces activation of phospholipase A2, which hydrolyzes plasma membrane phospholipids, chiefly phosphatidylcholine, generating arachidonic acid (AA). Further AA enzymatic proteolysis by cyclo-oxygenases (COX)

and lipoxygenase(5) rapidly produces prostaglandins (PG) and leukotrienes, respectively.[68] These *de novo* mediators have also been implicated as fibrotic stimuli.

Prostaglandins

Of the *de novo* mediators generated within seconds to minutes following mast cell activation, prostaglandins have important inflammatory roles. Increased prostaglandin synthesis was demonstrated in as little as fifteen seconds following IgE activation in human mast cells *in vitro*[69] and other studies have shown acutely increased prostaglandin concentrations following burn injury.[70,71] Prostaglandin D2 (PGD_2) is abundantly produced by mast cells and serves to recruit other inflammatory effectors such as basophils and Th2 cells. Although Th2 recruitment is considered anti-inflammatory, several investigations demonstrate that PGD_2 may be a fibrotic stimulus during wound healing. Abe *et al.* showed that dermal fibroblasts exposed to PGD2 significantly increased collagen-1 expression[72] and Kohyama and colleagues demonstrated that PGD2 was able to induce fibroblasts contraction in collagen gels *in vitro*.[73] Investigations are underway to determine other potential fibrotic roles for prostaglandins; however, fibrosis may be impacted to a lesser extent by other *de novo* mediators such as the leukotrienes by still unknown mechanisms.

Leukotrienes

Leukotrienes are another class of inflammatory mediators rapidly produced during mast cell activation. Early studies demonstrated significantly elevated leukotriene levels in the blister fluid of burn survivors with large wounds[74] suggesting that participation of this key mediator following burn injury is important. *In vitro*, leukotriene C4 (LTC_4) has been shown to upregulate TGF-β1 expression by pulmonary epithelial cells through activation

of p38-kinase, a critical mitogenic effector.[75] LTC$_4$ has also demonstrated capacity to increase collagen production and proliferation in bronchial fibroblasts in culture settings.[76] *In vivo*, LTC$_4$ was shown to exacerbate and sustain fibrogenesis in an animal model of pulmonary fibrosis. Importantly, fibrotic lesions were diminished considerably by treating animals with leukotriene receptor antagonists providing further evidence of the fibrotic potential by this critical mast cell mediator. By releasing small peptides, vasoactive molecules, matrix-degrading proteases and lipid mediators, mast cells are vitally important during inflammation and further suggests that mast cell modulation following burn injury may abrogate fibrotic pathology.

POTENTIAL MAST CELL MODULATION FOLLOWING BURN INJURY

Mast cells are resident within most tissues providing first-level responses of the innate immune system. They are found actively degranulating in increased numbers at sites of injury and numerous lines of evidence have demonstrated the fibrotic potential of released mediators. Perturbing the action of these mediators may reduce fibrotic signaling and strategies to attenuate mast cell-induced fibrosis are now being explored. This is further highlighted in published studies showing how scarring can be lessened upon obstructing mast cell activation.

Mast cell degranulation can be halted through pharmacologic stabilization. Several naturally-derived and synthetic compounds have demonstrated the ability to selectively block calcium and chloride channels on mast cell membranes as well as calcium and chloride channels on the endoplasmic reticulum membrane. Impeding calcium and chloride flow prohibits vesicle fusion to the plasma membrane and ultimately diminishes the ability of mast cells to degranulate.[77,78] While mast cell stabilizers have proved effective in

treating hypersensitivity disorders, their effects in preventing post-burn fibrosis are just now being elucidated.

Cromolyn sodium, a natural plant-derived compound, is one of the first mast cell stabilizers discovered and has been used to successfully relieve symptoms associated with allergic reactions such as conjunctivitis,[79,80] ulcerative colitis,[81] and systemic mastocytosis.[82] Used as a topical compound, cromolyn sodium has been shown to considerably reduce pruritus associated with atopic dermatitis and eczema in several clinical trials.[83,84] Importantly however, cromolyn sodium has demonstrated anti-fibrotic capabilities. *In vitro*, cromolyn sodium treatment reduced excessive collagen production by hepatocytes obtained from fibrotic human livers[85] and Chen *et al.* demonstrated reduced fibrosis in the excisional wounds of mice systemically treated with cromolyn.[86] Early investigations revealed that treatment with the synthetic mast cell stabilizer ketotifen prevented cutaneous fibrosis in mice.[87] More recently, studies showed that systemic ketotifen prevented wound contracture in a scarring model of the red Duroc pig[88] and Monument *et al.* demonstrated that ketotifen reduced joint contractures in a rabbit model of cutaneous scarring.[89] These investigations establish the importance of mast cells as moderators in fibrotic pathogenesis and underscore the need to explore new treatments.

Novel therapies may provide a fresh approach to combat the detrimental fibrosis of post-burn HTS. Anti-tryptase therapies have been suggested to reduce fibrosis by preventing permissive ECM remodeling or potential mitogenic activation of PAR2. Several studies show that anti-tryptase treatment with synthetic molecules were able to minimize mucosal inflammation during inflammatory bowel progression in several patient cohorts[90,91] and specific tryptase inhibition was also shown to minimize joint inflammation

in arthritic mice.[92] Inhibiting tryptase's enzymatic potential may be difficult due to its tetravalent active site structure; however, anti-tryptase therapy should be further explored to reduce fibrosis post-burn.

Pepducins have recently been reported as modulators of G-protein coupled receptor (GPCR) signaling and may have the promising ability to shunt tryptase-induced fibrotic signaling via PAR2. Pepducins are small peptides synthetically attached to lipids. Hydrophobicity allows incorporation into the plasma membrane, and specifically designed peptides permit interaction with distinct GPCRs to cause signal disruption. Pepducins directed against PAR2 (specific only for tryptase activation) have been shown to suppress itch and inflammation in a mouse model of atopic dermatitis[93] and other studies demonstrated that PAR2 pepducins were able to protect mice from the caerulein-induced onset of pancreatitis.[94] More recently, investigators were able to rescue mice from intermediate hepatic fibrosis with aggressive PAR2 pepducin treatment.[95] These investigations highlight mast cell importance in the progression of fibrotic pathologies and emphasize the need for new explorations in order to reduce post-burn fibrosis through mast cell modulation.

CONCLUSION

Mast cells are critical effector inflammatory cells and are found in considerably higher densities during injury and cutaneous wound healing. Chemoattractant molecules that recruit mast cells to wound sites, directly chemotactic stimuli, and other factors that potentiate degranulation are significantly increased following burn injury. While it is likely that a multitude of cell populations contribute to fibroproliferation, mast cells have been implicated in several scarring pathologies and should be considered integral during the

post-burn wound healing cascade. From inhibiting degranulation by membrane stabilization to direct targeting of potent pre-formed and *de novo* mediators, mast cell modulation may attenuate fibrosis as part of the detrimental post-burn HTS sequelae. Further investigations are warranted to explore mast cells influence in the healing burn wound.

CHAPTER 2: INCREASED MAST CELL DENSITY AND ELEVATED SERUM TRYPTASE CONTRIBUTE TO FIBROTIC PROLIFERATION IN PEDIATRIC POST-BURN HYPERTROPHIC SCARRING

INTRODUCTION

US burn centers treat over 400,000 injuries annually, with approximately 25,000 cases requiring intensive inpatient care.[96] Although with considerable reduction in mortality following severe burns,[2] attention is focused on long-term outcomes, with treatment of post-burn scars remaining the most significant challenge. Painful, pruritic, and raised hypertrophic scars (HTS), occurring subsequent to delayed wound healing, are a major sequela in up to 70% of severely burned patients; these pathologic scars significantly impair function and reduce quality of life.[4,97,98] Current therapeutic options have demonstrated limited effectiveness. Pressure garments can modulate collagen production, leading to thinner HTS,[99,100] however, compliance is demanding and premature abeyance or interruption in therapy can result in worse contraction and scar thickening.[101] Newer laser therapies can improve post-burn HTS considerably by reducing inflammation or physically ablating collagen allowing for partial restoration of normal wound healing,[102-104] but further clinical evidence is required to show sustained efficacy. These and other interventions continue to evolve and show potential for scar improvement, however, complete scar resolution remains elusive. Contractures persist and functional restoration is incomplete, limiting the post-burn quality of life.

In order to identify novel therapies that can improve post-burn wound healing, we have studied the role of mast cells in the innate immune response as moderators of

pathologic scarring. Expression of several pro-inflammatory cytokines and chemokines show sustained upregulation following severe burns.[22,23] Elevated factors produced in the burn wound, such as stem cell factor, can directly initiate mast cell cytoskeletal rearrangement through cKit activation, triggering chemotaxis.[31] TGF-β and macrophage inflammatory protein-1a (CCL3), both considerably increased post-burn, are major mast cell chemoattractants.[28,29,105] Such sustained increases in these key cytokines can provide a critical path that might account for mast cell accretion to burn wounds and fibrotic initiation.

There is now a growing body of investigations into mast cell involvement in several fibrotic pathologies. Studies have shown that mast cells play an important role in the induction of cardiac hypertrophy as well as pulmonary and renal fibrosis.[16,17,106] Vasoactive amines and other products released during mast cell degranulation are known to enhance collagen production and perturb normal wound healing.[107] Furthermore, mast cell proteinases contribute to both extracellular matrix remodeling and a fibrotic phenotype through a mast cell-fibroblast paracrine axis.[54] This signaling axis may point to a role for proteinase-activated receptors (PARs) in burn wound fibroblasts. Mast cell tryptase cleaves PAR2 and the resulting cleaved peptide, SLIGKV, acts as a tethered ligand activating the receptor. Subsequent PAR2 signaling is implicated in other fibrotic pathologies such as pulmonary fibrosis and rheumatoid arthritis[108,109] and may provide a valuable link between mast cells and dermal fibroblasts in the healing burn wound. Yet, despite this evidence, new investigations to identify roles for mast cells in post-burn scarring pathogenesis remain limited.

In this study, we examined the density, location, and activation status of mast cells within the post-burn HTS of pediatric patients. Additionally, we investigated the proliferative capacity of the major mast cell protease granules tryptase and chymase in primary post-burn HTS fibroblasts to determine a role for mast cells in HTS pathophysiology.

METHODS

Mast cell density, location, and activation status following severe burn injury

All tissues were obtained with informed consent and approved by the Institutional Review Board at the University of Texas Medical Branch. Non-burned skin (NBS) and hypertrophic scar (HTS) tissues were obtained from pediatric burn patients, with burns greater than or equal to 30% total body surface area, during revision surgeries at 6, 12, 18, 24, and 48 months post-burn (N=25, 5 per time point). HTS met histological and clinical criteria for hypertrophic classification by presence of thick, densely packed, highly eosinophilic and immature collagen, nodules with sharp borders, and global reduction in elastin. Tissues were then washed in PBS and antibiotic solution then placed in 10% neutral buffered formalin for 48-72 hours. After fixation, tissues were immersed in 70% ethanol prior to being processed and dehydrated to absolute ethanol over 12 hours. Tissues were then infiltrated with paraffin wax prior to sectioning at 4μm. A total of 7 different patient tissues were assessed at each time point post-burn.

Dual immunofluorescence for mast cell tryptase and chymase:

Sections were de-paraffinized and rehydrated to pure water. Sections were then immersed in antigen retrieval solution (DAKO, Agilent, Santa Clara, CA, USA) heated to 95ºC for 30 minutes, then blocked in 3% horse serum for one hour at room temperature.

Primary mouse monoclonal antibody to human mast cell tryptase (Abcam, Cambridge, MA, USA) diluted 1:350 in background-reducing antibody diluent (DAKO) was applied to each section overnight at 4°C. The next day, sections were washed and re-blocked in 3% horse serum for 1 hour at room temperature, then primary rabbit monoclonal antibody to human mast cell chymase (Abcam) diluted 1:350 in background-reducing antibody diluent was added to each section overnight at 4°C. The next morning, sections were washed in PBS then incubated for 1 hour at room temperature in fluorophore conjugated secondary antibody diluted in PBS corresponding to the primary antibody: goat anti-mouse AlexaFluor 568 (ThermoFisher, Waltham, MA, USA) or tryptase (1:500) and donkey anti-rabbit AlexaFluor 488 (ThermoFisher) for chymase (1:500). Sections were washed and nuclear stained in 1:10000 diamidino-2-phenylindole (DAPI) diluted in PBS for 20 minutes at room temperature. Each section was then cleared and mounted in resinous media. Fluorescence images of the papillary and mid-dermis were then captured at 450nm (blue-DAPI), 488nm (green-chymase) and 568nm (red-tryptase) then merged. Human lung tissue served as a positive control. Negative skin/scar controls received either no primary antibody or mouse/rabbit IgG to serve as an isotype control. Sections were washed thoroughly between each step in PBS with Tween 3 times, 10 minutes each.

Immunofluorescent quantification:

Each image was quantified for fluorescent intensity using ImageJ software (version 1.3 for Windows, NIH, Bethesda, MD). Five separate fields of the same mathematical area in the papillary and mid-dermis for each section were quantified by obtaining the integrated density of fluorescent stain at 488 and 568nm (blue signal was removed). Background

fluorescence was calculated and subtracted from red/green fluorescence to yield the corrected total tissue fluorescence (CTTF) in relative intensity units:

CTTF = Mean Integrated Fluorescence Density – Background Fluorescence Density

Mean CTTF was compared by one-way analysis of variance (ANOVA) to assess differences in means followed by a *post hoc* Bonferonni test to assess for significant differences between groups and time points.

Toluidine Blue stain:

Tissues were fixed, embedded, and prepared as before. Following rehydration, sections were stained in toluidine blue solution (Sigma, 89640, St. Louis, MO, USA) for 5 minutes then dehydrated in xylene. Each section was mounted in resinous media and enclosed by a glass coverslip. Trained observers in histopathology, and blinded to time point, quantified mast cells and separately qualified each as intact or degranulated to yield total mast cell density in the papillary and reticular dermis.

Serum mast cell tryptase in pediatric post-burn patients

Whole blood from pediatric burn patients (n=5) with ≥30% TBSA burns was collected with consent during the acute care stage (<30 days post-burn) and again at 6 months following injury. Samples were patient-matched over time (n=10 total samples). Age-matched blood from non-burned patients served as control (n=6). Serum was obtained and tryptase concentration was measured in triplicate by sandwich enzyme-linked immunosorbent assay (ELISA) specific to human mast cell tryptase- βII with a detection range between 0.25 – 8.0 ng·mL^{-1} (MyBioSource, San Diego, CA, USA). Colorimetric changes were measured on the FLUOstar Optima Microplate reader (BMG Biotech, Cary,

NC, USA). Mean serum tryptase concentration during the acute stage and again at 6 months post-burn was compared to age-matched non-burned control by one-way ANOVA.

Proliferative effects of mast cell proteases on burn wound fibroblasts

Primary human fibroblasts from NBS and HTS were obtained from pediatric burn patients during revision surgeries in this IRB approved study, washed in PBS and cultured in Dulbecco's Minimal Essential Media (DMEM) supplemented with 10% fetal bovine serum and 1% antibiotic antimycotic solution (Cellgro-Mediatech, Manassas, Virginia USA) at 37°C in 5% CO_2. Cell passages 3-7 were used for all *in vitro* experiments. Neonatal skin fibroblasts (PCS-201-010, ATCC, Manassas, Virginia USA) served as cellular controls and DMEM alone served as an assay control. Next, 2.50 x 10^3 cells were plated onto a 96-well microculture plate and allowed to attach. Cells were plated in 5 replicates for each treatment and cell line. Cells were then treated with either 0.002, 0.02, 0.2, 2.0 µg·mL^{-1} recombinant human (rh-) Chymase (R&D Systems, Minneapolis, Minnesota USA), 0.001, 0.01, 0.1, 1.0, 10.0 µg·mL^{-1} rh-Tryptase (Enzo Life Sciences, Farmindale, New York USA), or 0.1, 1.0, 10, 100 µM SLIGKV (MilliporeSigma, Burlingame, MA, USA) diluted in DMEM for assays. SLIGKV is the tryptase-cleaved peptide serving as a tethered ligand to activate PAR2 in the absence of mast cell tryptase. To assess metabolic and proliferative activity after 24 hours, an MTT assay (ATCC) was performed. Briefly, the soluble tetrazolium MTT reagent was added to each well and allowed to incubate for 3 hours for optimal metabolism of MTT. Following incubation, cells were lysed in detergent and the subsequent colorimetric change was analyzed by recording absorbance at 570nm. Mean absorbance for each cell line and treatment concentration was compared by one-way

ANOVA. Range of treatment for each compound was assessed by determining the concentrations that caused 50% cell death. This occurred at 100μg μg·mL^{-1} in rh-Tryptase, 1mM in SLIGKV, and at 100μg μg·mL^{-1} in rh-Chymase treatment, respectively. The experiment was repeated four times using matched NBS and HTS primary fibroblasts from four separate patients.

Mast cell density is significantly increased in post-burn **hypertrophic scars and remains elevated over time**

Quantitative CTTF shows increased expression of mast cell Tryptase and Chymase in post-burn HTS compared to non-burned skin. Moreover, this elevation continues for up to 4 years following burn injury. Mean tryptase/chymase dual stain CTTF values for post-burn HTS at 6 months (5.78 ± 2.21 x 10^4), 12 months (4.99 ± 0.199 x 10^4), 24 months (7.83 ± 0.193 x 10^4), and 48 months (1.219 ± 1.62 x 10^5) were significantly elevated (p<0.005) when compared to NBS (2.45 ± 0.74 x 10^4) (Fig 1a and 1b). Mean CTFF for HTS at 48 months was also significantly higher when compared to all other HTS time points (p<0.01). Moreover, the immunofluorescent data demonstrate gradual dissemination of mast cells in post-burn HTS, from initial localization around microvasculature to full propagation throughout the papillary and mid-dermis. These data demonstrate mast cell localization to burn scars after several years following the original injury, further showing that mast cell density increases significantly over time.
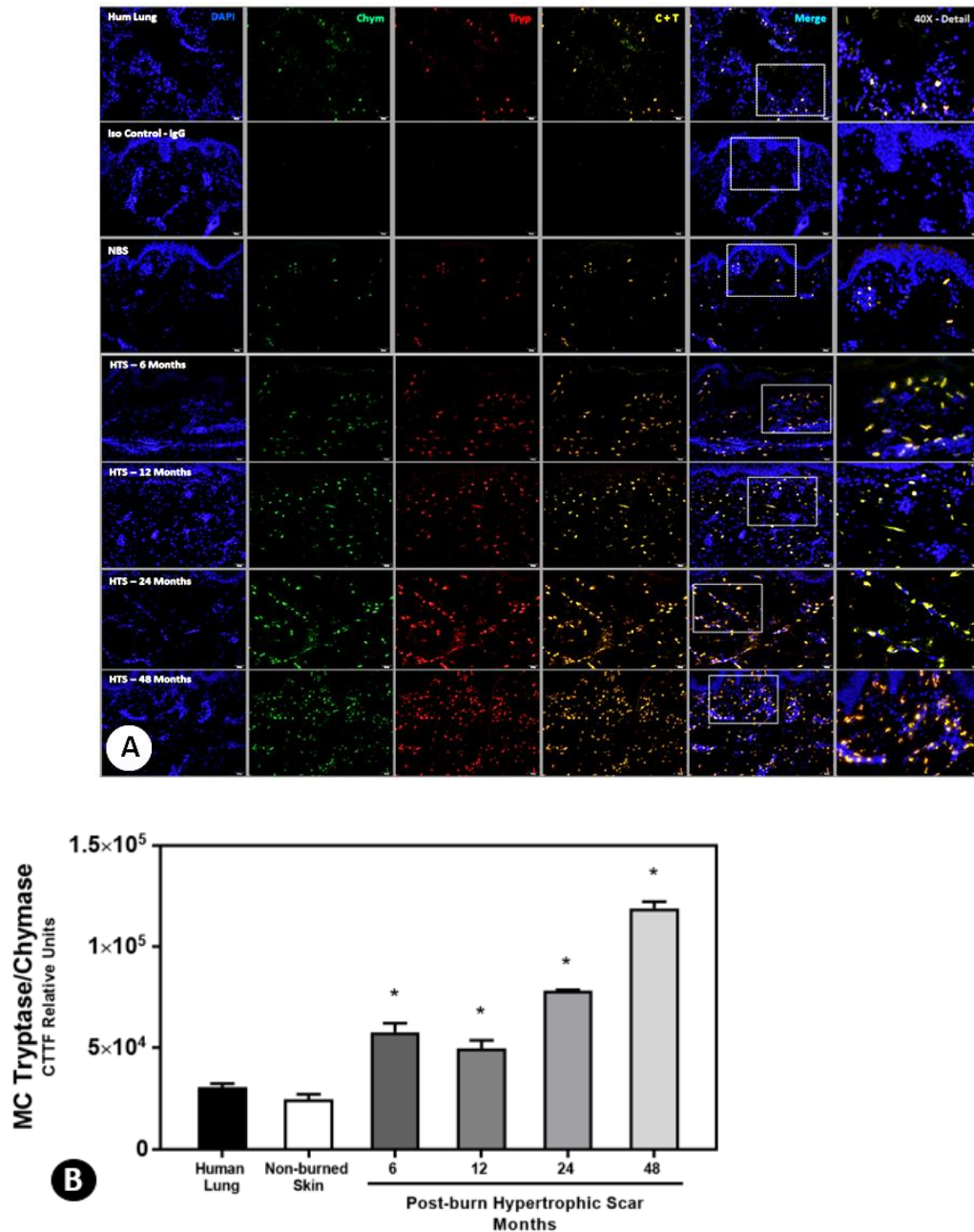
Figure 1:   Mast cell presence is significantly higher in pediatric post-burn **hypertrophic scars.**
Dual immunofluorescence intensity for mast cell tryptase and chymase increased considerably in pediatric HTS up to 4 years post-burn compared to that of non-burned skin (A). Quantification of corrected total tissue fluorescence (CTTF) indicates elevated mast cell density over time (B). Data presented is mean CTTF $\pm$ SEM. Non-burned skin (NBS) from non-burned patients served as control and human lung (Hum Lung) tissue served as an antibody staining control. A one-way ANOVA determined overall significance difference in group means followed by a post hoc Bonferonni test to confirm differences between groups and time points. *$p<0.001$ to non-burned skin.

Additionally, these data suggest that mast cells play a vital role in the maintenance of the post-burn scar tissue and provide further evidence that mast cells may indeed contribute to the fibrotic phenotype seen in hypertrophic scar pathology.

Intact and degranulating mast cells are significantly elevated in post-burn hypertrophic scars up to 2 years post-burn

Blinded observers' quantification shows significantly more intact and degranulating mast cells ($p<0.005$) over time in the papillary and mid-dermis of post-burn HTS compared to non-burned skin in toluidine blue stained tissues (Fig 2a and 2b). Intact mast cells increased from $1.72 \cdot 0.25$mm^{-2} at 6 months post-burn to $2.73 \cdot 0.25$mm^{-2} at 24 months post injury in HTS compared to $0.35 \cdot 0.25$mm^{-2} in non-burned skin ($p<0.005$). Degranulating mast cells were measured in increasing densities in HTS from $1.32 \cdot 0.25$mm^{-2} at 6 months post-burn to $1.55 \cdot 0.25$mm^{-2} at 18 months. Although increased in HTS, degranulating mast cell density was not significantly elevated at 2 years following injury. As analyzed by Fleiss' kappa statistic, there was substantial inter-rater agreement among four blinded observers (0.61-0.85) (Fig 2c). Taken together, these data indicate an active scar with degranulating mast cells persisting over time for at least 2 years following burn injury.
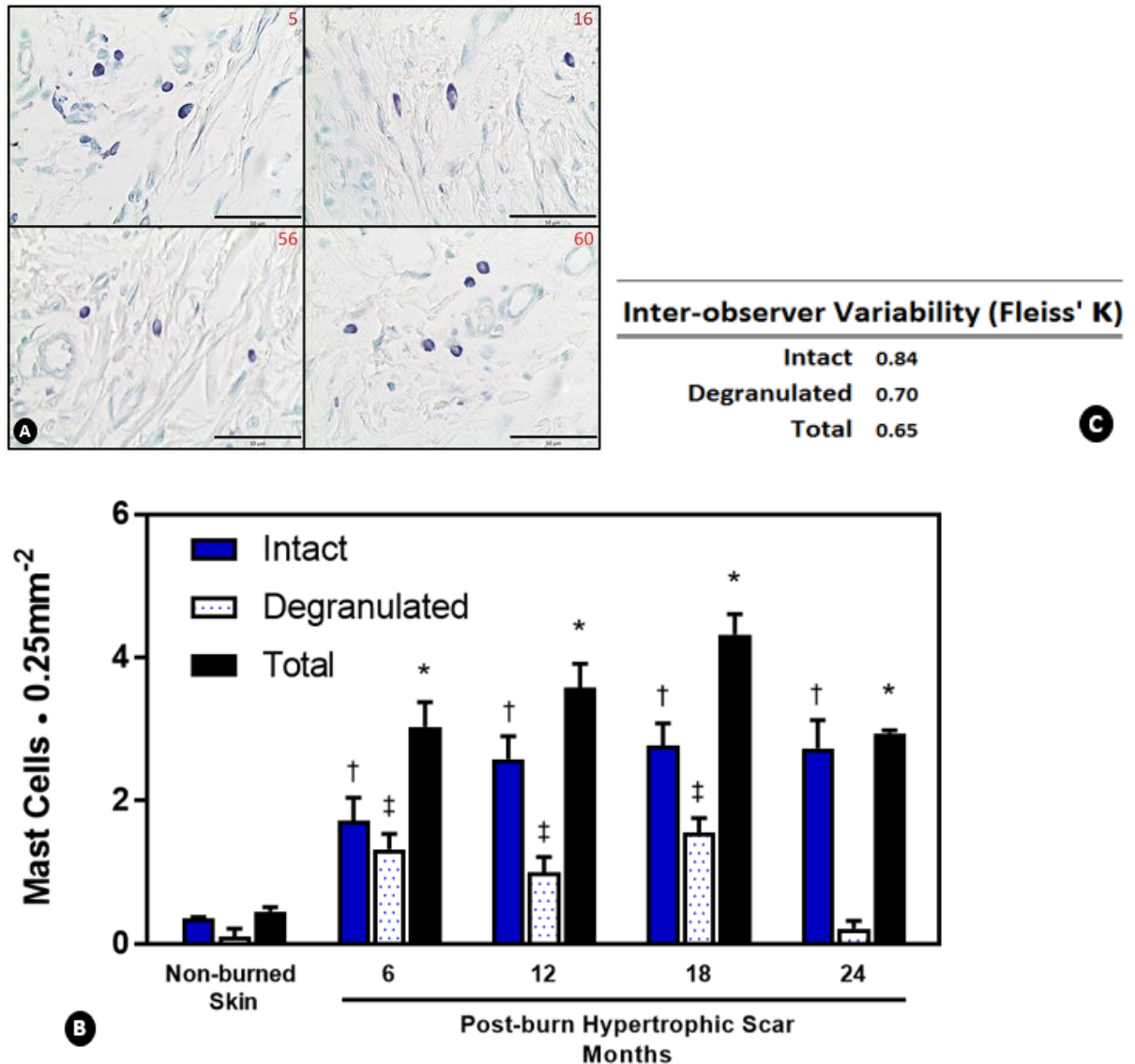
Figure 2: Both intact and degranulating mast cells are significantly increased in post-burn hypertrophic scars over time.

Toluidine blue stained tissues from NBS and HTS up to 2 years post-burn were imaged at 400X magnification (**A**, representative images). Scale bar represents 50μm. Mast cells in the papillary and mid-dermis were quantified as intact or degranulated by blinded observers trained in burn histopathology. Quantification shows significantly increased mast cell numbers, both intact and degranulating, in post-burn HTS compared to NBS indicating an active scar up to 2 years following injury. Data is presented as mean ± SEM among 4 blinded observers, *p<0.005 (**B**). Inter-observer variability was assessed as substantially in agreement (0.61-0.85) by Fliess Kappa statistic (**C**).

Serum mast cell tryptase concentration is considerably increased during the acute post-burn stage and at 6 months

Mean serum mast cell tryptase is significantly increased in pediatric burn survivors immediately following injury (6.104 ± 0.930 ng·mL-1) and at 6 months post-burn (5.105 ± 0.802 ng·mL-1) compared to non-burned children (0.7083 ± 0.2467 ng·mL-1) (Fig 3, p<0.001). Compared to age-matched non-burned controls, burn injury increases mast cell degranulation not only acutely following burn injury, but degranulation is sustained during initial HTS formation suggesting that active mast cell degranulation may contribute to HTS pathophysiology.
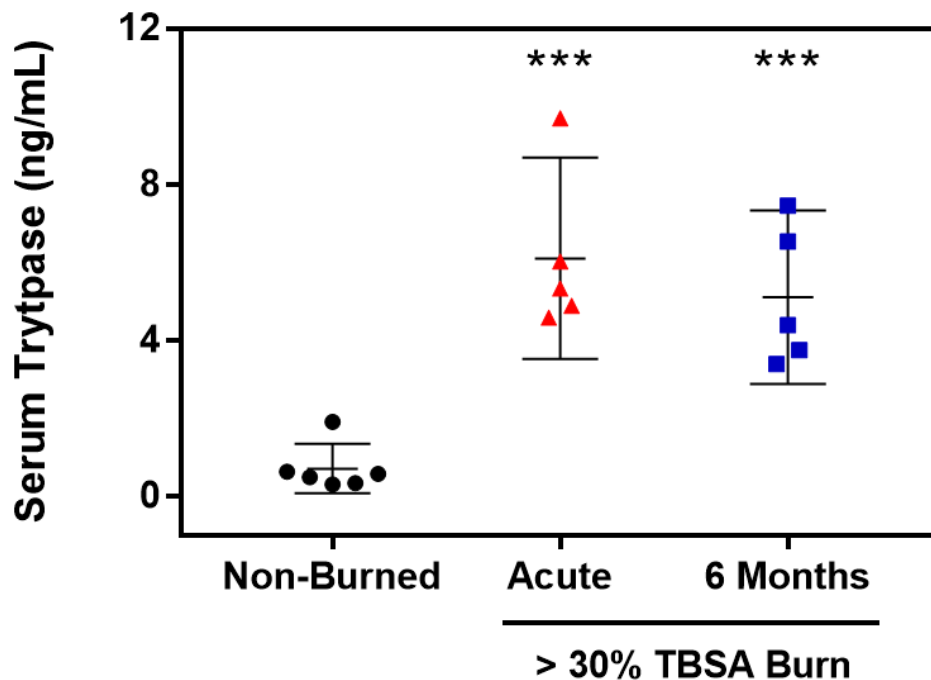
Figure 3: Mast cells are activated following severe burn injury.
Serum mast cell tryptase is significantly elevated during the acute care stage of burn injury and at 6 months post-burn compared to non-burned, age-matched controls, ***p<0.001 as measured by ELISA specific to human mast cell tryptase-βII. Data is presented as mean serum tryptase with 95% confidence interval.

Mast cell tryptase significantly increases proliferation in post-burn **dermal fibroblasts**

rh-Tryptase increased cell proliferation from control at only the highest concentration in NBS cells. Proliferation ranged from 89 ± 14 % at 0.001 μg·mL^{-1} up to 118 ± 17% at 10 μg·mL^{-1} in primary NBS fibroblasts. However, there was no significant difference in proliferation at any concentration. In contrast, rh-Tryptase significantly increased proliferation of primary HTS dermal fibroblasts at all concentrations. Proliferation increased steadily from 146 ± 18% at 0.001 μg·mL^{-1} to 176 ± 31% at 10 μg·mL^{-1}, peaking at 209 ± 23% at 1.0 μg·mL^{-1} (Fig 4a). The PAR2 activator, SLIGKV, showed similar effects on proliferation as did rh-Tryptase in each fibroblast type. Surprisingly, SLIGKV demonstrated no proliferative effect in NBS fibroblasts at any concentration, cresting at 95 ± 5% at the lowest concentration and reducing proliferation to 81 ± 6% at 100μM compared to control cells (Fig 4b). Still, in post-burn HTS fibroblasts, SLIGKV increased proliferation at all concentrations, peaking at 148 ± 8% from control at 0.1μM. These rh-Tryptase- and SLIGKV-induced proliferative increases were significantly different from those in NBS fibroblasts (p<0.01). Most notably, the other major mast cell protease, Chymase demonstrated no proliferative effect at any concentration on either NBS or HTS primary fibroblasts (Fig 4c). Peak proliferation of 88 ± 26% occurred at 0.02 μg·mL^{-1} in NBS fibroblasts and at 2.0 μg·mL^{-1} in primary HTS fibroblasts. Proliferations was not different from control cell (PCS) proliferation or from each other, NBS vs. HTS (p>0.05). To ensure cellular apoptosis did not artificially inflate proliferation measurements, cells morphology was monitored throughout the experiment. No morphological changes were noted in any of the cell populations.
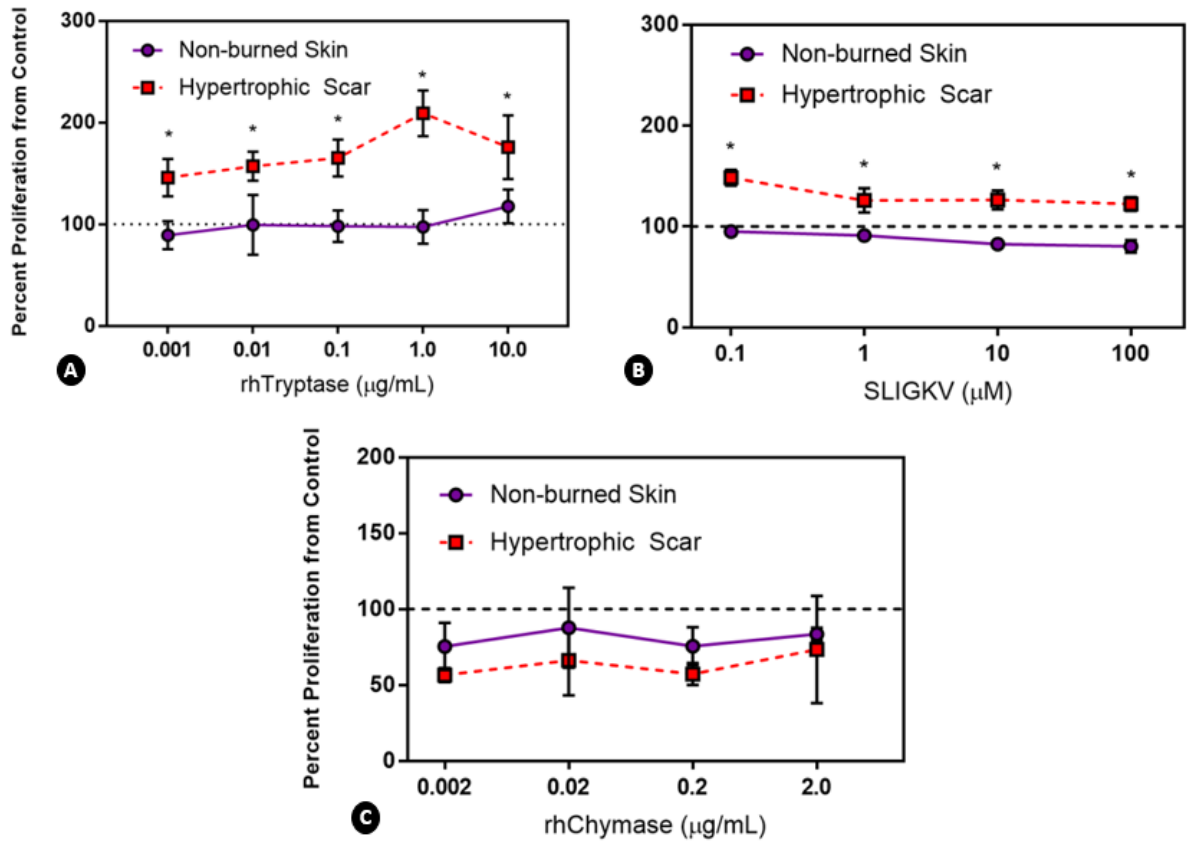
Figure 4: Mast cell tryptase increases burn wound fibroblast proliferation.

rhTryptase and PAR2 activator SLIGKV significantly increased the proliferation of primary post-burn dermal fibroblasts (**A** and **B**); proliferation was not altered by rh-Tryptase nor SLIGKV in non-burn skin primary fibroblasts. Additionally, rh-Chymase failed to induce any significant changes to proliferation in any NBS or HTS cell line at any concentration (**C**) demonstrating that tryptase is the main serine protease released by mast cells to cause proliferation of dermal fibroblasts. Furthermore, the data show that this proliferative effect occurs mainly in hypertrophic scar fibroblasts and not in non-burned fibroblasts. This differential response may indicate a fundamental phenotypic modification following burn injury to wound fibroblasts compared to their non-burned counterparts. Data is presented as mean percent proliferation from control (PCS) fibroblasts $\pm$ SD, *$p<0.05$.

Painful and disfiguring HTS remain one of the most challenging post-burn outcomes to treat clinically. Therapies such as compression garments, laser therapy, or surgical revision are used in order to reduce HTS by physical means, reducing excess collagen deposition, and minimizing many detrimental scar parameters. Cellular-based therapies are now incorporating the use of autologously derived adipose stem cells that beneficially alter ECM and flatten HTS, but the extent to which this unique cell population contributes to improved healing is still unknown.[110,111] Systemic pharmacologic interventions are receiving more attention as well. In addition to reducing cardiac load and blunting the hypermetabolic response following a severe burn, we have previously shown that the non-selective beta-blocker propranolol, with or without Oxandrolone, reduces HTS by reducing β-adrenergic receptor expression.[5,112] These current therapeutic options, although promising, remain inadequate for full scar resolution and painful and pruritic HTS persist for years after the initial injury. We must continue to look in new directions to develop more effective therapies and strategic immunomodulation may prove to be pivotal.

Recent evidence suggests that immune cell populations may play a fundamental role in post-burn HTS pathology. Macrophages and T-cells in the early burn wound release a plethora of pro-inflammatory cytokines that serve to recruit neutrophils and monocytes.[113-115] This immune milieu has been shown to be essential for the induction of post-burn fibrosis.[116,117] Studies show that when macrophages are depleted during early wound healing, subsequent scarring can be reduced.[118] Even with the evidence of increased immune cell activity, mast cells have been often neglected in the post-burn wound healing cascade, although they are implicated in several other fibrotic pathologies.[119-121] However,

growing evidence is demonstrating that mast cells may indeed play a more prominent role in HTS pathogenesis than previously thought.

Kischer and colleagues provided the earliest data that mast cells may be involved in cutaneous scarring following severe burns by observing increased mast cell numbers in granulation tissue compared to bordering non-burned skin.[19] Tredget *et al.* found elevated mast cell quantities and increased histamine metabolism in adult patients with hypertrophic scars.[20,122] Results from the current study show significantly elevated mast cell density in the hypertrophic scar tissues of pediatric burn patients. Importantly, mast cell presence increases with time, from 6 months post-burn up to four years after initial injury. Itch and pain from the scars during this time shows sustained impact on patient well-being and quality of life.[3] Moreover, during this same time, data indicate that mast cells disseminate from microvasculature to most areas in the papillary and reticular dermis suggesting that they have a sustained effect on dermal fibroblasts during HTS pathology.

As a part of their immune function, mast cells release an abundance of pre-formed and *de novo* synthesized mediators upon activation. The serine protease tryptase is the most abundant of these mediators and its actions are implicated in several fibrotic pathologies. Previous studies have shown that tryptase inhibits apoptosis of synovial fibroblasts in rheumatoid arthritis in a Rho-kinase dependent manner which further sustains a fibrotic phenotype.[123] Others have demonstrated that tryptase can trigger collagen production in circulating fibrocytes highlighting tryptase's fibrotic inducing potential. In the present study, we found increased serum tryptase levels in severely burned children. This considerable tryptase elevation, although not within "normal" levels and not rising to

concentrations associated with mast cell disorders such as mastocytosis, were up to 6 times higher than concentrations found in healthy non-burned children.

Increased tryptase levels were expected acutely following a major burn due to the canonical hypermetabolic response and general cellular necrosis that is part of large cutaneous full-thickness injuries. Notably however, a surprising finding was that tryptase concentrations remained elevated at 6 months post-burn from patient-matched samples. Such continuous increases would assuredly have fibrotic consequences in the healing burn wound. Studies have shown tryptase's ability to induce proliferation in fetal fibroblasts and adult skin fibroblasts through the activation of PAR2 and resultant MAPK signaling.[64,124] However, our investigations show differential effects of tryptase on proliferative capacity of primary fibroblasts from non-burned skin versus HTS. Tryptase treatment, or the PAR2 activator SLIGKV, induced significant proliferation in HTS fibroblasts but not in non-burned fibroblasts which suggests there is an inherent phenotypic difference in dermal fibroblast populations of burn survivors. Further studies are warranted to explore PAR2 expression and activation in post-burn fibrosis.

Chymase is another critical protease released during mast cell degranulation and strong evidence demonstrates that chymase promotes cardiac fibroblast proliferation, induces pulmonary fibrosis, and stimulates epithelial proliferation in lung carcinomas.[54,125,126] Contradictory evidence, however, suggested that chymase may inhibit proliferation by modifying cell-matrix adhesions.[127] Here, we show that chymase had no such proliferative effects in primary post-burn HTS fibroblasts at any experimental concentration. It is possible that chymase may have other effects on wound healing or ECM deposition. Although it did not affect proliferation of either non-burned skin fibroblasts or

HTS fibroblasts, chymase remains an important mast cell protease that requires further study in the context of cutaneous fibrosis and scarring.

Histamine is the major vasoactive amine released during mast cell degranulation and is most often associated with immune hypersensitivity reactions. Although not investigated here, others have reported increased histamine levels after a major burn[49,122] and the present study does provide evidence for actively degranulating mast cells during post-burn wound healing. Importantly, increased mast cell density in post-burn HTS would provide the source for histaminergic itch. Pruritus remains a significant factor reducing the quality of life for burn survivors and the majority of pediatric patients still report moderate itch up to 2 years after injury.[128,129] Understanding mast cell activation following a major burn may not only address scarring pathophysiology, but may also elucidate underlying mechanisms of post-burn itch and provide a therapeutic path to alleviate such burden.

In conclusion, this study demonstrated that mast cells accumulate in pediatric post-burn HTS in increasing densities long after the scar has matured. Moreover, mast cells were found to be fully disseminated throughout the entire dermis indicating chemoattractant stimuli are still present in the burn scar for years. Increased serum tryptase levels during acute burn treatment and at 6 months post-burn supports the hypothesis that active mast cell degranulation in HTS sustains a fibrotic environment over time. Finally, the current study helps increase our understanding of post-burn HTS pathophysiology and highlights the need for further investigations into potential cellular-based and immunomodulatory treatments to alleviate cutaneous fibrosis and other detrimental post-burn sequelae.

CHAPTER 3: MAST CELL TRYPTASE CONTRIBUTES TO POST-BURN FIBROSIS THROUGH PROTEASE-ACTIVATED RECEPTOR-2 ACTIVATION

INTRODUCTION

Worldwide, burns account for almost 11 million traumatic injuries annually that necessitate medical intervention and cause nearly 200,000 deaths. Emergent resuscitative measures, immediate surgical interventions, and reformed nutritional standards have remarkably reduced mortality in pediatric full thickness burn cases over the last few decades.[2,130,131] However, post-burn hypertrophic scarring (HTS) remains a critical morbidity with limited treatment options that ultimately diminishes quality of life for burn survivors. Impaired movement, limited by fibrosis, and itching persist for years after the initial injury and HTSs continue to be the most difficult treatment challenge.[4] Innovative therapies such as laser ablation and autologous adipose tissue injections have greatly improved detrimental scar sequelae. Novel treatments must be explored to restore normal wound healing after traumatic burns. To understand better the consequences of HTS, we have recently explored the roles of mast cells in post-burn HTS pathophysiology.

Mast cells are sentinel effector cells of the innate immune system activated to degranulate during allergic hypersensitivity reactions, anaphylaxis, and in response to certain bacterial and parasitic infections.[132] Released factors serve as inflammatory stimuli that initiate vasodilation and facilitate mobilization and infiltration of other immune cells populations to sites of injury. Inflammatory cytokines such as transforming growth factor-β (TGF-β), monocyte chemoattractant protein-1 (MCP-1), and macrophage inflammatory protein-1 (MIP-1) are significantly increased following burn injury[22] for sustained periods and are known chemoattractants for mast cells.[33,105,133] The increased expression of

cytokines may provide the impetus for mast cell chemotaxis and migration to sites of burn injury. Once established in wound tissue, we hypothesize that the mast cells may drive HTS progression.

Increased mast cell numbers are present in adult HTS with concomitant elevations in systemic histamine, an important mediator produced by mast cells. Additionally, mast cells are noted as key regulators of cardiac, adipose, and renal fibroses.[18,106,120,121] We have previously demonstrated increased mast cell density in pediatric HTS up to 4 years post-burn with simultaneously increased serum tryptase concentration up to 6 months following the initial injury, further supporting the notion of actively degranulating mast cells in long-term HTS.[134] Mast cells may be involved in a host of wound healing activities, but importantly may contribute to HTS progression through a fibroblast paracrine axis that is not well studied or understood.

Several studies have described mast cell – fibroblast interactions and their potential link to scarring. Indirect mechanisms may involve mast cell released factors such as vascular endothelial growth factor (VEGF), which stimulates vascular leakage and sustains further inflammation, while others have proposed fibroblast migration and collagen synthesis through the action of histamine, which is produced in ample amounts by mast cells.[48,135] Interestingly, evidence also points to the direct interaction of mast cells and fibroblasts and their ability to exchange proliferative signals through gap junctions.[136,137] Of all granules produced by mast cells, tryptase is the most abundant protease, accounting for up to 50% of the total protein contained in granules.[57,68] Tryptase is known to proteolytically cleave the protease-activated receptor-2 (PAR2) in dermal fibroblasts and is implicated in fibrotic pathologies including pulmonary fibrosis.[138] However, whether

this important protease's plays a role in post-burn scarring pathophysiology has not been explored.

The protease-activated receptors (PAR) are a unique class of G-protein-coupled receptors (GPCR) that are sensitive to a variety of enzymatic proteases in the extracellular environment including mast cell tryptase. There are four known isoforms (PAR1-4) that have a range of biological functions in many tissues. PAR activation and signaling is required for maintenance of vascular tone in the pulmonary system and regulation of secretion from pancreatic duct epithelial cells.[139,140] PARs share approximately 50% sequence homology over all isoforms, but the receptors are highly conserved across mammalian species.[141] GPCRs are canonically activated by distinct ligands that bind to complementary extracellular N-terminal moieties of the receptor. Binding catalyzes a physical conformation change that initiates G-protein mitogenic intracellular signaling.
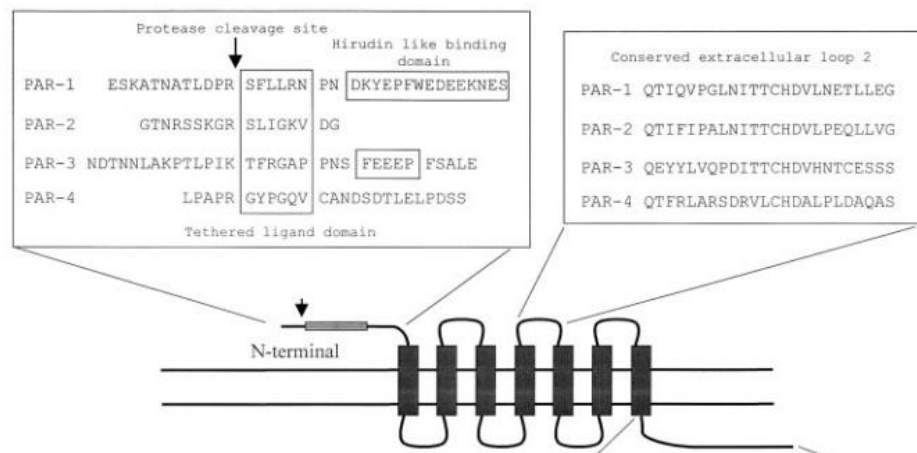
Figure 5: Primary sequences for proteolytic cleavage sites for PARs 1-4 are specific for distinct proteases including mast cell tryptase.

The extracellular portion of the second extracellular loop is specific for the tethered ligand binding site and subsequent activation of the signal. N-terminal cleavage is irreversible, therefore, PARs must be synthesized de novo for signal re-sensitization. Adapted from Macfarlane, S.R., *et al.*, *Proteinase-activated receptors.* Pharmacol Rev, 2001. **53**(2): p. 245-82.

However, PARs are very rare exceptions to classic GPCR activation and subsequent signaling. PAR activation is achieved by targeted proteolytic cleavage of N-terminal moieties. The cleaved peptide binds to the second extracellular loop of the receptor and acts as a tethered ligand that stimulates signaling (Fig 5 and 6).[142]
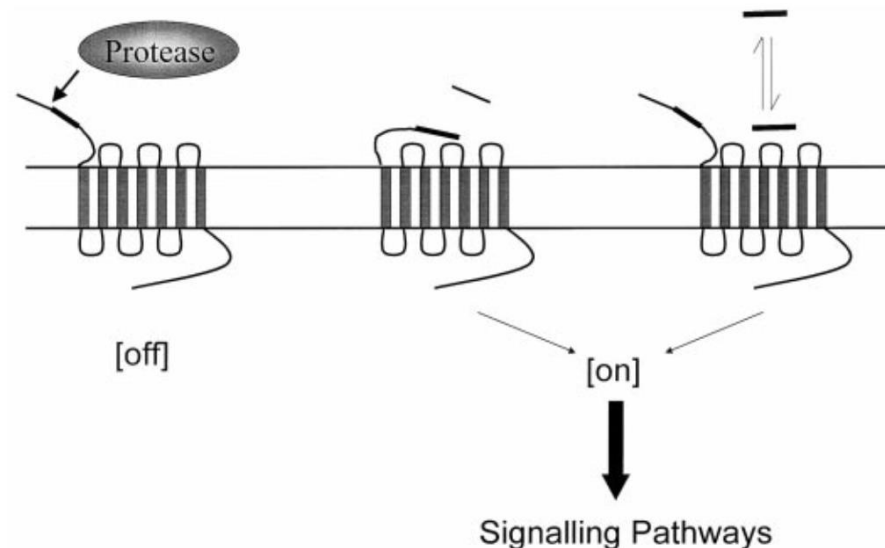
Figure 6: Diagram of proteolytic activation of PARs.
Adapted from Macfarlane, S.R., *et al.*, *Proteinase-activated receptors.* Pharmacol Rev, 2001. **53**(2): p. 245-82.

Following receptor activation, intracellular G-proteins are recruited and coupled to intracellular portions of the GPCR, which activates phospholipase C (PLC) and initiates calcium mobilization. Repeated PAR activation stimulates increased β-Arrestin expression and trafficking to the plasma membrane where β-arrestin and PAR interact to terminate signaling. This accompanies receptor internalization by clathrin-coated pits and initial direction to early endosomes with later delivery to lysosomes for degradation. Interestingly, MAPK signaling (Fig 7) has been shown to continue even upon receptor internalization, which may be a mechanism to target and activate specific kinases or

localize signal propagation.[141,143] Additionally, whereas most GPCRs can be recycled back to the plasma membrane, PAR proteolytic cleavage is irreversible. New receptors must be synthesized de novo to re-sensitize the cell for continued signaling.[144] Thus greater PAR expression indicates increased signaling.
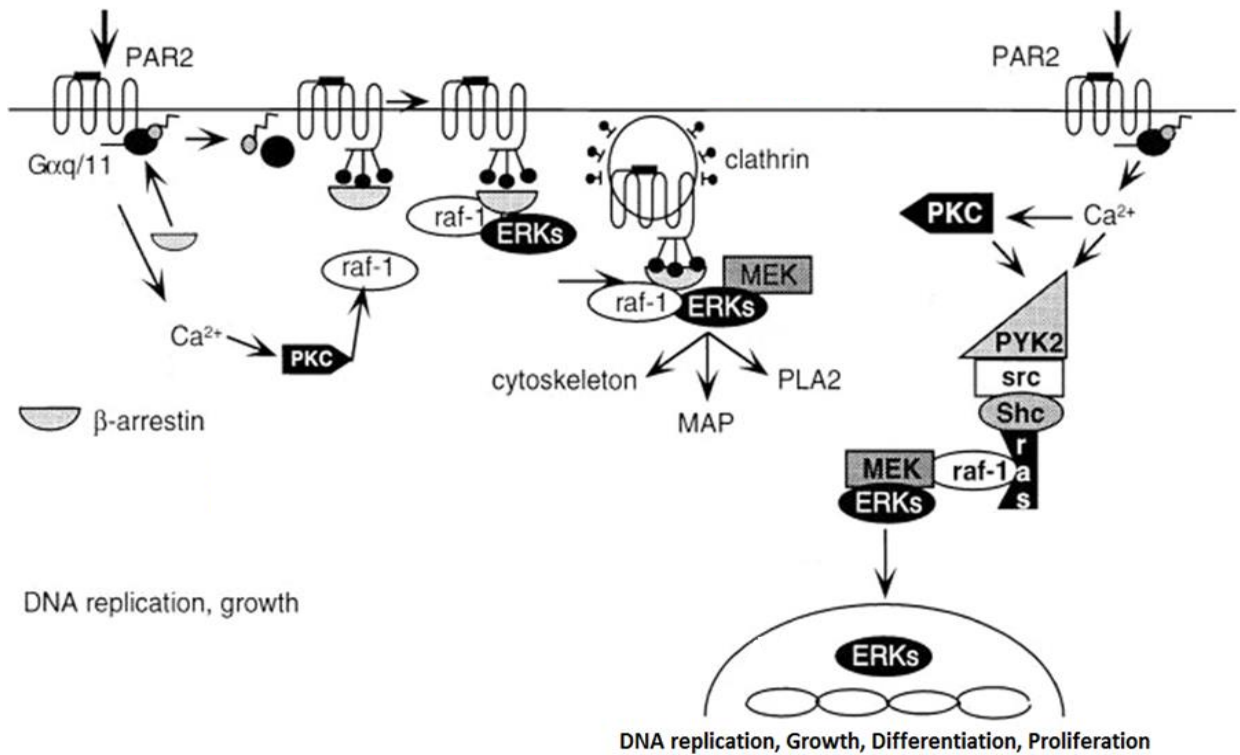
Figure 7:   PAR2 activation and MAPK signaling.
Following PAR2 activation by mast cell tryptase, G-proteins are rapidly recruited to propagate mitogenic signaling. Activation induces β-Arrestin expression and endocytosis of the signaling complex. Signaling continues even upon internalization prior to degradation in lysosomes. Unlike most GPCRs that can be recycled back to the plasma membrane, PARs are irreversibly cleaved upon activation and must be made de novo to re-sensitize the cell for continued signaling. Adapted from DeFea, K.A., *et al.*, beta-arrestin-dependent endocytosis of proteinase-activated receptor 2 is required for intracellular targeting of activated ERK1/2. J Cell Biol, 2000. 148(6): p. 1267-81.

Cleavage sequences for PARs provide specificity for distinct proteases. PARs-1, -3, and -4 are activated by thrombin, which plays a major role in the clotting cascade. Proteolysis at specific N-terminal moieties results in different tethered ligand activating peptides. Functional expression and receptor mutation studies revealed that the hexapeptide SLIGKV was the activating tethered ligand specific for PAR2 this peptide is a very potent agonist at low concentrations.[145] Unlike other isoforms, PAR2 is the only described physiologic receptor targeted solely by a single protease – tryptase, which is produced by mast cells. Importantly, the activation of PAR2 is implicated in several scarring pathologies which may have critical consequences in post-burn HTS.[146] Mast cell tryptase induces lung fibroblast proliferation and subsequent fibrosis via PAR2 activation[147] *in vitro* and is also implicated in liver and kidney fibrotic progression *in vivo*.[95,148] However, PAR2 expression, activation status and subsequent signaling post-burn has never been explored. In the current study, we demonstrate a function for mast cell-induced tryptase activation of post-burn PAR2 on post-burn HTS and establish a role for mast cells in the progression HTS following severe burn injury in children.

METHODS

Tissue procurement and primary cell culture

All tissues were obtained under a protocol approved by the University of Texas Medical Branch Institutional Review Board. Hypertrophic scar (HTS) and bordering non-burned skin tissues were excised and obtained during revision surgeries on pediatric patients with full-thickness burns covering at least 20% of the total body surface area (TBSA). Post-burn hypertrophic scar tissues were identified via clinical examination and histologically confirmed by a certified histopathologist. Tissue was washed in phosphate

buffered saline (PBS) and soaked in antibiotic solution for 1 hour prior to processing. Tissue was then minced and cultured in sterile Dulbecco's minimal essential media (DMEM, ThermoFisher, Waltham, MA, USA) supplemented with 1% antibiotic/antimycotic solution (ThermoFisher) and 10% fetal bovine serum (FBS, MilliporeSigma, St. Louis, MO, USA). Fibroblasts were isolated and further expanded in 10%-FBS supplemented DMEM (10% DMEM) at $37^{\circ}C$ and 5% CO_2 for experiments. Commercially purchased primary neonatal skin fibroblasts (PCS, American Type Culture Collection [ATCC], Manassas, VA, USA) served as natural non-burned controls and were cultured and expanded under the same conditions. *In vitro* experiments were completed in replicates with 3 sets of patient-matched, and 2 sets of non-matched, fibroblasts isolated from non-burned skin and HTS, between passages 3-7.

PAR2 immunocytochemistry

1.50 x 10^5 HTS and NBS cells were cultured as described and plated onto glass coverslips in 6-well plates and expanded for 24 hours to reach 30-40% confluence. After attachment, cells were washed in PBS and cultured in serum-free DMEM for 24 hours. Cells were then treated either with 10µM of the PAR2 activating peptide SLIGKV (S9192, MilliporeSigma, Burlingame, MA, USA) solubilized in water or 10% DMEM alone for 10, 20, 30, and 60 minutes. Independent experiments were performed for three patient-matched fibroblasts from non-burned skin and HTS in triplicate. At each time point, treatments were removed and cells were washed in ice cold PBS prior to fixation in 4% paraformaldehyde diluted in methanol for 20 minutes then blocked in 3% horse serum for 1 hour at room temperature. Cells were then incubated in rabbit monoclonal anti-PAR2

antibody (1:300, Abcam 180953, Cambridge, MA, USA) diluted in background-reducing antibody diluent (DAKO) at 4°C overnight. After washing 3 times in phosphate-buffered saline with Tween20, fibroblasts were incubated with secondary antibody AlexFluor488 (1:350, ThermoFisher A-21206) for 1 hour at room temperature. Subsequently, cells were counterstained with 4′,6-diamidino-2-phenylindole (DAPI) 1:10000 for fluorescent nuclear visualization and coverslipped for imaging.

Images were acquired on an Olympus BX41 microscope utilizing cellSens software (version 1.7, Olympus, Tokyo, Japan). Fluorescent intensity, indicative of PAR2 expression, was quantified by corrected total cell fluorescence (CTCF) in ImageJ (version 1.3 for Windows, NIH, Bethesda, MD). Briefly, a region of interest area was outlined around individual cells in the field of view. Background regions of interests were defined as non-cellular areas. Pixel intensity of each region of interest was calculated as integrated density; greater integrated density corresponds to increased fluorescent intensity and greater PAR2 expression. Integrated density was normalized to area of measurement to account for differences in cell size and subtracted from the mean background integrated density to correct for non-specific fluorescence to yield the corrected value CTCF[149]: CTCF = measured fluorescence intensity (PAR2) – background fluorescence. A one-way ANOVA assessed PAR2 expression (CTCF) differences produced by SLIGKV treatment between cell lines at each time point.

Proliferation and Wound Healing / Scratch Assays

Proliferation assay: Primary non-burned skin and HTS fibroblasts were cultured as described. In each well of a 96-well microculture plate, 3.0×10^3 fibroblasts were plated in

10% DMEM and allowed to attach overnight. The next day, media was removed and cells were treated with 10μM of the PAR2 inhibitor, GB83, (Axon MedChem, Reston, VA, USA) solubilized in dimethyl sulfoxide (DMSO) and diluted in 10% DMEM, for 2 hours prior to treatment with either $10\mu g \cdot mL^{-1}$ recombinant human mast cell tryptase (Enzo Life Sciences, Farmingdale, New York USA), $20ng \cdot mL^{-1}$ recombinant human mast cell chymase (R&D Systems, Minneapolis, Minnesota USA), or the combination of both. The placebo controls were independent treatments with 10% DMEM or 0.01% DMSO. Following 1-hour treatment, an 3-(4,5-dimethylthiazol-2-yl)-2,5-diphenyltetrazolium bromide (MTT) assay (ATCC, Manassas, VA, USA) measured percent proliferation from control. Briefly, tetrazolium dye (MTT) was added to each well and incubated for 3 hours at 37°C until a purple precipitate formed from the metabolism of MTT reagent. Cells were then lysed in detergent buffer and the ensuring color change was spectroscopically measured at 570nm. Mean absorbance values were normalized to control treatment and compared by one-way analysis of variance to assess differences in proliferation between cell lines and treatments.

Wound healing / Scratch assay: Both non-burned skin and HTS fibroblasts were cultured as before. In each well of a 6-well culture plate, 2.5×10^6 fibroblasts were plated and allowed to grow 24-48 hours to reach 100% confluence. Next, cells were treated with 10μM GB83. After 2 hours, GB83 pre-treatment was removed and the fibroblasts were then treated with either 10% DMEM (control), 0.01% DMSO, 10μM of the PAR2 activator SLIGKV, or inverse peptide VKGILS as control. Immediately following treatment, a sterile 100μL pipette tip was used to form two artificial scratches approximately 1cm apart in each well. The scratch created a uniform gap averaging 500-600μm. Culture plates were

re-incubated at 37°C and brightfield images of the scratch were captured every two hours over the course of 12 hours on an inverted Nikon Diaphot 300 (version 3.22.15, NIS software, Melville, NY, USA). The same area of each well and scratch gap was imaged during each time point. TScratch software (version 1.0, Koumoutsakos group (CSE Lab), ETH Zurich, Zurich, Switzerland)[150] quantified the percent open area for each wound and a 2-way ANOVA analyzed differences between treatments at each time point. Significance was accepted at $p<0.05$. Experiments were repeated three times for three patient-matched non-burned skin and HTS fibroblast cell lines.

RT-qPCR for mRNA markers of fibrotic signaling

HTS and NBS cells were cultured and treated as before in 6-well plates in three independent experiments. After 2-hour GB83 pre-incubation and following 1-hour SLIGKV treatment, mRNA was harvested to investigate fibrotic and mitogenic signaling pathways. RNA was isolated via the RNEasy Mini Kit (Qiagen, Los Angeles, California USA) and proceeded according to manufacturer's instructions. Briefly, cells were lysed in RLT buffer and RNA was allowed to precipitate in 75% ethanol before transfer to the RNA mini column. Following centrifugation, the column was washed twice in wash buffer, once in RPE buffer, and RNA was eluted in approximately 20 µL RNase-free water. RNA concentration and purity were assessed by UV spectroscopy (NanoDrop 1000, ThermoFisher) with absorbance measured at the ratio of 260 and 280nm. Next, 500µg of isolated RNA was reverse transcribed to yield pure complimentary DNA (cDNA) via iScript Reverse Transcriptase kit (Biorad, Hercules, California USA). Thermocycling was set to 5 minutes at 25°C, 30 minutes at 42°C, and then 5 minutes at 85°C. After cycling was

complete, cDNA was held at 4°C until gene expression assessment via polymerase chain reaction (PCR). Prior to PCR, cDNA was diluted in DNase-free water 1:10. Transcripts were then amplified using the StepOne Plus PCR system (Applied Biosystems, Foster City, California USA) with SYBR Green Master Mix (Biorad) along with primer pairs for markers of PAR2 activation and subsequent fibrotic signaling (Table 1). Melt curves were analyzed to ensure the purity and specificity of the primer. Gene expression was then normalized to β-Actin and fold change was calculated utilizing the delta-delta threshold cycle (ΔΔCt) method for comparisons between treatment groups.

Target	Primers (5' - 3') Sense	Antisense
PAR-1	CAGTTTGGGTCTGAATTGTGTCG	TGCACGAGCTTATGCTGCTGAC
PAR-2	GGGTTTGCCAAGTAACGGC	GGGAACCAGATGACAGAGAGG
PAR-3	TCCCCTTTTCTGCCTTGGAAG	AAACTGTTGCCCACACCAGTCCAC
PAR-4	AACCTCTATGGTGCCTACGTGC	CCAAGCCCAGCTAATTTTTG
β-Arrestin-1	CAAAGGGACCCGAGTGTTCA	TGGGAACGACTGTACGTTGG
Collagen-I	CGACCGCTTCACCTACAG	TTTTGTATTCAATCACTGTCTTGC
Collagen-III	GGGAACAACTTGATGGTGCT	CCTCCTTCAACAGCTTCCTG
α-SMA	GACGAAGCACAGAGCAAAAGAG	TGGTGATGATGCCATGTTCTATCG
bFGF	GGCTTCTTCCTGCGCATCCA	GCTCTTAGCAGACATTGGAAGA
KGF	AGGGACCCAAGAGATGAAG	TGATTGCCACAATTCCA
VEGF	GGGCAGAATCATCACGA	CCGCCTCGGCTTGTCACA
MMP-1	CTGAAGGTGATGAAGCAGCC	AGTCCAAGAGAATGGCCGAG
MMP-2	GCGACAAGAAGTATGGCTTC	TGCCAAGGTCAATGTCAGGA
MMP-9	CGCAGACATCGTCATCCAGT	GGATTGGCCTTGGAAGATGA

Table 1: Primer pairs for proliferative and fibrotic targets in post-burn hypertrophic scar pathophysiology signaling.

PAR2 knockdown

In three independent experiments with three patient matched non-burned skin and hypertrophic scar fibroblasts cell lines, 1.50×10^5 HTS fibroblasts were grown to 50%

confluence in 6 well tissue culture plates and treated with 10μM siRNA to PAR2 (ThermoFisher). Lipofectamine served as the transfection reagent. Control fibroblasts received 10% DMEM, lipofectaime, or scrambled siRNA alone. siRNA pre-treatment was removed after 72 hours and then cells were treated with 10μM SLIGKV for 1-hour. Following treatment, protein was harvested to confirm efficient PAR2 knockdown and RNA was collected to analyze markers of fibrotic signaling as previously described. Primers are listed in Table 1.

Human mast cell and burn wound fibroblast direct co-culture

Patient-matched primary non-burned skin and HTS fibroblasts were cultured and expanded as previously described. Human mast cells (LUVA) were purchased commercially (Kerafast, Boston, MA, USA) and expanded in StemPro-34 media (ThermoFisher) supplemented with 200mM L-glutamine, 1% penicillin and streptomycin, and 0.2% primocin at 37°C in 5% CO_2. LUVA mast cells proliferate independent of stem cell factor, but express a non-mutated and functional c-kit receptor. These mast cells have also been shown to express the full complement of endogenous pre-made and *de novo* mediators including tryptase and chymase. Following expansion, 1.0×10^6 mast cells were treated with 20μg·mL^{-1} compound 48/80 (MilliporeSigma) overnight to activate the cells and potentiate degranulation.[151] The next morning, mast cells were removed and the conditioned media (MC Cond Med), containing the contents of the degranulated mast cell granules, was harvested for use *in vitro*. Depleted mast cells were discarded.

For co-culture experiments, 2.50×10^5 patient matched non-burned skin and HTS fibroblasts were separately plated in each well of 6-well culture plates and allowed to reach

approximately 90% confluence in DMEM supplemented with 10% fetal bovine serum. For immunocytochemistry experiments, fibroblasts were grown to approximately 30-40% confluence on glass coverslips in 6-well culture plates. Next, media was removed and the fibroblasts were washed in warm PBS. Fibroblasts were then treated either with 2% DMEM, 10% DMEM, 1.0×10^6 LUVA MC Cond Med with or without PAR2 inhibition (GB83), or 1.0×10^6 activated LUVA mast cells with or without PAR2 inhibition. Fibroblasts were pre-treated with10μM GB83 for 2 hours prior to subsequent treatments. Fibroblasts and mast cells were in direct contact for described treatment conditions. Treatment conditions were applied for 1 hour. Subsequent processing to assess myofibroblast differentiation and protein expression differences in order to elucidate proliferative and fibrotic signaling is described below.

Myofibroblast immunocytochemistry in mast cell – fibroblast co-culture

Following co-culture, all treatments including mast cells and media were removed from culture dishes. Fibroblasts, grown on glass coverslips, were prepared as before (see PAR2 Immunocytochemistry). Briefly, cells were washed in ice-cold PBS, fixed in 4% paraformaldehyde, and blocked in 3% goat serum for 1 hour. Following heated antigen retrieval, cells were incubated in 1:300 mouse IgG to human alpha-smooth muscle actin (αSMA, MilliporeSigma) overnight at 4°C to assess myofibroblast phenotype. The next day, coverslips were washed and incubated in secondary fluorophore conjugated 1:500 anti-mouse IgG AlexaFluor 568 (ThermoFisher) for 1 hour. Subsequently, nuclei were stained with 1:10,000 DAPI and coverslips were washed in PBS and mounted onto slides for visualization. Fluorescent images were captured on an Olympus BX41 microscope utilizing cellSens software. CTCF for αSMA expression was calculated as previously

described. Individual actin filaments within the same microscopic plane were measured via cellSens software. A minimum of 10 filament measurements were obtained for individual cells.

Western Blot

Co-cultured fibroblasts were washed in PBS and lysed in buffer containing 20mM Tris, 150mM NaCl, 1mM EDTA, 1% Triton-X, and a cocktail containing protease- and phosphatase inhibitors (ThermoFisher). Protein concentration was determined by Pierce bicinchoninic assay (BCA) (ThermoFisher). Thirty-five micrograms of total protein were loaded onto a 4-15% gradient polyacrylamide gel under denaturing conditions. Following electrophoretic separation, proteins were transferred to a polyvinylidene difluoride (PVDF, MilliporeSigma) membrane. The membrane was then blocked in 5% bovine serum albumin for 1 hour at room temperature, washed thoroughly in tris-buffered saline with Tween 20 (TBST), and incubated in 1:1000 anti-Collagen-1 (Abcam) or αSMA (MilliporeSigma) primary antibody diluted in TBTS overnight at 4°C. The next day, membranes were again washed and then incubated in anti-rabbit or anti-mouse HRP-conjugated secondary antibody for 1 hour at room temperature. Pierce enhanced chemiluminescence solution (ThermoFisher) served as the substrate for detection on autoradiography film. Expression was quantified via densitometry using ImageJ (ver. 1.3); mean expression was quantified from a minimum of three independent experiments.

Statistical analyses

Standard parametric tests including two-tailed student's t tests, one-way or two-way ANOVAs with Bonferonni post hoc analyses compared differences between treatment

groups for normally distributed data using GraphPad Prism (version 7.03, GraphPad Software, La Jolla California, USA). Non-parametric tests including the Mann-Whitney rank sum test for 2 groups and the Kruskal-Wallis test for more than 2 groups were applied in cases where data were not normally distributed. Unless otherwise indicated, data is presented as mean ± standard deviation; significant was accepted at $p \leq 0.05$.

RESULTS

PAR2 expression in primary post-burn HTS fibroblasts is significantly elevated

PAR2 fluorescence intensity is significantly increased in primary post-burn HTS fibroblasts compared to primary non-burned skin fibroblasts (Fig 1a-b). PAR2 expression, reported as mean CTCF, in untreated post-burn HTS fibroblasts ($1.0 \times 10^6 \pm 4.2 \times 10^4$) was significantly greater than untreated non-burned skin fibroblasts ($1.3 \times 10^5 \pm 2.9 \times 10^5$), p<0.001.

Additionally, PAR2 expression increases over time following treatment with the PAR2 activating peptide SLIGKV and expression is significantly elevated compared to SLIGKV treated non-burn controls (Fig 8c-d). Mean CTCF values for non-burned skin fibroblasts remained stable from just prior to SLIGKV activation at $2.0 \times 10^4 \pm 6.2 \times 10^3$ (0 minutes) to $1.8 \times 10^4 \pm 6.1 \times 10^2$ (60 minutes) indicating that receptor expression remains unchanged with PAR2 activation. However, PAR2 CTCF was significantly elevated in primary HTS fibroblasts at each time point compared to PAR2 expression in non-burned skin fibroblasts, peaking at $4.9 \times 10^4 \pm 9.5 \times 10^3$ at 10 minutes following SLIGKV treatment. The CTCF values remained elevated over the 1 hour course of treatment and were significantly higher in HTS fibroblasts compared to either PCS control fibroblasts or

non-burned skin fibroblasts at each time point (p<0.001). This evidence may represent two distinct and phenotypically different fibroblast populations and suggests that HTS fibroblasts, derived from burn survivors, are primed for PAR2 activation by mast cell tryptase. Moreover, PAR2 activation initiates increased receptor expression that may help maintain tryptase sensitization over time in post-burn HTSs.
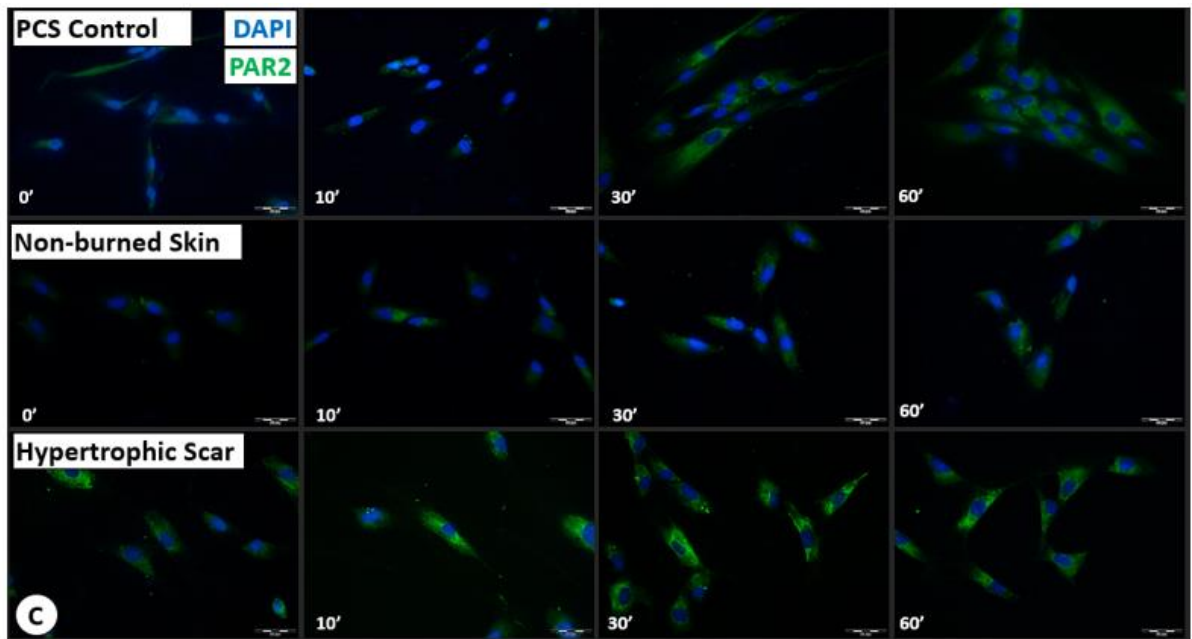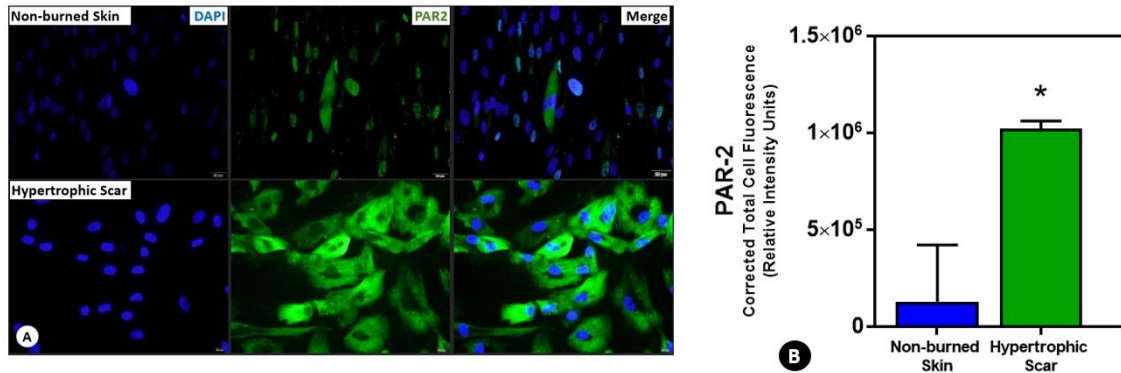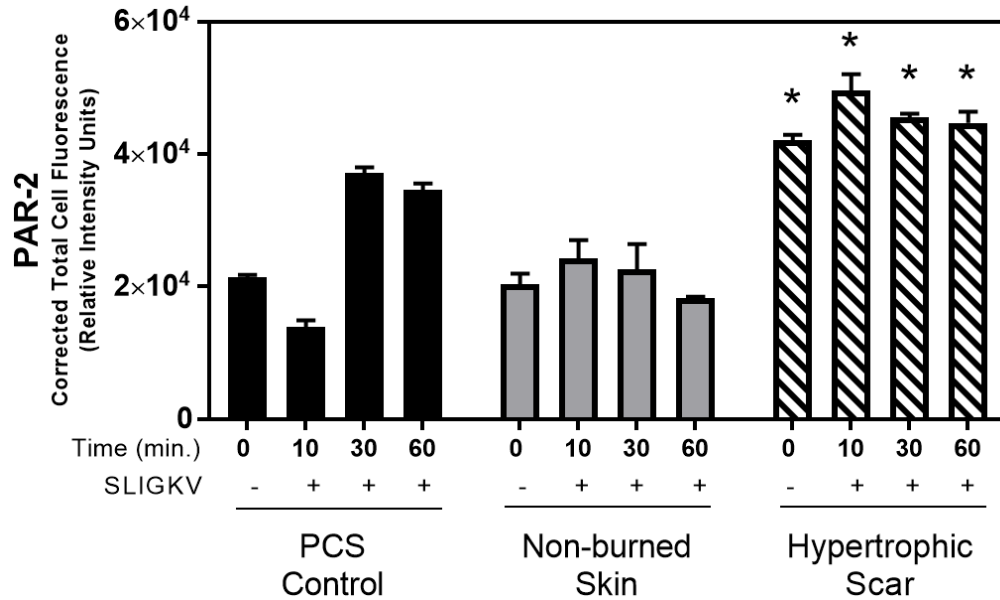
Figure 8: PAR2 expression is increased in hypertrophic scar fibroblasts.
Post-burn hypertrophic scar fibroblasts express significantly increased basal levels of PAR2 (green) compared to non-burned skin fibroblasts (*p<0.0001, t-test) (**A and B**). Scale bar = 20μm. Following SLIGKV treatment, PAR2 expression is elevated and remains consistently elevated after 1 hour in hypertrophic scar fibroblasts. A two-way ANOVA compared mean CTCF values between SLIGKV-treated cell lines at each time point. (**C and D**). CTCF values for HTS fibroblasts were significantly higher, *p<0.001, than CTCF values in PCS control or non-burned skin fibroblasts for each time point tested. Data is presented as mean CTCF ± SD.

PAR2 inhibition significantly reduces tryptase-induced post-burn HTS fibroblast proliferation

Mast cell tryptase treatment increased the proliferative capacity of primary post-burn HTS fibroblasts compared to non-burned fibroblasts. Mean percent proliferation significantly increased in response to tryptase from 84.8 ± 11.8% in non-burned skin fibroblasts to 121.4 ± 13.6% in HTS fibroblasts (Fig 9a, p<0.001). Furthermore, tryptase-induced proliferation was significantly diminished in HTS fibroblasts, from 121.4 ± 13.6%

to 64.2% ± 31.3% (p<0.01) with GB83 pre-treatment. However, the same proliferative reduction did not occur in non-burned skin fibroblasts with PAR2 antagonism.

Mast cell chymase treatment did not affect proliferation in either post-burn HTS fibroblasts or in non-burned skin fibroblasts. Additionally, GB83 pre-treatment did not alter proliferation in either cell line. No significant differences were found in proliferation following chymase or PAR2 antagonism treatment between cell lines (Fig 9b).

Combined tryptase and chymase treatment demonstrated similar results as tryptase treatment alone (Fig 9c). Mean percent proliferation was unchanged from 107.1 ± 16.8% in non-burned skin fibroblasts compared to 121.2 ± 9.2% in HTS fibroblast with combined treatment. Proliferation was considerably reduced in GB83-treated HTS fibroblasts, from 121.2 ± 9.2% to 36.8 ± 33.4% (p<0.001), but not in non-burned skin fibroblasts (107.1 ± 16.8% to 98.1 ± 12.8%).
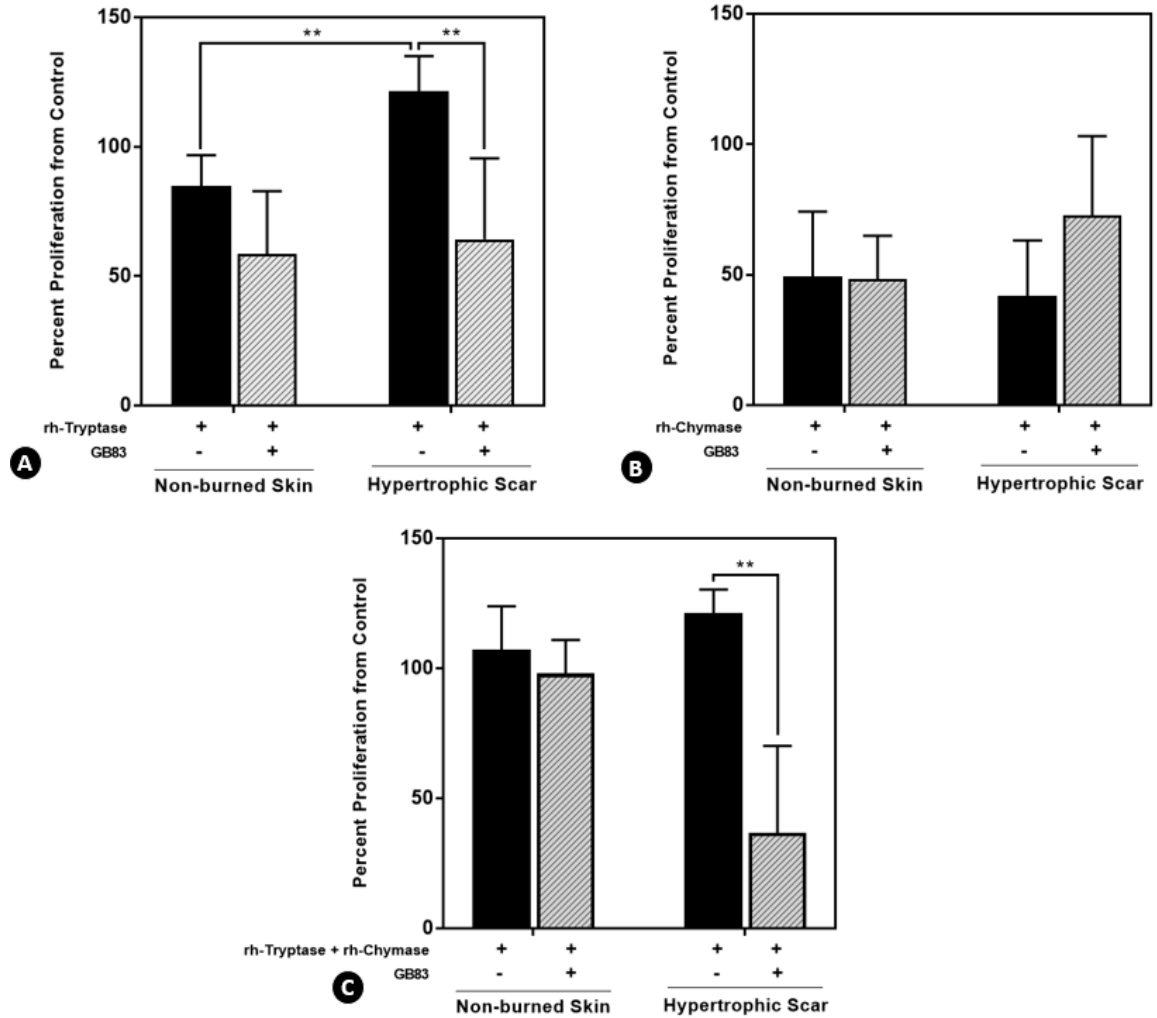
Figure 9: PAR2 blockade reduces hypertrophic scar fibroblasts proliferation.

MTT assays show that mast cell tryptase increases the proliferation of hypertrophic scar fibroblasts compared to non-burned skin fibroblasts. However, PAR2 antagonism by GB83 significantly reduces the tryptase-induced proliferative effect (**A**, **p<0.01). Mast cell chymase or GB83 treatment does not effect the proliferative capacity in ether non-burned skin or hypertrophic scar fibroblasts (**B**). The combination of both mast cell tryptase and chymase treatment did not increase cellular proliferation, however, tryptase-induced proliferation was significantly reduced again in primary hypertrophic scar fibroblasts compared to non-burned skin fibroblasts when cells were pre-treated with the PAR2 inhibitor, GB83 (**C**, **p<0.01). Data is presented as mean percent proliferation from untreated controls ± SD.

Comparable differential proliferative effects between cell lines were also demonstrated in the wound healing scratch assay (Fig 10a). In non-burned skin fibroblasts, open wound gap percent decreased from $92.9 \pm 6.9\%$ to $59.0 \pm 25.6\%$ after 12 hours with SLIGKV treatment. In GB83 pre-treated non-burned fibroblasts, open wound percent decreased to $70.5 \pm 4.5\%$ after 12 hours with SLIGKV treatment. However, there were no significant differences in wound closure with GB83 in non-burned skin fibroblasts (Fig 10b). However, in post-burn HTS fibroblasts, GB83 pre-treatment resulted in $70.7 \pm 7.6\%$ wound closure after 12 hours, but $26.2 \pm 5.7\%$ closure in fibroblasts treated with SLIGKV alone (Fig 10c), a significant difference ($p<0.05$) indicating PAR2 inhibition with GB83 significantly reduces SLIGKV-induced proliferation. Additionally, wound gaps closed only 4.4% in treatment with the inverse peptide VKGILS after 12 hours in non-burned skin fibroblasts and 10.3% in hypertrophic scar fibroblasts, which was significantly less from SLIGKV treatment ($p<0.05$), indicating that SLIGKV is the activating peptide for PAR2, which is consistent with previous studies.[152,153]
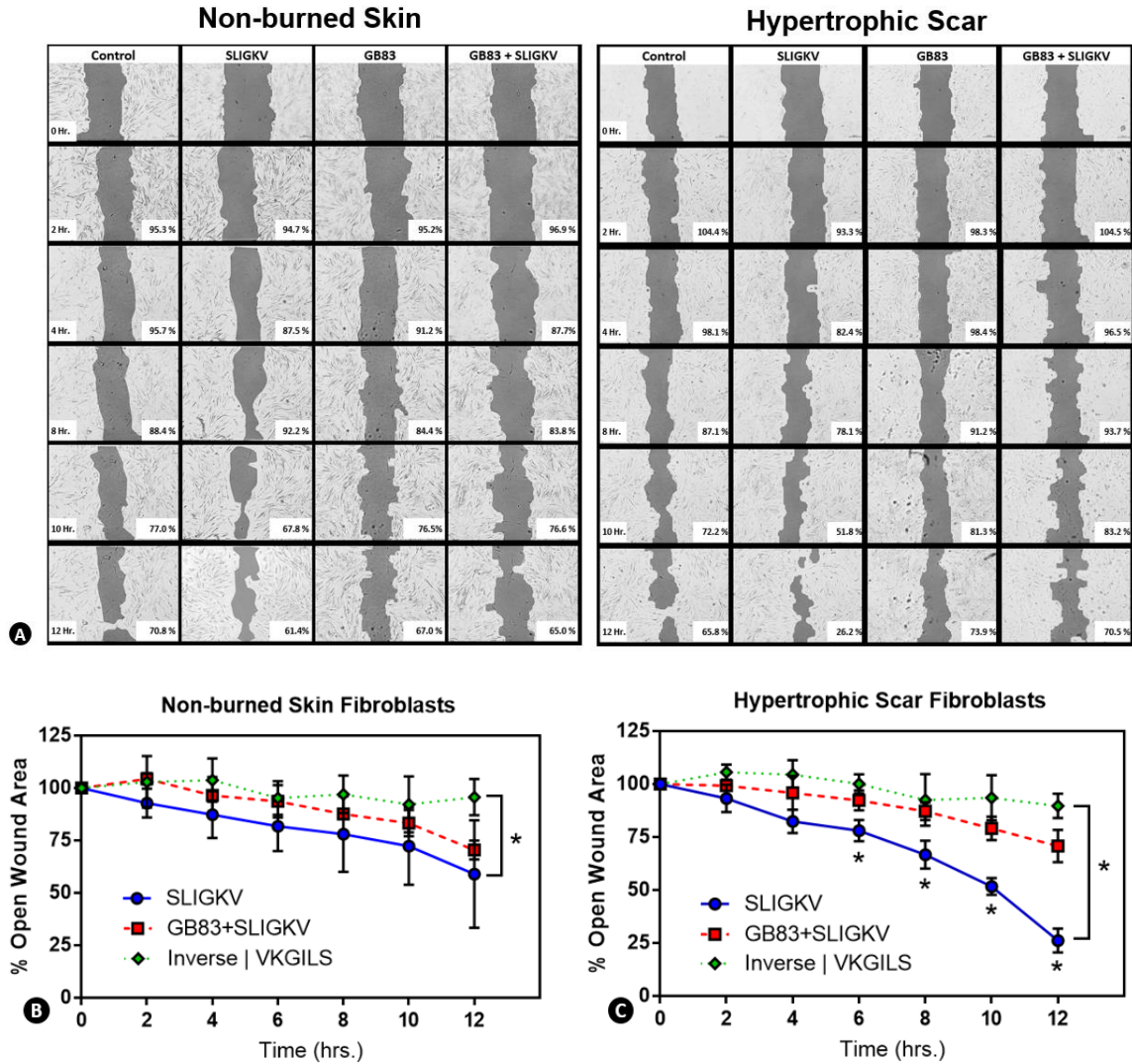
Figure 10: GB83 reduces tryptase-induced proliferation in hypertrophic scar fibroblasts.
Percent wound closure was measured over 12 hours in both non-burned skin and post-burn hypertrophic scar fibroblasts (**A**). Scale bar = 200μm. Scratch assay results show PAR2 antagonism with GB83 does not alter non-burned skin fibroblast proliferation as no difference in wound closure was calculated between treatments at any time point (**B**). However, GB83 pre-treatment significantly impeded wound closure in hypertrophic scar fibroblasts after 12 hours compared to PAR2 activation with SLIGKV treatment alone (**C**, *$p<0.05$). Data is presented as mean % open scratch area from 0 time point ± SD. Treatment with inverse peptide VKGILS did not produce wound closure, indicating SLIGKV is the activating peptide for PAR2.

71

PAR2 activation stimulates fibrotic and proliferative signaling in HTS fibroblasts

Following SLIGKV treatment, PAR2 activation significantly increased mRNA expression of mitogenic and fibrogenic signaling effectors. Expression of PAR2 transcripts increased by almost 2-fold in HTS fibroblasts following PAR2 activation compared with non-burned skin fibroblasts, but this effect was significantly blunted with GB83 pre-treatment ($p<0.01$, Fig 11a). No comparable attenuation was measured in non-burned skin fibroblasts. PAR2 activation is initiated by N-terminal cleavage and endocytosis of the G protein-coupled receptor complex. For re-sensitization, PAR2 must be synthesized de novo; consequently, elevated PAR2 mRNA expression is likely the result of increased signaling. This is confirmed by concomitantly increased β-Arrestin-1. HTS expression of β-Arrestin-1 was increased nearly 5-fold from non-burned fibroblasts ($p<0.01$), but decreased significantly with GB83 PAR2 inhibition (Fig 11b). Elevated β-Arrestin-1 would signify increased receptor internalization suggesting further PAR2 activation and signaling.

Keratinocyte growth factor (KGF) and basic fibroblasts growth factor (bFGF) are important elements in the wound healing cascade conveying mitogenic signaling, specifically during the inflammatory phase. Here, we show two-fold increases in both factors produced in HTS fibroblasts compared to non-burned skin fibroblasts after PAR2 activation with SLIGKV (Fig 11c-d). Both KGF and bFGF mRNA expression was significantly reduced with GB83 pre-treatment ($p<0.01$) suggesting PAR2 inhibition may be critical to reduce fibrotic signaling stimuli.

Vascularity is another essential feature in wound healing. Increased vascularity accompanies initial inflammation and numerous factors contribute to angiogenic signaling,

chief among these is vascular endothelial growth factor (VEGF). SLIGKV-treated post-burn HTS fibroblasts produced an almost 2-fold increase compared with non-burned fibroblast controls, but again, mRNA expression was significantly reduced (p<0.01) with PAR2 blockade back to levels comparable to those produced by non-burned skin fibroblasts (Fig 11e).
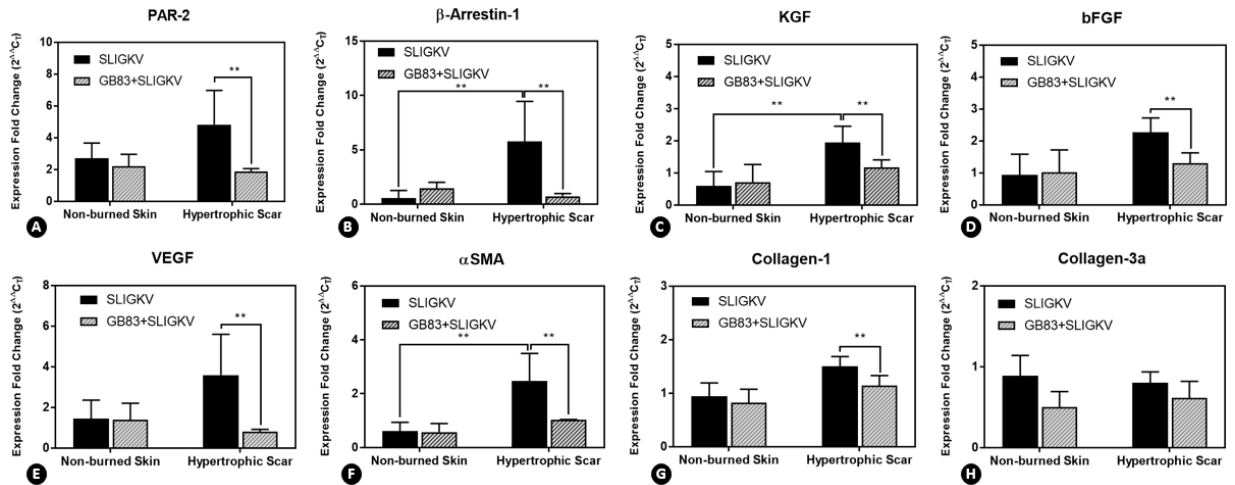
Figure 11:   PAR2 activation stimulates fibrotic and proliferative signaling in HTS fibroblasts.
Quantitative reverse transcriptase polymerase chain reaction results show significantly elevated expression levels of proliferative signaling markers PAR2 (**A**) β-Arrestin-1 (**B**), Keratinocyte Growth Factor (KGF) (**C**), and basic Fibroblast GF (bFGF) (**D**) following SLIGKV activation of PAR2. Similarly, vasoactive vascular endothelial GF (VEGF) mRNA was considerably upregulated (**E**). Furthermore, PAR2 activation also stimulated significantly elevated mRNA expression in the fibrotic markers αSMA (**F**) and Collagen-1 (**G**); however, there were no comparable increases in Collagen-3 (**H**). The proliferative and fibrotic signaling induced by PAR2 was significantly abated by pre-treatment with the PAR2 inhibitor, GB83 in all markers except Collagen-3. These effects only occurred in post-burn hypertrophic scar fibroblasts and not in non-burned skin fibroblasts suggesting fundamental phenotypic differences between burned and non-burned fibroblasts. **p<0.05. Data is presented as mean mRNA expression fold change to control-treated cells ± SD.

In cutaneous scar pathophysiology, increased proliferative and mitogenic signaling contributes to fibrosis with excessive collagen production and subsequent contraction. As a result of this aberrant signaling, normal fibroblasts are converted to myofibroblasts. αSMA is an important indicator of this phenotypic switch. Here, we show αSMA expression is considerably increased 3-fold following PAR2 activation (Fig 11f) in HTS fibroblasts compared to non-burned skin fibroblasts. The SLIGKV-induced increased αSMA expression was abated by PAR2 blockade ($p<0.01$) producing an approximate 4-fold decreased expression. Additionally, GB83 pre-treatment showed similar results in collagen-1 expression, but not in collagen-3 (Fig 11g-h). This data demonstrates differential effects of PAR2 activation between non-burned skin fibroblasts and post-burn HTS fibroblasts *in vitro* and importantly, shows the fibrotic and proliferative-inducing capacity of PAR2 activation by mast cell tryptase can be diminished through PAR2 antagonism.

PAR2 knockdown attenuates fibrotic gene expression in HTS fibroblasts *in vitro*

In the previous set of experiments, we demonstrated that PAR2 activation stimulated elevated mitogenic signaling with accompanying increases in αSMA and Collagen-1 mRNA transcript expression in HTS fibroblasts derived from severely burned children. To ensure that this fibrotic stimulus was initiated through PAR2 signaling, we next treated these fibroblasts with siRNA to reduce PAR2 expression. SLIGKV treatment in control fibroblasts significantly elevated expression of several proliferative and fibrotic genes including PAR2, collagens-1 and 3, αSMA, and matrix metalloproteinases (MMP)-2 and -9 (Fig 12a-f). All mRNA targets were significantly elevated in comparison to

74

control-treated cells by at least 1.5-fold (p<0.01). Similar expression increases were shown following PAR2 activation with SLIGKV in HTS fibroblasts pre-treated with scrambled siRNA for PAR2. Expression of mRNA transcripts for all proliferative and fibrotic targets was significantly decreased in HTS fibroblasts pre-treated with siRNA to PAR2 alone. Furthermore, expression of PAR2, collagens-1 and 3, αSMA, and MMP-2 and -9 was decreased by at least 2-fold (p<0.01) even after SLIGKV treatment in HTS fibroblasts with PAR2 knockdown via siRNA, confirming PAR2 activation is important in the initiation of signaling necessary for post-burn wound healing and HTS progression. The siRNA to PAR2 was specific to only this isoform as mRNA expression for PARs -1, -3, and -4 was not significantly altered from control (Fig 12g-j). PAR2 expression was significantly diminished (p<0.05) at all siRNA concentrations tested (Fig12h). Supplemental figure 16 shows PAR2 protein expression was considerably decreased, confirming qRT-PCR results.
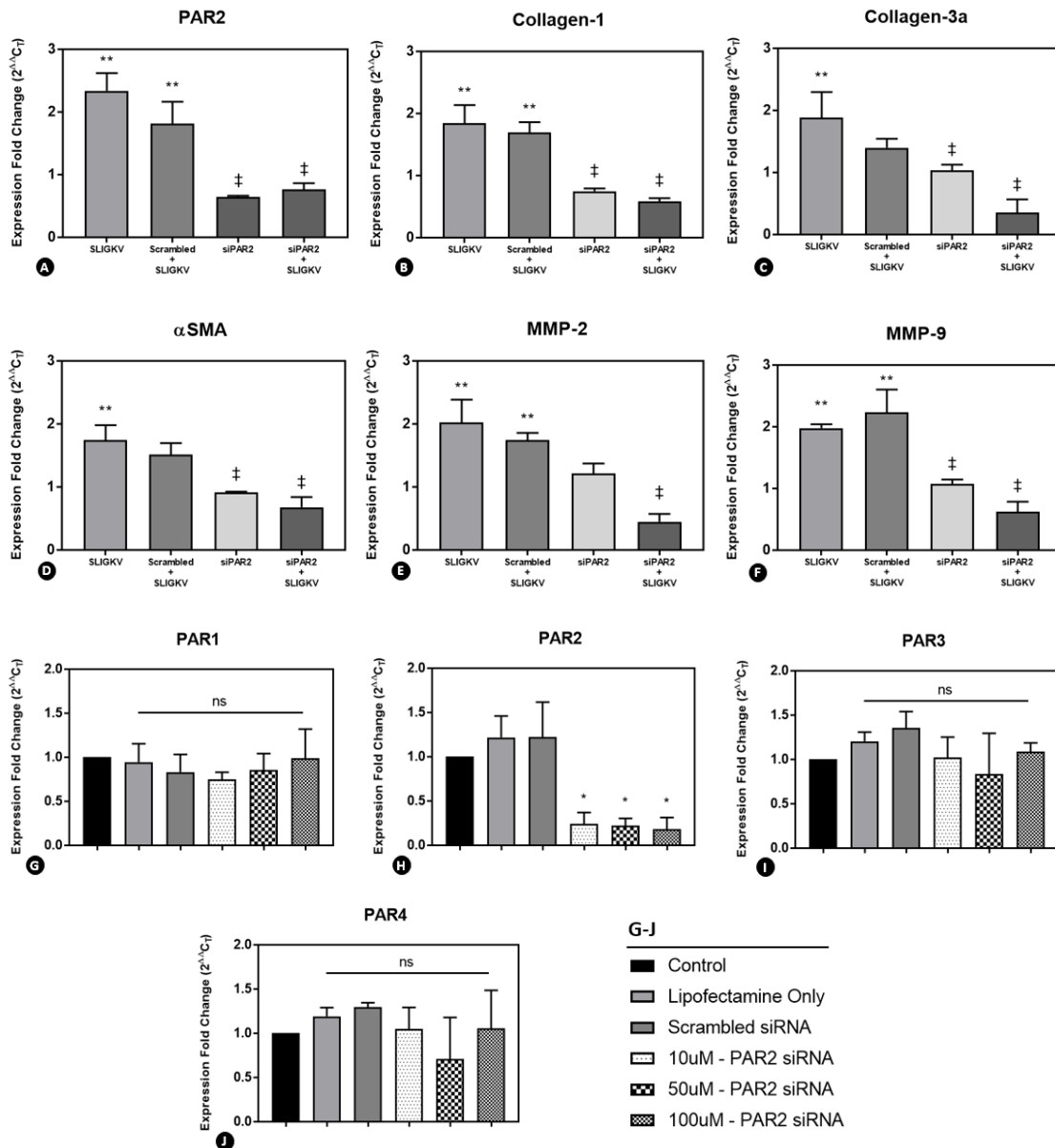
Figure 12: PAR2 knockdown attenuates fibrotic gene expression in HTS fibroblasts *in vitro*.
Primary post-burn hypertrophic scar fibroblasts were pre-treated with 50μM siRNA to PAR2 for 72 hours followed by 1 hour treatment with 10μM PAR2 activator SLIGKV. qRT-PCR results show significantly increased expression of several important fibrotic markers (*p<0.01 compared to DMEM-treated controls) following SLIGKV treatment including PAR2, Collagens-1 and -3, α-αSMA and martrix metalloproteinases(MMP)-2 and -9 (**A-F**). However, SLIGKV-increased transcriptional expression of all fibrotic markers was also significantly decreased with siRNA to PAR2 pre-treatment (‡p<0.01 to SLIGKV or Scrambled+SLIGKV treatment). Synthesized siRNA to PAR2 was specific only to PAR2 and no other PAR isoform as transcriptional knockdown was measured only in PAR2 (**G-J**). Scrambled = random sequence siRNA to PAR2.

PAR2 antagonism reduces the fibrotic phenotype in HTS fibroblasts co-cultured with human mast cells

A co-culture approach was then used to elucidate possible paracrine interactions between mast cells, their released factors, and primary dermal fibroblasts on subsequent fibrotic signaling; Non-burned skin and HTS fibroblasts were immunostained for αSMA (Fig 13a). αSMA expression and filamentous(F-)actin length were increased in control, non-burned, and HTS fibroblasts following treatment with either degranulation of co-cultured mast cells (Active MC) or culture with conditioned media from activated mast cells (MC Con Med) compared to non-treated (2-10% DMEM only) control cells (Fig 13b-c). Expression of αSMA was highest in HTS fibroblasts with both Active MC and MC Con Med treatments, 4.3×10^6 and 4.5×10^6, respectively, compared to non-burned skin fibroblasts with the same treatments, $3. \times 10^6$ and 3.9×10^6 relative expression ($p<0.05$). Additionally, F-actin length was similar across all cell types with treatment, averaging approximately 20-22μm. Importantly, this myofibrotic conversion was considerably diminished ($p<0.001$) with PAR2 inhibition via GB83 pre-treatment in all cell types. Mast cell-induced αSMA expression was most significantly decreased in HTS fibroblasts, declining from 4.5×10^6 with MC Con Med to 2.4×10^6 and 4.3×10^6 to 2.2×10^6 with Active MC alone, a 2-fold decrease in relative expression. A decline in αSMA expression with PAR2 inhibition was confirmed by significant decreases in F-actin length across all cell types ($p<0.001$), again with the most significant reductions in HTS fibroblasts. F-actin was reduced from 20.9 ± 7.3μm in MC Cond Med-treated HTS fibroblasts to 8.8 ± 2.7μm with GB83 pre-treatment. Additionally, F-actin length decreased from 23.2 ± 6.4μm to

15.1 ± 6.5μm in Active MC-treated HTS fibroblasts pre-treated with GB83 indicating PAR2 inhibition impeded transition into myofibroblasts.
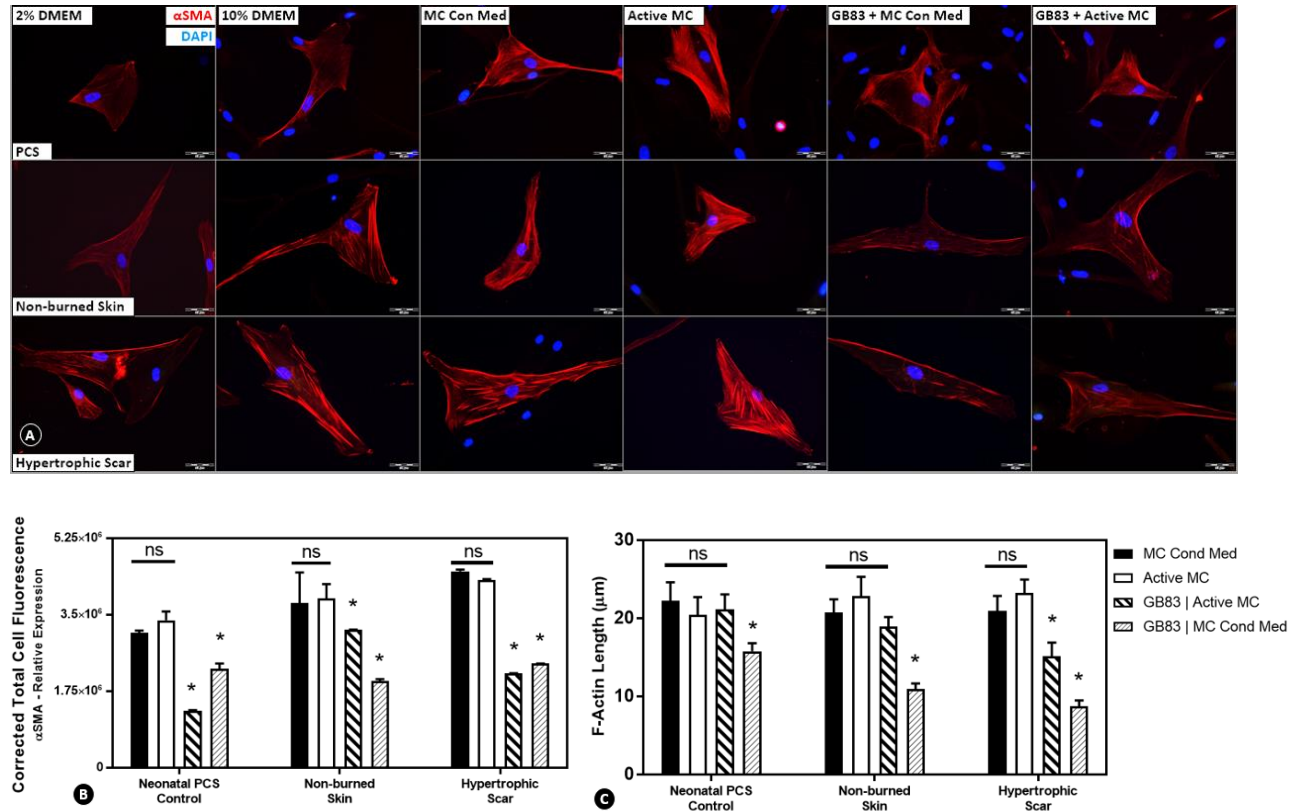
Figure 13: PAR2 blockade reduces myofibrotic phenotype in post-burn hypertrophic scar fibroblasts.

Representative images (**A**) show immunostained hypertrophic scar fibroblasts for αSMA (red) treated with 2% or 10% serum-supplemented DMEM, activated mast cell conditioned media (MC Con Med), or activated mast cells (Active MC) (columns 1-4). Cells were also pre-treated with the PAR2 inhibitor GB83 for 2 hours prior to treatment with either MC Con Med or Active MC (columns 5-6). Cell nuclei were stained with 4′,6-diamidino-2-phenylindole (DAPI, blue). αSMA expression, as quantified by CTCF, was increased in all cell lines with MC Cond Med or Active MC alone, most notably in hypertrophic scar fibroblasts. CTCF expression was significantly reduced with PAR2 blockade in all cell lines (**B**). Additionally, filamentous(F-) actin length was concurrently decreased with GB83 pre-treatment (**C**) indicating PAR2 blockade effectively reduces a myofibrotic phenotype in fibroblasts.

Similarly, both Active MC and MC Con Med treatment increased fibrotic signaling in HTS fibroblasts. Expression of mRNA transcripts for PAR2, αSMA, MMP-1 and -2, and collagens-1, -3, and -5 was elevated in HTS fibroblasts during co-culture conditions compared to TGF-β1-treated controls. Mast cell-induced proliferative and fibrotic gene expression was significantly suppressed with GB83 treatment (Fig 14a-e); PAR2 and αSMA mRNA transcripts were reduced by 2-fold ($p < 0.05$), whereas MMP-1, -2, collagens-1, -3, and -5 were decreased by up to 4-fold ($p < 0.01$).
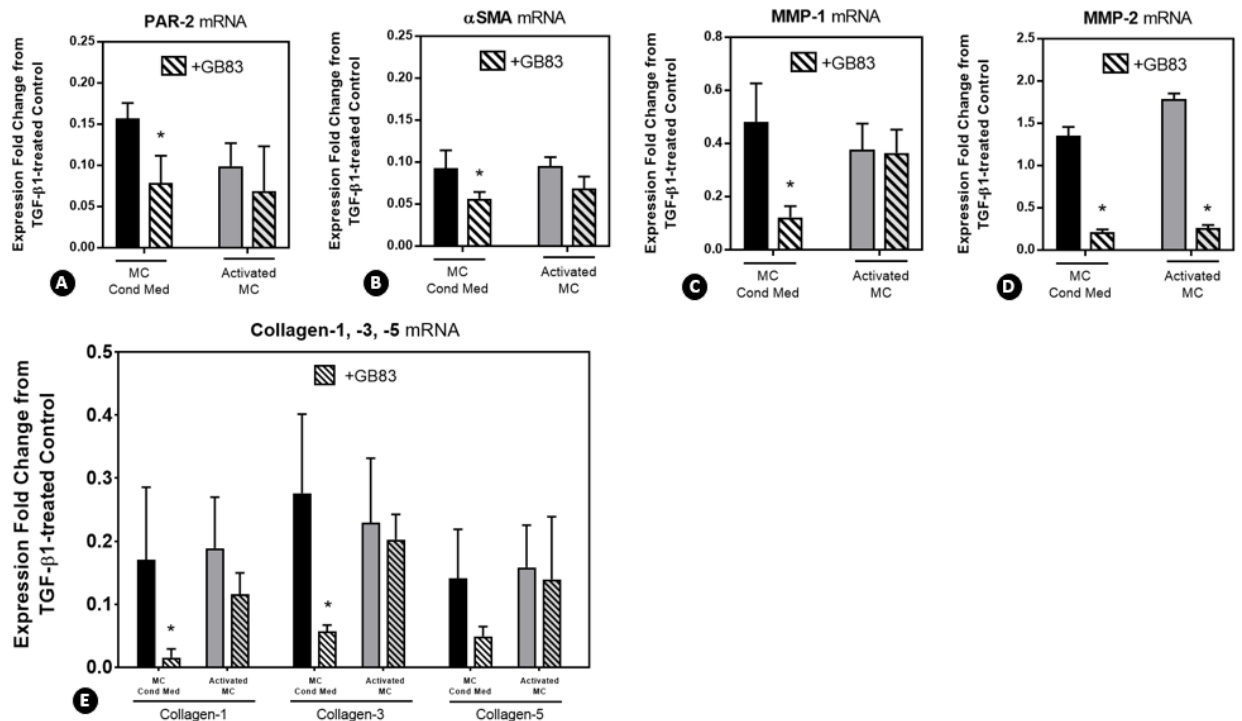
Figure 14: Mast cell-induced fibrotic phenotype is reduced with PAR2 antagonism in hypertrophic scar fibroblasts *in vitro*.
Activated mast cell conditioned media (MC Cond Med) or activated mast cells (Activated MC) alone co-cultured with post-burn hypertrophic scar fibroblasts caused elevated expression of several proliferative and fibrotic genes. However, PAR2 blockade with the synthetic molecule GB83 significantly diminished mast cell-induced expression of PAR2 (**A**), αSMA (**B**), matrix metalloproteinases-1 and -2 (MMP1, -2, **C,D**) and collagens-1 and -3, but not collagen-5 (**E**) in hypertrophic scar fibroblasts. *$p < 0.05$ compared to TGF-β1-treated control fibroblasts.

79

These results were further confirmed as mast cell-induced expression of αSMA and collagen-1 protein was blunted with GB83 pre-treatment (Fig 15a-b). Compared to TGF-β1-treated controls, HTS fibroblasts treated with MC Con Med or co-cultured with Active MC produced equivalent amounts of collagen-1 (Fig 15a) and αSMA (Fig 15b) protein. However, when pre-treated with GB83, then subsequently treated with either Active MC or MC Con Med, HTS fibroblasts produced significantly less collagen-1 (4-fold decrease, $p < 0.01$) and αSMA (4-fold decrease, $p < 0.05$), further confirming that PAR2 blockade can reduce a myofibrotic phenotype in post-burn HTS fibroblasts.
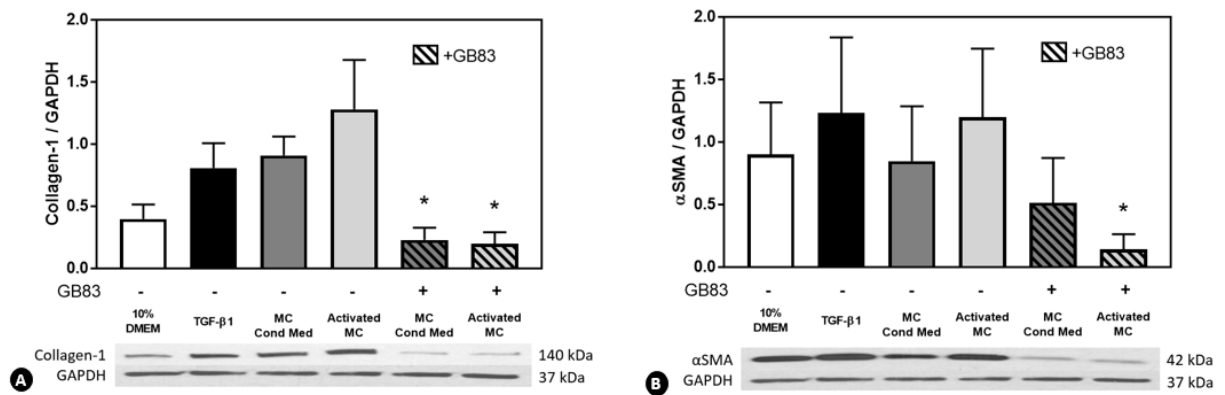
Figure 15: **GB83 reduces protein expression of collagen-1 and α-SMA in post-burn hypertrophic scar fibroblasts.**
Primary post-burn hypertrophic scar fibroblasts were pre-treated with PAR2 inhibitor GB83 prior to co-culture with either activated mast cell media or activated mast cells alone. Following 1 hour of co-culture, protein expression of collagen-1 and αSMA are significantly elevated. However, PAR2 blockade reduced the fibrotic expression (**A and B**) indicating PAR2 activation via mast cell tryptase contributes considerably to fibrosis in post-burn hypertrophic scar pathophysiology. *$p < 0.05$, expression is significantly reduced from TGF-β1-treated controls; samples were normalized to GAPDH.
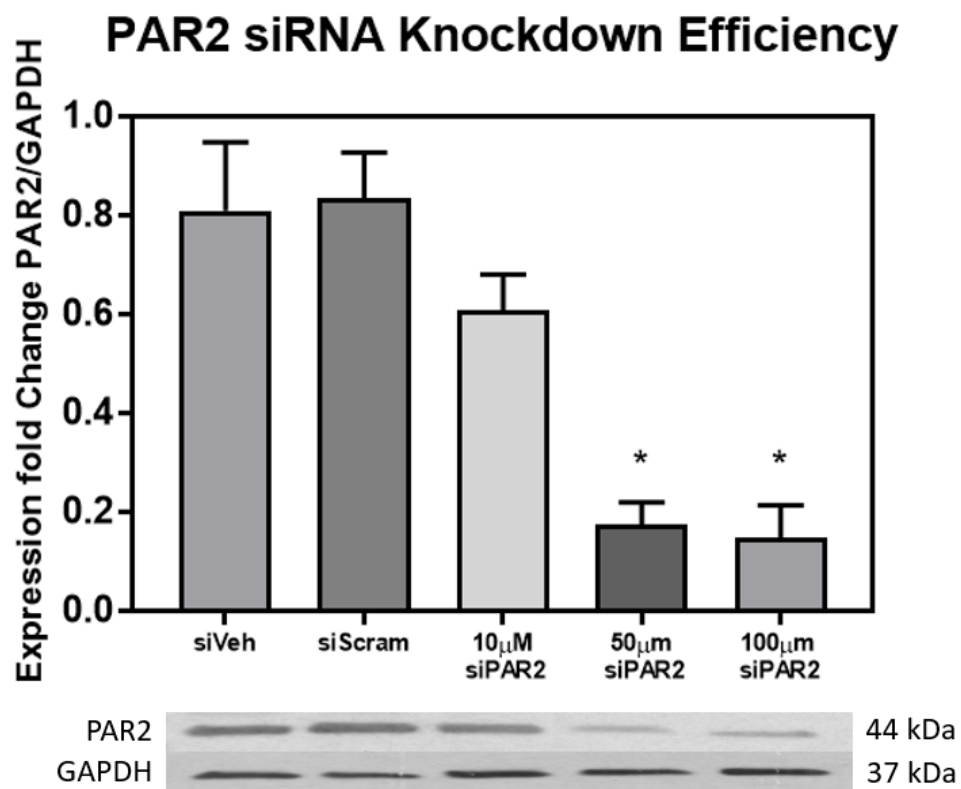
Figure 16: **PAR2 siRNA efficiently knocks down PAR2 protein expression.**
PAR2 expression is significantly reduced at PAR2 siRNA concentrations ≥50μM in this immunoblot for
PAR2 following 72 hours treatment. Expression was normalized to GAPDH. siVeh = siRNA Vehicle,
lipofectamine; siScram = Scrambled siRNA control.

DISCUSSION

Severe burn injury is a devastating and traumatic event that has lifelong emotional and physical consequences. Painful and pruritic HTS develop in up to 70% of burn survivors[4,97,154,155] with massive full-thickness injury and are much more prevalent in children than in adults.[156] The wound healing cascade following burn injury is a complex process classically defined by three overlapping phases that involve a multitude of interactions among numerous cell populations: inflammation, proliferation, and remodeling. The initial inflammatory phase lasts approximately 3-4 days and begins immediately following hemostasis. Neutrophils are attracted to wound sites by elevated concentrations of TGF-β and complement protein, and act to clear necrotic tissue and phagocytize bacteria to prevent systemic infection.[12] Post-burn neutrophil secretory profiles show significantly elevated IL-1 and IFN-γ along with other dynamic growth factors that serve as stimuli for macrophage migration during the proliferation phase.[157] Macrophages not only engulf depleted neutrophils but also serve as reservoirs for potent cytokines that direct continued wound healing and influence infiltrating lymphocytes. However, these inflammatory phase cytokines remain elevated up to 5 weeks after initial injury in severely burned children,[22] which protracts the inflammatory and proliferation phases for weeks and results in aberrant development of deep dermal fibroblasts.[158]

The cellular and molecular basis for post-burn scarring has been well defined, yet, mast cells remain a noticeably understudied cell population in the wound healing literature, and there is limited evidence suggesting mast cells as potential moderators in post-burn HTS progression. However, mast cells are clearly implicated in many non-cutaneous scarring pathologies and are found in greater numbers within adult hypertrophic scar

tissue.[20]   Concordantly, we have shown significantly elevated mast cell density and dissemination throughout dermal layers in pediatric HTS tissue up to 2 years post-burn with concomitantly increased serum tryptase levels up to 6 months post-burn. Shiota *et al.* demonstrated that active mast cells in hypertensive cardiac tissue upregulated *de novo* production of profibrotic growth factors that induced cardiac fibrosis.[16] More recent evidence has shown that pulmonary fibrosis fails to develop in mast cell deficient mice suggesting a causal link between mast cells and fibrotic pathogenesis.[17]

Mast cells exert influence through release of pre-formed or *de novo* synthesized mediators and chief among these is the potent serine protease tryptase. Elevated serum tryptase levels occur in mice with ventilator-induced lung fibrosis.[138] Furthermore, tryptase exposure enhanced the proliferative and fibrogenic capacity of primary human lung fibroblasts and increased the collagen production of fibrocytes *in vitro* through PAR2 activation.[65,159]

In the present study, we showed significantly elevated PAR2 expression in post-burn HTS fibroblasts after receptor activation with SLIGKV treatment. The data confirms signaling re-sensitization via *de novo* PAR2 expression over time. Moreover, we also demonstrated a differential PAR2 profile in non-burned skin fibroblasts where PAR2 expression remained unchanged over time with or without receptor activation. Importantly however, PAR2 expression was significantly increased in HTS fibroblasts without SLIGKV stimulation (basal expression), demonstrating a distinct phenotypic difference between non-burned skin fibroblasts and post-burn HTS fibroblasts and further suggests that burn injury may prime wound fibroblasts for PAR2 signaling. Several studies have previously established important phenotypic differences in fibroblast populations

attributed to burn trauma. El Ayadi *et al* showed that β-adrenergic receptor expression, localization, and degradation was significantly altered in burn wound fibroblasts resulting in modified catecholamine signaling that may account for part of the over exuberant fibrotic response after a severe burn.[5] Zhang and colleagues (2012) showed that HTS fibroblasts express elevated levels of Smurf2 protein, associated with increased TGF-β1 mediated fibrosis.[160] Others have revealed adverse and differential responses to cytokines in post-burn fibroblasts compared to their non-burned counterparts.[161,162] It is our understanding that this is the first study to show distinct PAR2 expression differences between non-burned skin fibroblasts and HTS fibroblasts. Ultimately, these differences aberrantly affect dermal fibroblast responses to stimuli and have devastating consequences in HTS progression. Interestingly, we also show increased PAR2 expression in neonatal fibroblasts (PCS control), which may indicate a functional role for PAR2 activation during dermal remodeling as is consistent with neonatal skin formation.

In addition to expression differences, the current study also demonstrated functional proliferation differences between fibroblast populations. We showed that tryptase treatment significantly increased proliferation almost 2-fold in post-burn HTS fibroblasts compared to non-burned skin fibroblasts, but importantly, proliferation could be effectively blunted through PAR2 antagonism with GB83. GB83 is a small molecular weight synthetic compound that is a specific and potent inhibitor of PAR2.[152] Although PAR2 activation induces significant proliferation in epidermal keratinocytes,[163,164] effects on signaling in dermal fibroblasts are largely unknown. Other investigations have suggested that the other major serine protease, chymase, has proliferative potential. Several studies have demonstrated that mast cell chymase promotes cellular proliferation

independent of PAR2 activation.[54] Recent enzymatic evidence demonstrates that chymase can directly cleave and activate stromelysin and collagenase MMPs.[125,126] These data indicate chymase's potential to indirectly influence proliferation by aiding in ECM reconstruction and reducing dermal fibroblast contact inhibition, thereby, creating a conducive environment for growth and proliferation. Only one investigation has exhibited the potential for chymase activation of PAR2. Groschwitz *et al* indicated that chymase increased MAPK expression and activity in intestinal epithelial cells solely through PAR2 activation; [165] however, other studies have failed to confirm chymase's ability to activate PAR2. Moreover, contradictory results show chymase has no proliferative potential in fibroblasts. Indeed, chymase inhibited proliferation of airway epithelia by enzymatically reducing CD44 contact with pericellular matrix.[127] Similarly, other studies have shown that chymase has no effect on calcium mobilization in fibroblasts – including that induced by tryptase, which implicates PAR2 activation.[166] In the present study, we have demonstrated that chymase treatment alone did not induce proliferation or increase metabolism in either fibroblasts from non-burned skin or HTS. Tryptase-induced dermal fibroblasts proliferation may contribute to the injurious consequences of post-burn HTS.

Results from functional wound healing assays confirm the PAR2-dependent proliferative effect of tryptase. We show that PAR2 antagonism with GB83 pre-treatment significantly reduced SLIGKV-induced proliferation in HTS fibroblasts prevented closure of the artificial wound in scratch assays; SLIGKV treatment alone, however, rapidly closed the scratch by almost 75% after 12 hours. Artificial wounds were only closed approximately 40% in SLIGKV treated non-burned skin fibroblasts, further demonstrating functional differences in addition to the phenotypic differences between fibroblast

populations. This has important implications in post-burn and general wound healing. Whereas rapid wound closure is evolutionarily beneficial, excessive proliferation is considered pathologic and significantly promotes scar formation. In the present study, GB83 blockade of PAR2 activation decreased excessive proliferation in our *in vitro* investigations. PAR2 antagonism may result in returning the wound environment back to a more normal physiologic state which would be beneficial to reduce post-burn HTS.

Gene and protein expression profiles are also significantly altered in dermal fibroblasts following severe burn injury. Fibroblast inflammatory cytokine profiles are known to be severely deranged acutely following burn injury,[167] an effect thought mainly induced by catecholamine surges and increased TGF-β signaling. Protracted aberration of mitogenic fibroblast signaling is a critical underlying cause of post-burn HTS formation. PAR2 activation is part of this detrimental cascade that stimulates mitogenic signaling through ERK phosphorylation and targeted activation of MAPK intermediates, which ultimately induces expression of fibrotic markers and modulators of ECM.[146] In the present study, we show increased SLIGKV-induced expression of KGF, FGF, αSMA and collagen-1 mRNA in HTS fibroblasts. KGF and FGF are potent growth factors that are able to stimulate enhanced proliferation and fibrotic output in an autocrine fashion,[168,169] whereas collagen-1 overproduction contributes directly to fibrosis. Most importantly however, PAR2 antagonism attenuated SLIGKV-induced expression of these proliferative and fibrotic markers, restoring a normal fibroblast phenotype. Similar results observed upon transcriptional PAR2 knockdown *in vitro* confirmed that limited PAR2 activation may minimize mast cell-induced fibrosis after severe burn injury.

Increased vascularity is another important hallmark of HTS pathology and is associated with scars that are more active. Sustained increases in VEGF bolster this effect and serve to initiate endothelial cell proliferation and vascular structure formation. Critical studies have shown that VEGF neutralization decreased fibrotic scarring in adult wounds and that fetal wounds were less vascular, due to inherently reduced VEGF levels, and healed scar-free.[135] Previous investigations have also shown that tryptase exposure enhanced the production of VEGF in fibrotic chondrocytes.[63,123] Similarly, in the present study, we show that PAR2 activation by SLIGKV significantly elevated VEGF expression by HTS fibroblasts compared with non-burned skin fibroblasts, and PAR2 blockade diminished the response considerably. Reducing pathological angiogenesis in the burn wound is considered fundamental to reduce scarring.

Myofibroblast transdifferentiation is another important manifestation in HTS pathogenesis. Myofibroblasts secrete significantly greater amounts of ECM and provide the initial contractile force to pull the wound edges together. However, aberrant wound healing following burn injury reinforces myofibroblast dysregulation, contributing greatly to post-burn HTS development. Numerous mechanisms driving this critical change have been proposed; however, increased αSMA expression is the identifying feature. αSMA is abundantly expressed in HTS fibroblasts and is functionally responsible for HTS contraction clinically.[170] In the present study, both mast cells and their activated conditioned media, cultured directly with post-burn fibroblasts, significantly elevated αSMA expression by the fibroblasts. Tryptase activation of PAR2 is thought to increase αSMA expression through MAPK signaling as well as to induce increases in β-arrestin expression, allowing filamentous actin arrangement.[171] PAR2 inhibition reduced

expression of αSMA, decreasing fiber length even in the presence of actively degranulating mast cells. Moreover, mast cell-induced αSMA and collagen-1 expression *in vitro* was reduced as well, both at the mRNA and protein levels, supporting previous evidence that PAR2 blockade can reduce the fibrotic phenotype of burn wound myofibroblasts.

Overall, this investigation identified a central role for mast cells during post-burn wound healing and confirmed MAPK-mediated upregulation of fibrotic phenotype in HTS fibroblasts. Through paracrine interactions, we demonstrated that these effects were induced by mast cell tryptase activation of PAR2. This evidence provides a potential mechanism that mast cell degranulation may contribute directly to HTS progression through continued expression and activation of this important receptor. Most importantly, we show that tryptase-induced fibrotic stimulus can be attenuated through PAR2 blockade. Although numerous post-burn HTS treatment options exists, most are expensive and require therapy that lasts for years. With future investigations, suppression of this paracrine axis through targeted PAR inhibition might provide a beneficial adjunct therapy to reduce HTS following a severe burn injury.

CHAPTER 4: TOPICAL MAST CELL STABILIZER CROMOLYN SODIUM REDUCES POST-BURN HYPERTROPHIC SCAR FIBROSIS IN THE FEMALE RED DUROC PIG

INTRODUCTION

The majority of severe, full-thickness burn wounds result in extremely debilitating and disfiguring hypertrophic scars (HTS). These scars are a major source of itch and pain that critically affect function and are notoriously difficult to treat. Although treatment options such as corrective surgeries, compression garments, and ablative lasers show promise, long-term efficacy is limited and scars persist for years.[4,172,173] Complex molecular mechanisms that regulate post-burn scar pathogenesis have been identified, but have yet to be translated into viable clinically therapies. The lack of success in human trials coupled with the paucity of post-burn tissue samples have led investigators to use human cell cultures and animal models to study human HTS. Consequently, recent investigations have focused on new cellular targets and signaling pathways to uncover novel treatment approaches that may alleviate post-burn HTS.

The immune system plays a major role in the response to burn injury by triggering sustained inflammation. After initial hemostasis, macrophages and T lymphocytes are stimulated to release an abundance of pro-inflammatory cytokines to attract neutrophils and monocytes to the burn wound. These cell populations are essential during wound healing and are critical regulators of fibrosis that drive pivotal changes in dermal fibroblasts.[174,175] Manipulations of these cell phenotypes or their secretomes have shown limited success in reducing inflammation or fibrosis.[176,177] Despite mast cells having been

linked to fibrosis, their role in post-burn fibroproliferative pathogenesis is not well understood.

Mast cells are of hematopoietic origin and play important roles in both innate and adaptive immunity. In addition to protecting against pathogens including bacterial infections and,[132,178] mast cells serve as sentinels and are located in large numbers in tissues with proximity to the external environment such as the skin and lungs. These highly versatile cells are principally identified as mediators of hypersensitivity or allergic reactions, but their presence and activity have been documented in several disorders including hepatic ischemia,[179] hypertensive cardiac disease,[180] and even cancer.[181] Moreover, previous studies have demonstrated increased mast cell numbers in the HTS of adults[20] and children[19] with concomitantly elevated histamine metabolites during scar progression.[122] There is now considerable evidence confirming that mast cells have major impacts in fibrogenesis.[18,182]

Several factors released by mast cell degranulation may be responsible for induction of fibrosis. The vasoactive amine histamine is produced in large quantities by mast cells and promotes fibroblasts proliferation and increases collagen synthesis.[183,184] *De novo* synthesis of prostaglandin-2 and leukotriene C4 enhances fibroblast proliferation *in vitro* and also increases the collagen expression of pulmonary fibroblasts.[72] Furthermore, studies have demonstrated that mast cell chymase can convert pro-collagen-1 to collagen-1 and directly activate latent TGF-β,[53,185] the inflammatory cytokine known to sustain fibrotic signaling. However, mast cell tryptase is the most abundant stored protease[186] and may have the greatest direct effect, driving fibrotic pathologies.

Unlike chymase, mast cell tryptase has been shown to promote angiogenesis by activating endothelial cells[62] and significantly reducing skin fibroblast apoptosis.[123] Of all released factors, only tryptase has demonstrated a consistent ability to induce myofibroblast differentiation.[187] Myofibroblasts produce significantly more collagen than other fibroblasts, contribute directly to wound contraction, and are the defining phenotype in post-burn HTS. Mast cell tryptase directly cleaves protease-activated receptor-2 (PAR2) on dermal fibroblasts, which we have shown to be significantly upregulated in HTS fibroblasts from pediatric burn patients.[188] PAR2 signaling promotes fibroblast proliferation and significantly induces myofibroblast differentiation,[189] further suggesting that the mast cell tryptase-fibroblast paracrine axis contributes to post-burn HTS progression. Together, this ample evidence suggests that, given the involvement of mast cells in the development and persistence of scarring, pharmacologic mast cell stabilization may provide a viable anti-scarring intervention following severe burn injury.

Cromolyn sodium (CS) is a small, 500 Dalton synthetic compound that has been FDA-approved for over two decades as a mast cell stabilizer. Although the mechanism of action remains unclear, evidence suggests that the compound interrupts mast cell plasma membrane and endoplasmic reticulum calcium (Ca^{2+}) channels.[190,191] Inhibiting this ionic flux impedes vesicle transport and fusion to the cellular membrane. This ultimately obstructs vesicle exocytosis and blocks mast cell degranulation. CS demonstrates broad anti-inflammatory properties with very low toxicity at high doses and is safely prescribed to prophylactically manage symptoms associated with mast cell disorders such as mastocytosis. Several clinical trials have demonstrated the efficacy of CS for reducing pruritus associated with atopic dermatitis[192] and symptoms associated with atopic

eczema.[193] However, stabilization of cutaneous mast cell localized to post-burn HTSs has not been explored.

To investigate the anti-fibrotic effects of the mast cell stabilizer CS, we utilized the red Duroc pig model of HTS. Several animal models have tried to recapitulate human HTS with limited success, but current evidence shows the red Duroc as a reliable model to reproduce HTS most similar to human pathology, especially following burn injury.[194,195] In the current study, we show for the first time that topical application of CS, localized to HTS tissue, may be a beneficial treatment to reduce fibrosis following burn injury.

METHODS

Post-burn hypertrophic scar model in the female red Duroc pig

Animals: The institutional Animal Care and Use Committee of the University of Texas Medical Branch-Galveston (UTMB) approved all protocols. Healthy female red Duroc pigs (N=6) weighing 10-40 kg were acquired from the University of Texas MD Anderson center (Bastrop, Texas) and were socially housed at UTMB with free access to food and water. Animals were acclimatized for one week and were fasted for eight hours before all surgical procedures.

Burn wound: Prior to surgery, animals received a combination cocktail of telazol, ketamine, and xylazine (TKX, 0.25 mL/kg) for pre-procedural anesthesia. The dorsum of the animal was then shaved and scrubbed with betadine antiseptic. Following intubation, 1-5% inhaled isoflurane was continuously administered throughout the procedure. A brass block, heated to 200°C,[196] was applied for 40 seconds at 0.04kg/cm^2 to create 6.5 cm^2 full thickness 3rd- degree burns spaced evenly apart, bilaterally on the dorsum of the animal. After completion of the procedures, animals were extubated and provided intensive acute

care until ambulating and respiring normally. Animal subjects were then transferred to individual housing to maintain wound sterility. Wounds remained uncovered until excision and grafting procedures were performed the next day. Animals were administered buprenorphine-sustained release (SR, 0.6 mg/kg, q. 72 hours) for continuous pain control. Short-acting Buprenorphine (0.02 mg/kg) was administered as needed to relieve acute pain.

Excision and autograft: To simulate clinical care as practiced at our institution, excision and grafting procedures were conducted 24 hours following burn injury. Animals received anesthesia and analgesia as before and wounds were scrubbed with betadine solution. Individual wounds were tangentially excised down to viable tissue using a cold scalpel and then were electrocauterized to achieve hemostasis. Excised wounds were frozen and fixed in formalin for later analyses; histological evaluation of each excised wound confirmed a full-thickness burn. Split-thickness autologous donor skin (500-700μm) was then obtained by pneumatic dermatome (Integra, Plainsboro, NJ, USA) bilaterally from the non-burned thigh. Donor skin was aseptically meshed 1:4 and trimmed to match the wounds to be grafted, positioned on each wound bed, and stapled in place to the non-burned edges creating a split-thickness skin graft (STSG) (Supplemental Fig 1A-C). Wounds were dressed in sterile oil-emulsion gauze and surgical non-adhesive absorptive padding, then wrapped in elastic bandages that would not impede movement. Dressings were removed and wounds were debrided at 2, 5, 7, and 14 days post-burn to prevent infection and to promote wound closure. Complete closure of all wounds occurred approximately 3 weeks after initial injury for each animal. Healed wound fields remained open throughout the study. Porcine HTS morphologically resembling human HTS

93

developed and progressed throughout the experiment (Supplemental Fig 1D). Animals were euthanized after 4 months.
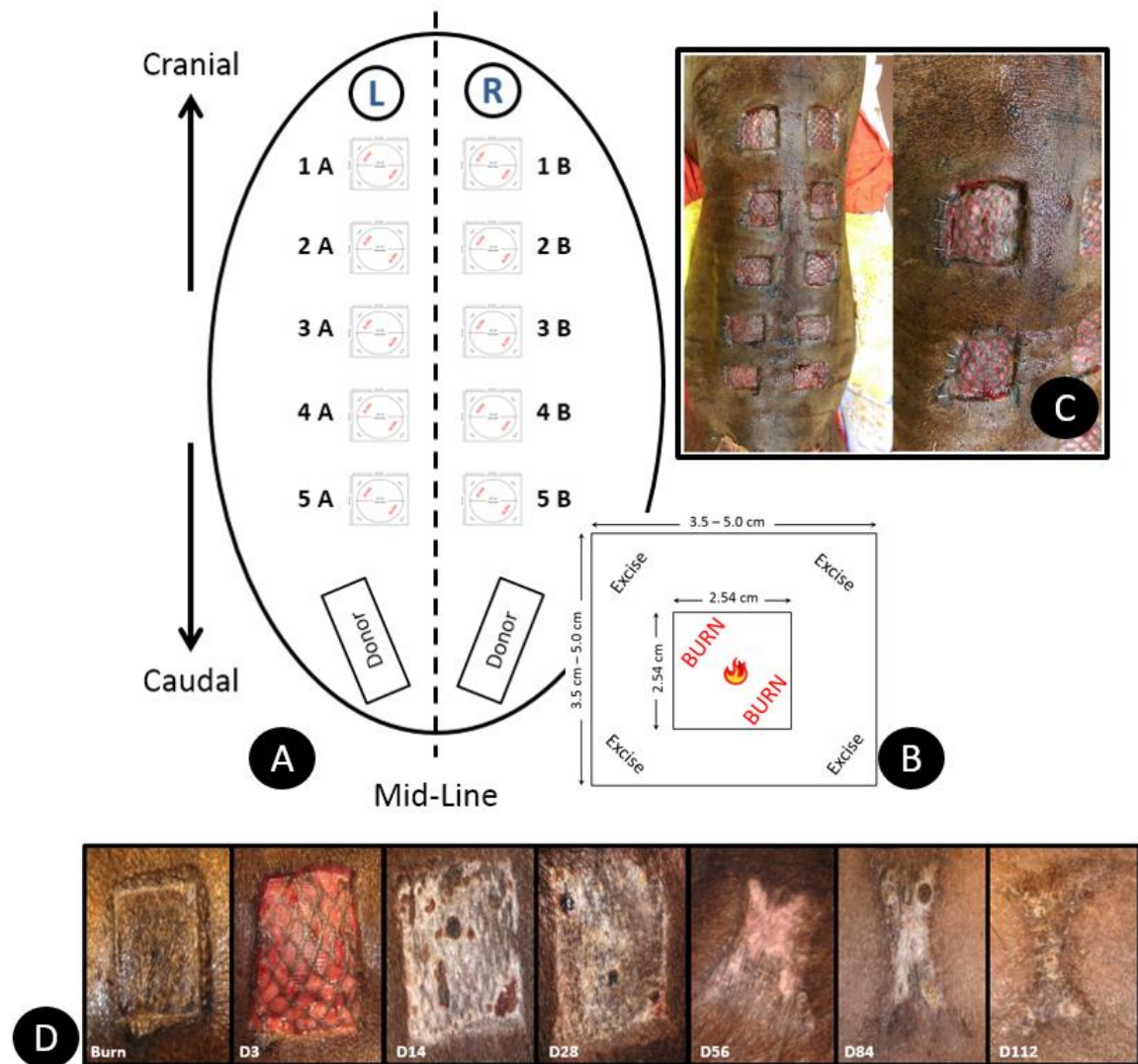
Figure 17:   Post-burn hypertrophic scar model in the red Duroc pig.
Bilateral paraspinal burns were created on the dorsum of female red Duroc pigs utilizing a brass block heated to 120°C for 40 seconds (**A**). Wounds were excised after 24 hours and grafted with 1:4 meshed split-thickness skin autologously derived (**B** and **C**). All wounds were closed around 3 weeks post-burn and were followed by raised and erythematous HTSs that were allowed to progress for approximately 4 months following initial injury (**D**). This model consistently recapitulated progression of human hypertrophic scars.

Cromolyn sodium preparation and treatment: Formulations of all substances administered to animals were prepared, stored, and administered sterilely. Cromolyn sodium (CS, MilliporeSigma C0399, Burlington, MA, USA) was emulsified in Hydrocerin® cream (Geritrex, Mt. Vernon, NY, USA) to achieve 4% (wt/vol) concentration. Hydrocerin cream is used in many burn centers to relieve skin dryness and was used for this study as the vehicle control (CS Vehicle). Immediately following wound closure (21 ± 3 days) study personnel, blinded to treatment, applied 2mL CS (N=10) or CS Vehicle (N=9) topically to wounds, twice per week until the end of the study. Untreated STSG (N=9) served as a standard-of-care control.

Tissue sampling: Prior to sampling procedures, animals received anesthesia and analgesia as before. Dorsal hair was then shaved and 5 mm punch biopsies inclusive down to the underlying fascia were obtained once per month following wound closure. To reduce confounding wound healing effects in HTS pathophysiology, biopsy locations were alternated over wound sites each month, and biopsies were preferentially taken from the lattice of the grafted area. For histology, non-burned tissue was obtained from sites distant from the wounds at each time point. Tissues were snap frozen in liquid nitrogen or fixed in 10% neutral buffered formalin for future analyses.

Mast cell density

Biopsies were fixed in 10% neutral buffered formalin for 72 hours then dehydrated to 100% ethanol prior to paraffin embedding. HTS samples were cut transversely to 4 μm sections and mounted on slides. Tissues were cleared in xylene, rehydrated to pure water, and stained in 10% toluidine blue (MilliporeSigma, 89640) solution at pH 2.2 for 5

minutes. Excess stain was removed in ethanol washes and then the sections were cleared in xylene, mounted in resinous media, and coverslipped. Metachromatic-stained mast cells were identified by observers trained in cutaneous histopathology and blinded to treatment. Mast cells were quantified in the papillary and reticular dermis and averaged for each section to yield mast cell density (mast cells · mm^{-1}) at 1, 2, 3, and 4 months post-burn.

PAR2 and myofibroblast expression

Immunohistochemistry for PAR2: Tissues were fixed, paraffin embedded, and cut as previously described. Following rehydration, tissues were immersed in target antigen retrieval solution (S1699 DAKO, Agilent Technologies, Santa Clara, CA, USA) heated to 95°C for 30 minutes, and then rinsed in phosphate buffered saline with Tween20 (PBST). Endogenous peroxidase activity was quenched by a 30 minute incubation of the tissues in 3% hydrogen peroxide diluted in methanol. The sections were then blocked in 5% goat serum for 1 hour at room temperature. Next, sections were thoroughly washed in PBST prior to antibody incubation. Tissues were incubated in primary antibody to PAR2 (180953, Abcam, Cambridge, MA, USA) diluted in background-reducing antibody dilutent reagent (S3022, DAKO) 1:300 overnight at 4°C. The next morning, sections were again washed in PBST and incubated in biotinylated secondary antibody (PK6101, Vector Laboratories, Burlingame, CA, USA) diluted 1:500 in PBST for 30 minutes. Next, sections were incubated with avidin and biotinylated-horseradish peroxidase (HRP) reagents for 30 minutes at room temperature. After washes in PBST, tissues were immersed in Diaminobenzidine (DAB) substrate, pH 7.5 for 3 minutes and counterstained in

hematoxylin for nuclear visualization. Slides were dehydrated through progressive xylene washes and mounted in resinous media.

Brightfield images of each section were captured at 200X magnification on an Olympus BX41 microscope and digitized utilizing cellSens software (version 1.7, Olympus, Tokyo, Japan). Images were gridded and positive PAR2 DAB stained cells in the papillary and reticular dermis were identified and quantified using ImageJ (version 1.3 for Windows, NIH, Bethesda, MD, USA),[197] and utilizing the validated IHC toolbox for image analysis.[198] Hematoxylin stained nuclei were counted for total dermal cellularity. The ratio of PAR2-postive cells to total cellularity was used to calculate the percent positive PAR2 (PAR2$^+$) expression for each condition and time point.

Immunoblot: PAR2-induced myofibrotic expression of alpha-smooth muscle actin (αSMA) and collagen-1 was assessed by western blot. Epidermis and subcutaneous tissues were first removed from frozen biopsies leaving intact dermal tissue. The remaining dermis was ground under liquid nitrogen then lysed in buffer containing protease and phosphatase inhibitor cocktails (11836170001 and P5726, MilliporeSigma). Protein separation was achieved by electrophoresis on 4-15% gradient polyacrylamide gels under denaturing conditions, and then transferred to a PVDF membrane. Membranes were blocked in 5% bovine serum albumin (BSA) and washed in tris-buffered saline with Tween20 (TBST) after protein transfer. Next, membranes were incubated in primary antibody to PAR2 (1:2000, 180953, Abcam), αSMA (1:1000, A5228, MilliporeSigma), collagen-1 (1:1000, 34710, Abcam), or β-actin (1:2000, 4970, Cell Signaling Technologies, Danvers, MA, USA) diluted in 1% BSA in TBST overnight at 4°C. The next day, membranes were thoroughly washed in TBST and then incubated in HRP-conjugated secondary antibody

for 1 hour at room temperature. Pierce ECL served as the chemiluminescent substrate for autoradiographic detection. Expression was quantified through densitometry in ImageJ and normalized to β-actin.

3-dimensional (3D) HTS imaging and analysis

Prior to each biopsy procedure, the 3D LifeViz II system (Quantificare, San Francisco, CA, USA) was used to capture individual wound field images in order to calculate wound or scar volume. To ensure accurate calculations, uniform distances from the camera system lens to the wound surface were calibrated using the two onboard lasers. Images were digitized and rendered in 3D by proprietary scar analysis software (DermaPix, Quantificare) validated to be reliable for post-burn wound assessment.[199] For each post-burn time point, the edges of each HTS outlined digitally for each wound to define the scar baseline Quantitative analyses for scar perimeter (mm), surface area (mm^2), total volume (mm^3), and height (mm) were performed within the software. Roughness measurements were based on the regularity of the skin surface adjacent to wound edges and defined as the average height of the scar surface variation compared to surrounding normal skin. Mean roughness = (|Positive Volume| + |Negative Volume|) / Surface Area). Differences in measured scar parameter values were calculated as percent change from the previous month to account for differences in wound healing, in addition to variation of absolute skin depths between animals. Percent change was then averaged for each treatment time point for all animals.

HTS Epidermal Height

Tissues were fixed and mounted to slides as previously described. Following rehydration, sections were stained in hematoxylin and eosin (H&E). H&E Images were digitized at 200X magnification using an Olympus BX41 microscope utilizing CellSens software. Composite color images were split resulting in separate red, blue, and green channel images. Utilizing the blue color channel image, the epidermis of each scar was outlined in ImageJ to yield a calibrated area (mm^2). Mean epidermal height (mm) was derived by dividing the measured area by the length of the epidermal basal lamina (Supplemental Fig 2). Epidermal height was normalized to non-burned skin at the same post-burn time point to yield the epidermal thickness index (ETI) as previously described.[200] ETI was compared between treatments for each time point.
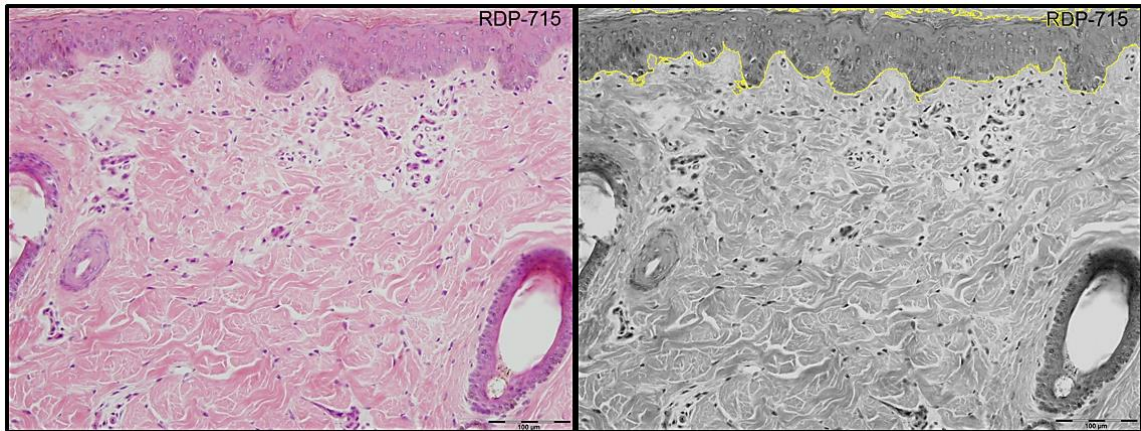
Figure 18:   Objective epidermal thickness measurements.
Histological images were captured at 200X magnification and digitized. H&E images were converted to binary, 8-bit images and the epidermis was outlined in ImageJ to yield a calibrated area (mm^2). Area was divided by the average length to yield the mean epidermal height (mm). Mean epidermal scar heights were then compared to epidermal heights of non-burned skin at the same time point post-burn to yield the epidermal thickness index (ETI) as previously defined by Tandera and Mustoe.[200] Scale bar = 100μm.

Dermal collagen density

HTS tissue sections were cut to 4 μM, mounted to slides and stained in Masson's trichrome (KTMTRPT, American MasterTech, Lodi, CA, USA) to allow quantitative measurement of collagen density and quality over time. Brightfield images were captured at 40X magnification on an Olympus BX41 microscope and digitized with CellSens software. Integrated optical density (IOD) was measured as changes in pixel intensity in ImageJ, with higher values corresponding to increased density and closely packed collagen fibers. Mean IOD was measured over 15 independent and non-overlapping regions for each HTS biopsy and normalized to non-burned skin at each time point to yield a ratio known as the collagen density index. Collagen density index was compared across treatments for each time point.

HTS vascular density

Tissues were processed using the immunohistochemistry method as described above in *Immunohistochemistry for PAR2*. Primary antibody for CD31 (28364, Abcam) diluted in background reducing solution (DAKO) 1:350 was used to identify endothelial cells in vascular structures within the papillary and reticular dermis of HTS and non-burned samples. Brightfield images of DAB stained tissues were captured at 100X magnification on an Olympus BX41 microscope and analyzed in imageJ. Optical density of CD31^{+} expression was quantified by validated methods.[201] Briefly, all images were first white-balanced for consistent color. For maximal separation of DAB chromogen, color was deconvoluted and monochromatic pixel values for staining intensity were converted to optical density (OD = log[max pixel intensity/mean pixel intensity]). Background staining

was removed by density standardization using a blank field image that was white-balanced as before. Epidermal and blank areas were digitally removed from analysis resulting in CD31 OD·mm^{-2}. Higher OD values per area indicated denser areas of DAB chromogen, greater expression of CD31, and marked increased vasculature within the tissue, which was then compared at each post-burn time point between treatments.

Statistical analyses

Unless otherwise noted, normally distributed data was compared by standard parametric tests. One-way analysis of variance (ANOVAs) assessed total differences in means followed by a *post hoc* Bonferonni test to assess significant difference between treatment groups and time points. In cases of non-normal distributions, non-parametric tests including the Mann-Whitney rank sum test for 2 groups or the Kruskal-Wallis test for more than 2 groups were applied. Significance was accepted at $p \leq 0.05$.

<u>**RESULTS**</u>

Topical cromolyn sodium reduces both mast cell density and PAR2 expression in post-burn red Duroc HTS

Mast cell density decreases after 2 months of cromolyn sodium treatment following post-burn wound closure (Fig 19). Mast cells were found in significantly higher densities in HTS at 1 month (28 days) following burn injury when compared to non-burned skin, $p<0.05$. At 1 month post-burn, mast cell density averaged $59.4 \pm 6.7 \cdot$mm^{-2} with STSG standard of care, $57.4 \pm 12.3 \cdot$mm^{-2} in CS Vehicle treatment, and $60.9 \pm 2.9 \cdot$mm^{-2} in CS 4% treatment compared to $22.5 \pm 7.2 \cdot$mm^{-2} in dermal areas of non-burned skin. Mast cell densities in all treatment groups remained considerably elevated over non-burned skin mast

cell densities (24.1 ± 3.8 ·mm^{-2}) at 2 months post-burn, p<0.05. However, 3 months following burn injury, and approximately 2 months after the start of treatment, mast cell numbers were significantly reduced in CS 4%-treated HTS (27.8 ± 12.9 ·mm^{-2}) compared to CS Vehicle-treated (66.1 ± 11.2 ·mm^{-2}) HTS, p<0.01. At 4 months post-burn, mast cell numbers continued to decrease in HTS treated with CS 4% (25.9 ± 4.6 ·mm^{-2}), which was statistically indistinguishable from non-burned skin (20.9 ± 8.1 ·mm^{-2}). Moreover, these densities were significantly reduced from mast cell densities in both CS Vehicle-treated (36.5 ± 9.6 ·mm^{-2}) and STSG-only treated (37.8 ± 6.8 ·mm^{-2}) HTS.
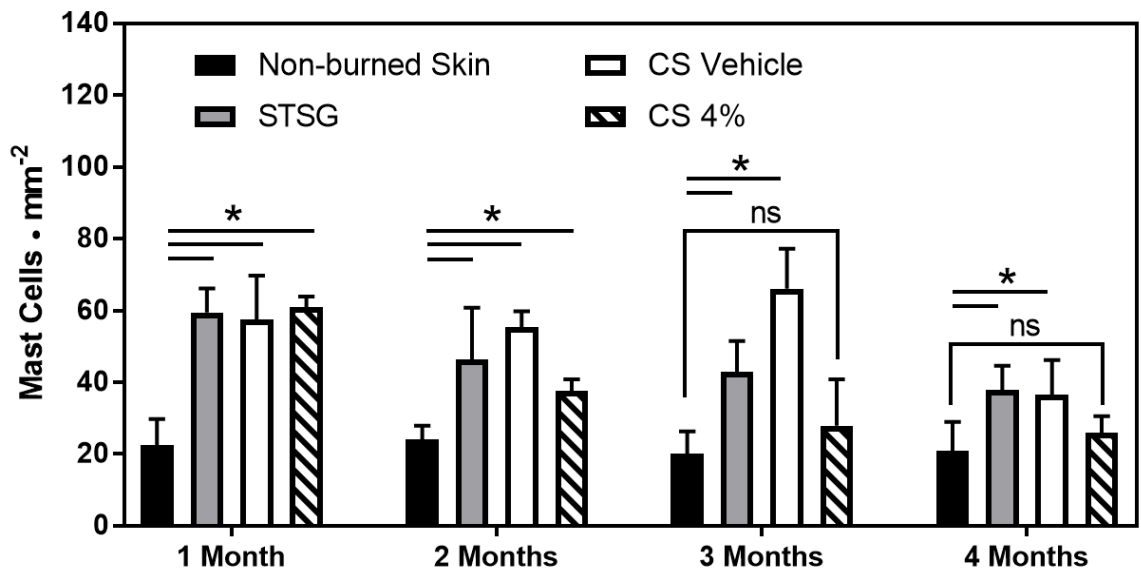
Figure 19: **Cromolyn sodium significantly reduces mast cell density in post-burn red Duroc HTS.** In toluidine blue stained tissues, mast cell density is significantly elevated following burn injury in HTSs compared to non-burned skin. However, beginning at 3-months post-burn, mast cell density decreases in HTS with CS treatment to statistically similar densities found in non-burned skin. Mast cell numbers remained elevated in STSG or CS Vehicle treated wounds over 4-months. *p<0.05, data is presented as mean number of mast cells · mm^{-2} ± SD.

Mast cell tryptase is a potent serine protease that cleaves and activates PAR2, inducing proliferation and initiating fibrotic signaling within dermal fibroblasts. Here, we show that topical CS treatment substantially diminished PAR2 expression in dermal fibroblasts up to 3 months in DAB immunostained HTS of red Durocs compared to CS vehicle treatment or STSG alone, $p<0.05$ (Fig. 20A). Quantitatively, the percent of PAR2+ fibroblasts (Fig 20B) were significantly lower at 1, 2, and 3 months post-burn with topical CS treatment (mean $= 2.5 \pm 0.9\%$) compared to standard of care STSG alone (mean $= 7.1 \pm 1.2\%$) and CS Vehicle treatment ($8.6 \pm 2.3\%$). With CS treatment, the percent of PAR2+ fibroblasts was reduced to that of non-burned skin at 1, 2, and 3 months following burn. However, at 4 months post-burn, there were no differences between any groups due to an increase in PAR2+ fibroblasts in all conditions.
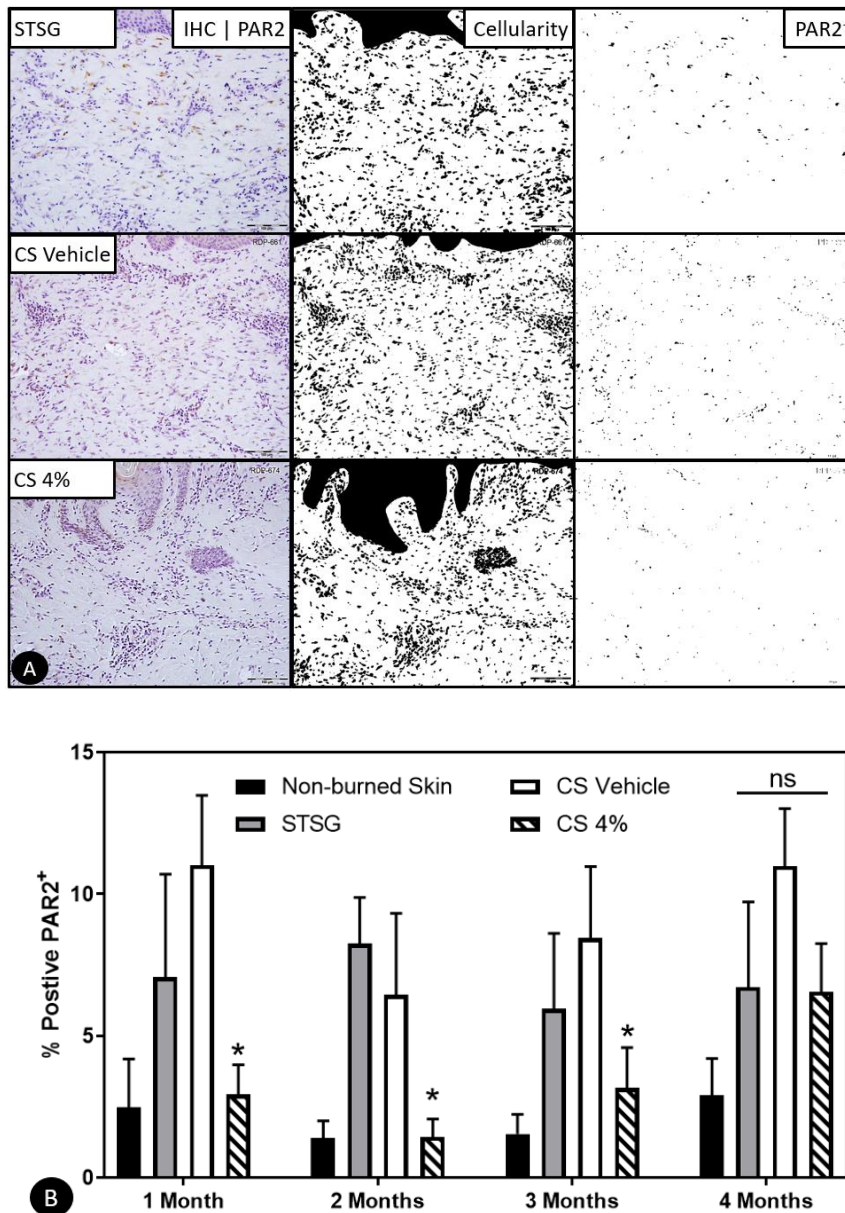
Figure 20. Post-burn cromolyn sodium treatment significantly alters PAR2 expression in HTS.
Representative images showing PAR2^{+} DAB immunostained HTS samples from STSG, CS Vehicle, and topical CS at 3-months post-burn (**A**). Scale bar = 100μm. Total cellularity as measured by the sum of individual nuclei (second column) was averaged for each treatment and divided by the average of PAR2^{+} cells (third column) to yield percent positive PAR2 staining within the dermis. Epidermal staining was not quantified. The percentage of PAR2^{+} immunoreactive cells was reduced with CS treatment at 1-, 2-, and 3-months post-burn compared STSG and CS Vehicle treated wounds (**B**). Data is presented as mean ± SD, *p≤0.05.

Mast cell stabilization diminishes fibrotic phenotype during early treatment in post-burn scar fibroblasts

Western blots show that PAR2 protein expression is considerably increased after burn injury in red Duroc HTS compared to non-burned skin. CS treatment significantly reduced PAR2 protein expression after 2 months compared to STSG or CS Vehicle treatment (Fig 21A, p<0.05), but expression increased 3 and 4 months post-burn, statistically insignificant between all three treatments. Contractile protein αSMA showed minimal expression in non-burned skin throughout the investigation, but was significantly upregulated in all HTS wounds (Fig 21B). However, αSMA expression was reduced at 2 months in CS treated HTS compared to both STSG and CS Vehicle treatment, p<0.05), but expression returned at 3 and 4 months post-burn to statistically similar levels for all three treatments. Additionally, immunoblots showed that collagen-1 protein expression decreased in CS treated wounds at 3 months post-burn (Fig 21C), but remained similar at all other time points.
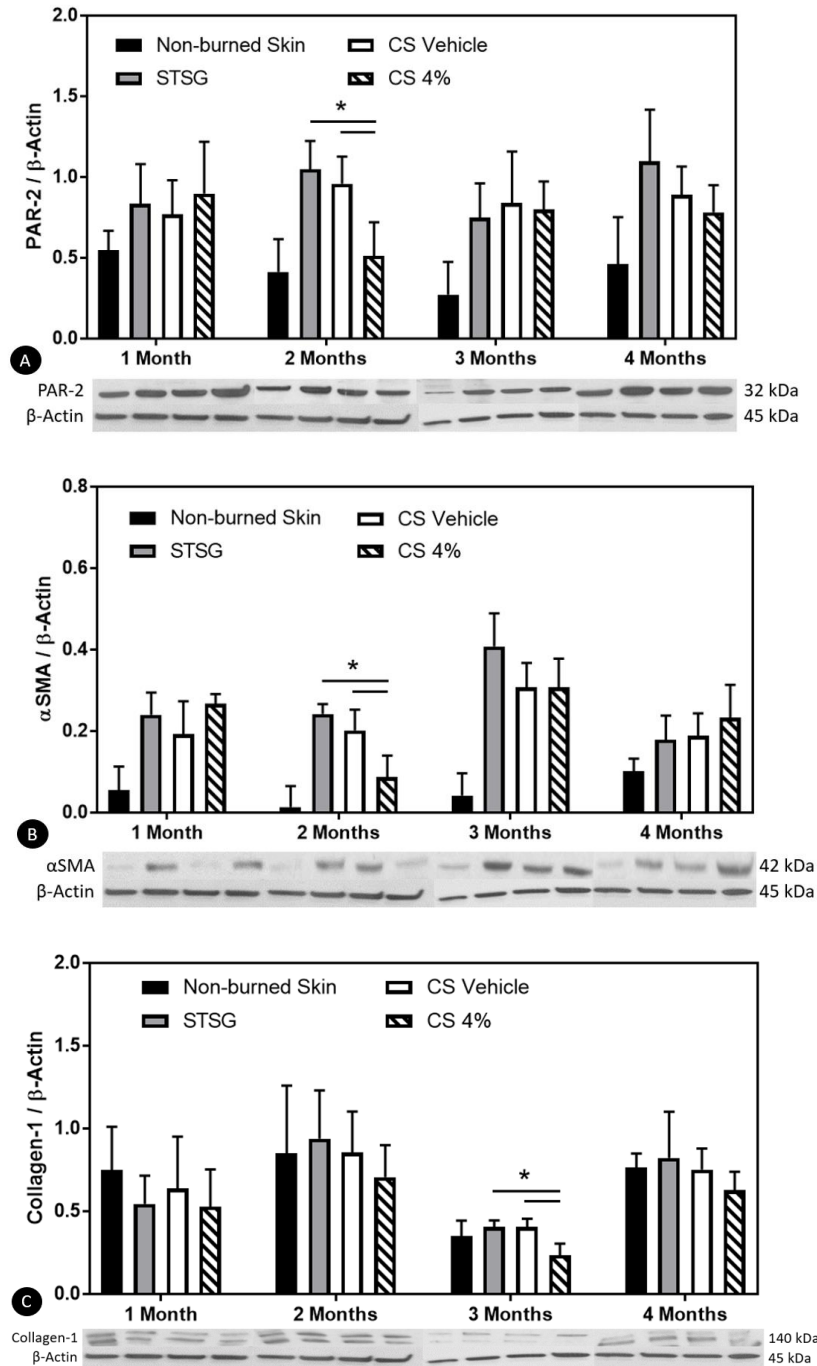
Figure 21: **Topical cromolyn sodium attenuates PAR2-induced fibrotic phenotype during early treatment in red Duroc scars.**

Immunoblots showed that both PAR2 and αSMA (**A** and **B**) expression was significantly reduced at 2 months post-burn, and collagen-1 was reduced at 3 months post-burn (**C**), compared to STSG and CS vehicle-treated HTS. Expression of these fibrotic markers in CS-treated HTS rebounded at 4 months post-burn. Data is presented as mean expression ± SD, *p<0.05.

Cromolyn Sodium flattens and smooths post-burn hypertrophic scars over time

Three-dimensional imaging revealed significant alterations in several detrimental scarring parameters after 3 months of biweekly topical cromolyn sodium application (Fig 22A). The percent change in scar height was significantly reduced from 1 to 2 months (-30 ± 6%) and again from 3 to 4 months (-6 ± 5%) compared to standard of care STSG (6 ± 5% and 11 ± 7%) and CS Vehicle treatments (17 ± 7% and 15 ± 7%) which increased over the same period, p<0.001 (Fig 22B). Both the perimeter of the scar and the total surface area increased with topical CS over the course of the treatment period. Percent change in scar perimeter increased significantly from 2 to 3 months (8 ± 6%) and from 3 to 4 months (11 ± 5%) with CS treatment whereas perimeter decreased in both STSG and CS Vehicle-treated scars over the same period (Fig 22C), p<0.001. Although the percent change in surface area increased over time for all treatments, there were no significant differences between groups at any time point (Fig 22D).

CS treatment had a major impact on scar volume and roughness as well. Analysis showed that topical CS 4% application decreased scar volume from 1 to 2 months (percent change: -21 ± 8%) and again from 3 to 4 months post-burn (0 ± 5%) which was significantly different from STSG (-4 ± 6% and 10 ± 5%) and CS Vehicle-treated HTS (4 ± 9 and 24 ± 8%) over the course of treatment, p<0.001 (Fig 22E). The percent change in scar roughness decreased considerably as well in CS-treated HTS during the same time periods (Fig 22F). Overall, 3D analysis showed that CS treatment reduced the height and volume of red Duroc post-burn HTS while increasing the perimeter and surface area. Whereas, in STSG or CS Vehicle-treated wounds, both height and volume increased and perimeter decreased, which indicated a contracting wound and more pathologic scar.
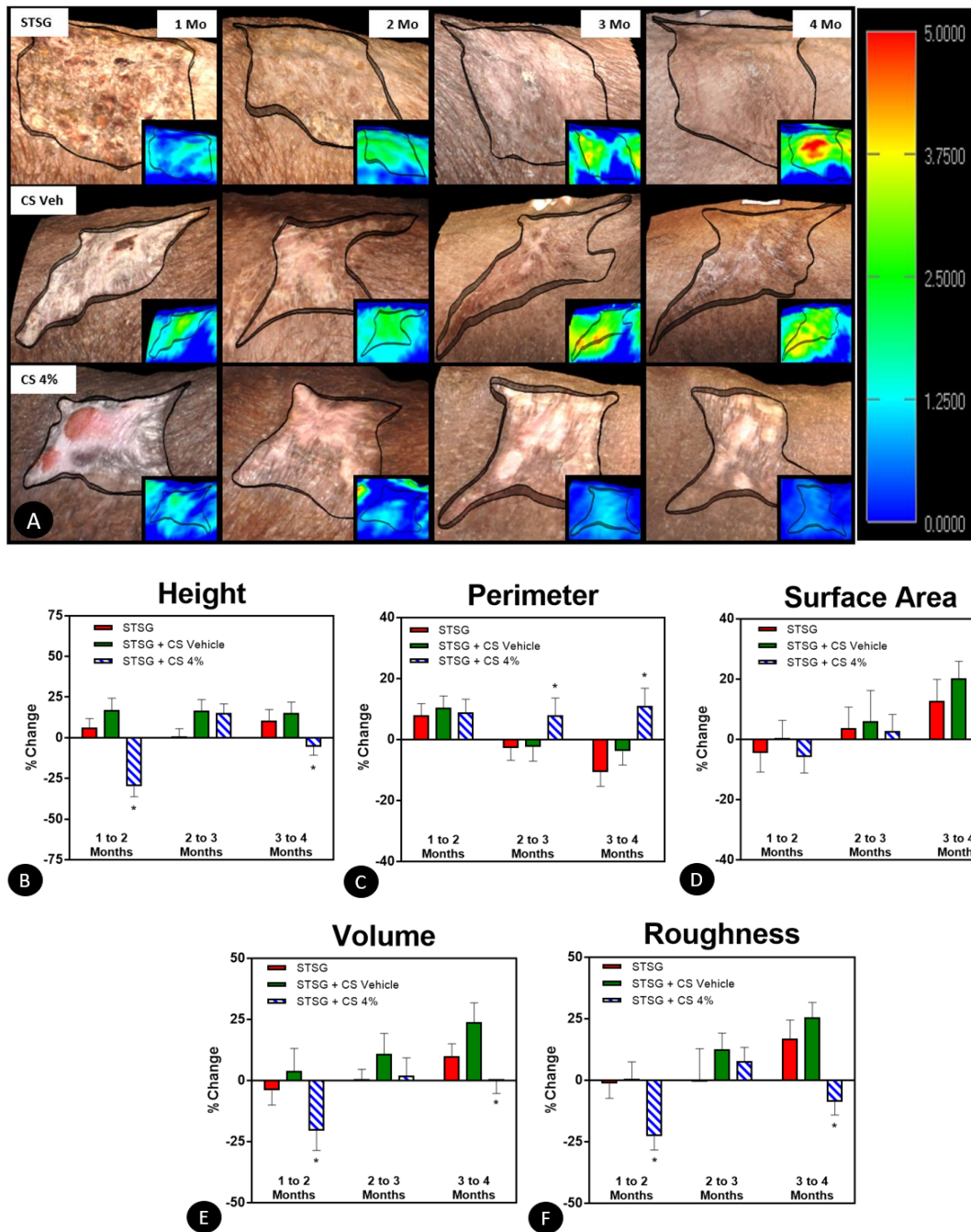
Figure 22: **Cromolyn treatment flattens red Duroc burn-induced HTS.**

3-Dimensional topographical analysis shows decreased scar height (inset images) over time in CS treated HTS in the red Duroc pig compared to STSG or CS vehicle only treated scars (**A**) after 4 months of treatment; scale = 0 (blue) – 5 mm (red). Quantitatively, scar height % change significantly decreased from 1 to 2 months and again from 3 to 4 months in CS treated wounds compared to either STSG or CS Vehicle treatment (**B**). Wound edges (outlined) were measured as the baseline and defined by DermaPix® software. HTS perimeter (**C**) increased steadily over the treatment period and this, together with increasing surface area (**D**) and

decreased volume (**E**), indicated a flattening scar with CS treatment. Additionally, HTS roughness was decreased (**F**) as well over time suggesting a smoothened interface with surrounding non-burned skin. *p≤0.05, data is presented as mean % percent change ± SD.

Topical cromolyn treatment reduces hypertrophic scar epidermal thickness

H&E stained transverse sections of red Duroc HTS showed decreased epidermal height in CS treated wounds over time (Fig 23A). There were no statistical differences in epidermal thickness index (ETI) at either 1 month or 2 months following burn injury between any treatment groups, but all were significantly thicker than non-burned skin. However, ETI was significantly reduced in CS-treated scars (1.3 ± 0.3) compared to STSG (1.7 ± 0.1) or CS Vehicle-treated HTS (1.7 ± 0.2) at 3 months post-burn, $p<0.01$ (Fig 23B). Again at 4 months, ETI was significantly diminished with CS treatment (1.0 ± 0.2) when compared to STSG (1.6 ± 1.3) or CS Vehicle treatment (1.5 ± 0.9), $p<0.01$. Interestingly, epidermal height was reduced to the thickness of non-burned skin after 4 months with CS 4% treatment, unlike in STSG or CS Vehicle treated HTS.
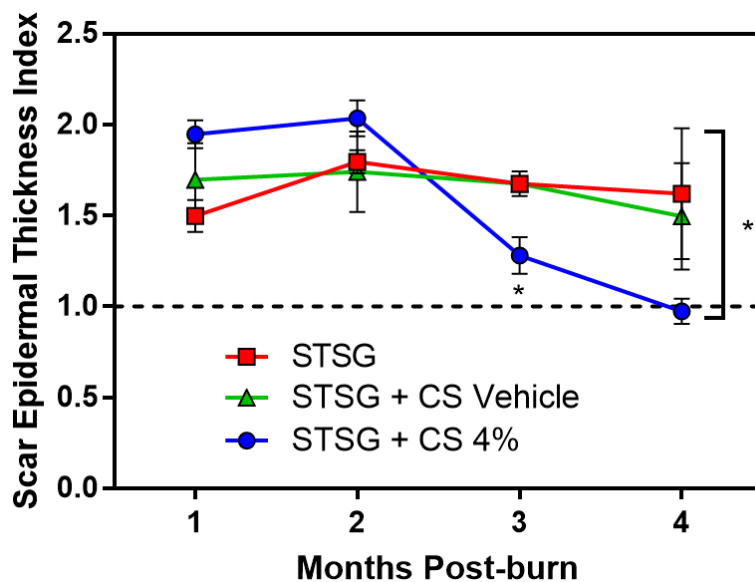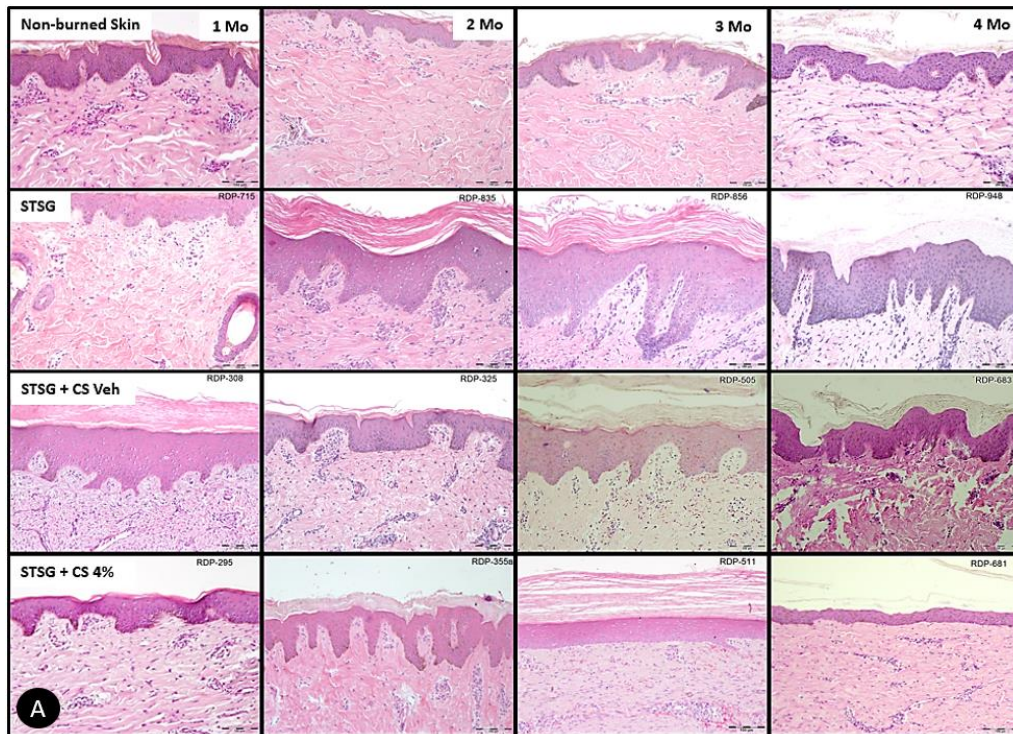
Figure 23: **HTS epidermal thickness index (ETI) is reduced in cromolyn treated post-burn scars.** Representative images demonstrate reduced HTS with CS treatment over 4-months (**A**). Scale bar = 100μm. Mean epidermal height was normalized to non-burned skin epidermis at each time point post-burn to yield ETI. Epidermal thickness was reduced following 4% topical CS treatment in red Duroc HTS 3- and 4-months (*$p<0.05$) post-burn compared to CS vehicle or STSG alone (**B**). ETI = 1.0 is the equivalent thickness of non-burned skin. Thinner epidermal layers indicates an improved water barrier compared to vehicle-treated

or STSG alone further suggesting regular mast cell stabilization may optimize wound healing following severe burn injury. Data is presented as mean ETI ± SD.

Cromolyn sodium treatment improves collagen organization and reduces collagen density

Masson's trichrome stained HTS sections show significant changes in collagen density and organization over time following CS treatment (Fig 24A). At each time point, non-burned skin biopsies maintained equal collagen density throughout the tissue and demonstrated orderly collagen fibers with no particular orientation. There were no significant differences in collagen density index between any treatment group for the first 3 months after initial burn injury. However, at 4 months post-burn, collagen density was significantly reduced with CS treatment (0.79 ± 0.06) compared to standard-of-care STSG (0.97 ± 0.13) or CS Vehicle-treated (0.95 ± 0.11) post-burn HTS, $p<0.05$ (Fig 24B). Compared to non-burned skin, collagen fibers ran relatively parallel to the skin surface at all time points post-burn in all treatments. However, after 4 months, CS treated wounds demonstrated less densely packed collagen.
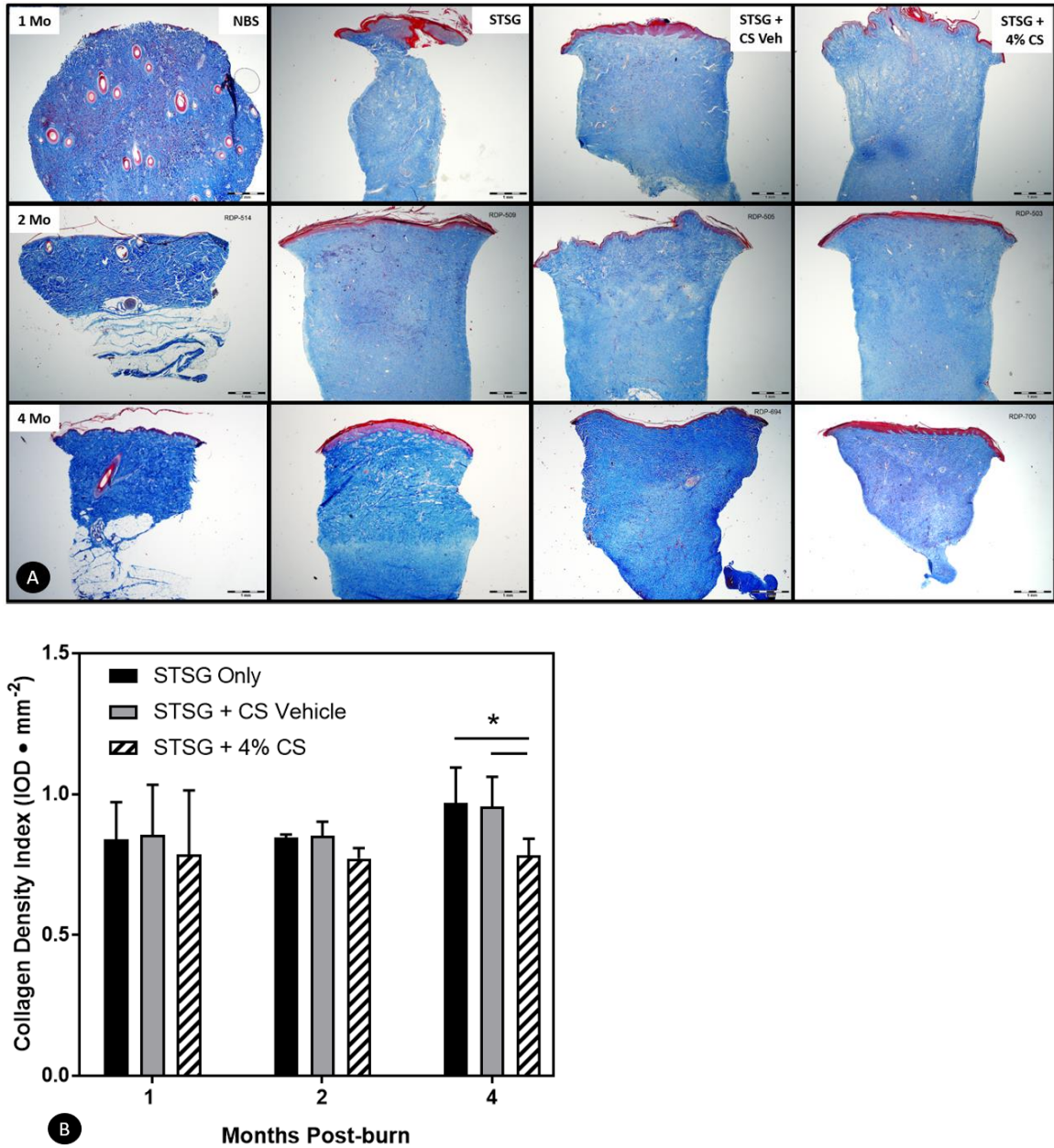
Figure 24: **Collagen density decreases in post-burn HTS treated with topical cromolyn.**

Biweekly topical CS treatment reduced collagen density in post-burn red Duroc HTS after 4-months compared to STSG alone or CS Vehicle treatment in Masson's Trichrome stained HTS biopsies (**A**). Scale bar = 1mm. Mean integrated optical density (IOD) was measured over 15 independent regions for each HTS biopsy and normalized to non-burned skin IOD at each time point to yield the collagen density index ratio. Mean collagen density was significantly reduced in 4% CS treated HTS compared to STSG or CS Vehicle treatment alone at 4-months post burn, *p=0.02, p=0.04, respectively; collagen density remained unchanged between treatment groups prior to 4 months (**B**).*p≤0.05, data is presented as mean collagen density index ± SD.

Topical cromolyn reduces HTS vascular density

Immunohistochemical identification of HTS dermal microvasculature showed that CS treatment significantly diminished vascularity over the treatment time course (Fig 25A). DAB stained CD31$^+$ HTS sections demonstrated reduced vascular density at 4 months post-burn (IOD: 0.061 ± 0.008) compared to STSG-treated (0.134 ± 0.056) or CS Vehicle-treated wounds (0.119 ± 0.052), $p<0.05$ (Fig 25B). Vascular density was statistically equivalent for all treatment groups prior to 4 months.
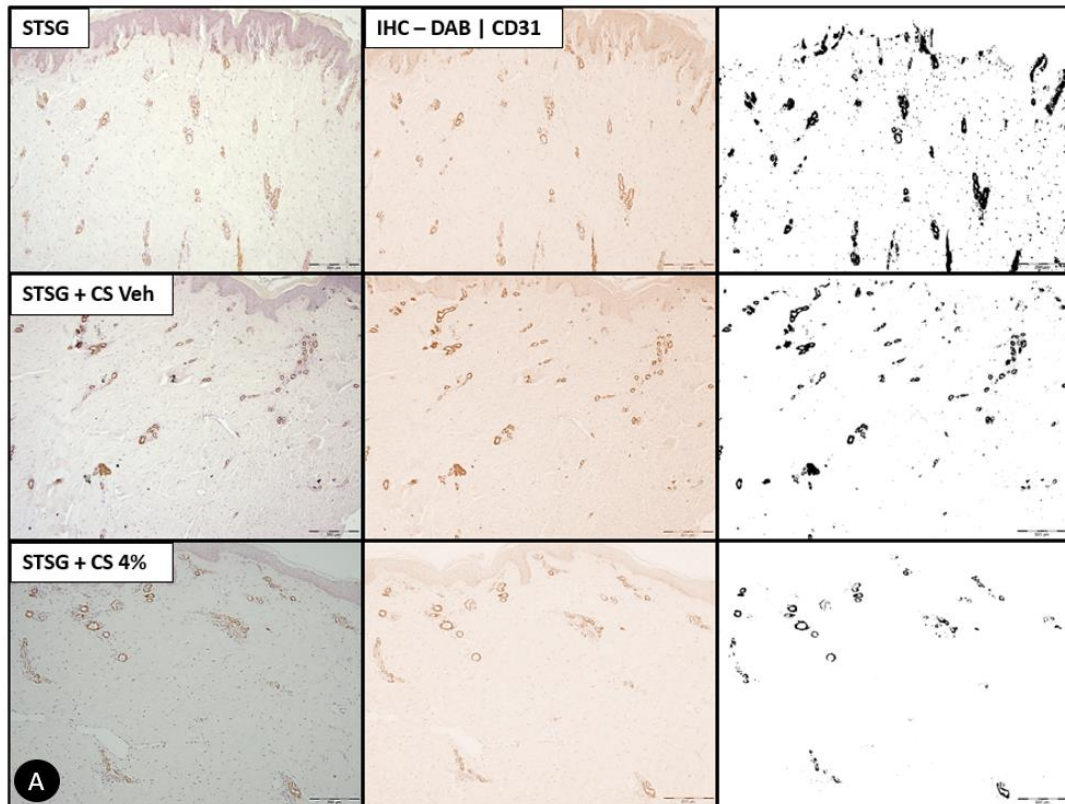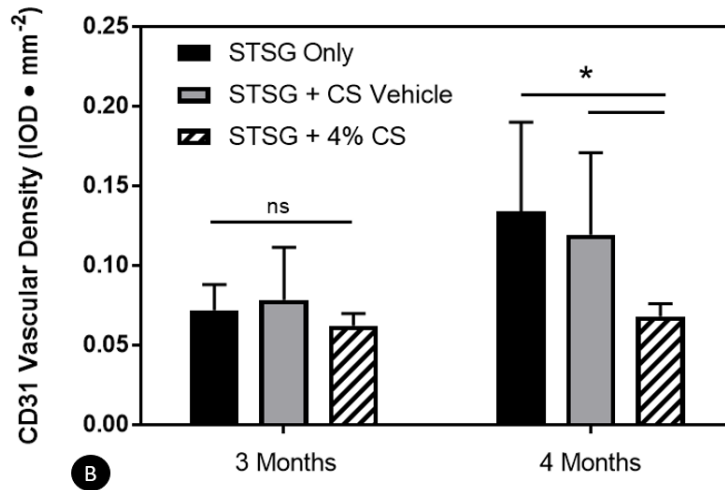
Figure 25: **HTS Vascularity is diminished during cromolyn treatment following burn injury.**
Representative images of CD31 immunostained 4 month biopsies (A); scale bar = 200μm. DAB-stained images (first column) were digitally deconvoluted in ImageJ to measure specific CD31 staining intensity (second column); with background removed (third column). Topical CS treatment significantly reduced dermal HTS vascularity compared to both STSG and CS vehicle treatment alone after 4 months post-burn, $*p<0.05$ (B). No significant differences in vascularity were measured prior to 4 months. Data is presented as mean vascular density IOD ± SD.

DISCUSSION

What is known about the cellular and molecular basis of post-burn HTS is well described in the literature. Much of this work is focused on the role of the fibroblast in HTS development. However, recent investigations are revealing a more complex pathogenesis than previously understood, changing how we think about the healing burn wound and subsequent scarring. Prolonged inflammation, directed primarily by tissue macrophages, neutrophils, and lymphocytes, supports differentiation of deep dermal myofibroblasts. Protracted inflammatory signaling drives these fibroblasts to produce contractile proteins and excess collagen, which promotes HTS development and progression. However, treatments targeting this aberrant process and investigations to prevent or correct the phenotypic switch were marginally effective.[202-204] Newly identified cell populations within the scar are now revealing fresh insights into the pathophysiology of post-burn HTS.

Mast cells are sources of potent growth factors and protease, and evidence indicates that they may directly contribute to the initiation and progression of post-burn scars. These multifaceted cells are recognized regulators of anaphylaxis and hypersensitivity reactions; however, ample evidence indicates that mast cells are pivotal in several fibrotic pathologies. We have previously found elevated mast cell densities in post-burn HTS of pediatric burn survivors up to 4 years after initial injury compared to uninjured tissue[205] and other investigations show increased mast cell numbers in pulmonary, renal, and myocardial fibroses.[180,182,206] This evidence is corroborated in the current study. Examination of biopsies from the red Duroc model confirm that mast cells aggregate in significantly greater densities acutely following burn injury within the wounds and scars. Moreover, mast cell densities remain elevated through HTS progression, further

confirming that mast cells are involved in cutaneous fibrosis following burn. Importantly, these data indicate that inhibition of the critical mast cell-dermal fibroblast paracrine axis may prove beneficial to reduce scarring.

Mast cells are blocked from releasing their contents by antagonizing degranulation pharmacologically in a process known as "stabilization." Although definitive evidence is lacking, mast cells are thought to be stabilized by inhibiting plasma membrane chloride and Ca^{2+} channels as well as and endoplasmic reticulum Ca^{2+} channels. Obstructing membrane chloride flux or endoplasmic reticulum calcium exchange prevents granule-containing vesicle exocytosis, thus, stabilizing mast cell membranes and preventing degranulation.[77,190,191] Several mast cell stabilizers have been developed to combat allergic reactions or reduce symptoms associated with mastocytosis. However, CS is the most extensively studied stabilizer in clinical trials and is documented to prevent mast cell degranulation. Several trials concluded that topical CS was effective at reducing mast cell-induced pruritus,[84,207-209] but importantly, newer investigations have indicated that CS may reduce fibrosis as well. Choi *et al.* (2015) reported that CS ameliorated TGF-β-induced fibrosis in a validated *in vitro* model of hepatic cirrhosis where mast cell numbers were increased.[85] Recently, Jiang and colleagues (2018), using a polycystic kidney rat model, concluded that CS may be beneficial to reduce fibrosis in mast cell-induced renal cystic disease.[210].

In the present study, we observed that mast cell densities are increased in post-burn HTS of red Duroc pigs and demonstrated that CS treatment significantly reduced mast cell accumulation in HTS over time. Through 3D analysis, we also showed that topical CS considerably decreased scar volume and height over time, while flattening and smoothing

the scar corroborating its anti-fibrotic effect. Together, these data indicate that CS treatment in the post-burn model of HTS mitigates additional mast cell recruitment, which serves to improve the wound healing cascade and reduce fibrosis.

Re-epithelialization is a hallmark of cutaneous wound healing that acts to restore the critical epithelial barrier to retain fluid and prevent infection. Greater transepidermal water loss during wound healing is linked with increased scarring.[211,212] Major burn injury compromises the barrier capacity of the epidermis and keratinocytes are rapidly induced to proliferate and migrate to replenish the barrier. Acutely, increased epidermal thickness is normal following wound closure, but continued keratinocyte proliferation is considered pathologic and results in elevated scars, abnormal formation of cellular junctions, and increased fibrotic progression. Formation of a thinner epidermis during re-epithelialization results in a more effective water barrier and less fibrosis in HTS pathology.[200] In our study, histological sections show HTS epidermis was significantly thinner in CS-treated wounds after 3 months and resembled a more mature and flattened scar. These data validate previous 3D wound analyses, which showed significantly decreased scar height over the treatment period and further suggests that CS treatment may restore normal keratinocyte signaling and proliferation to provide a more natural cutaneous barrier and a reduction in scarring.

Mast cells release multiple effectors through degranulation and tryptase, as the most abundant stored protease, is a powerful proliferative stimulus in the context of fibrotic pathogenesis. Tryptase robustly induces pulmonary, hepatic, and cardiac fibroblast proliferation[65,138,213] and we have previously shown that serum tryptase is significantly elevated in pediatric burn survivors.[205] Molecularly, mast cell tryptase cleaves and activates

117

the protease-activated receptor-2 (PAR2). PAR2 is a unique G-protein coupled receptor (GPCR) that is activated by amino-terminal cleavage. The cleaved hexapeptide (SLIGKV) then binds to the second extracellular loop, acting as a tethered ligand to stimulate a conformational change and potent mitogenic signaling. Physiologically, since the receptor must be cleaved for activation, PAR2 must be synthesized *de novo* to re-sensitize the cell for continued stimuli. This is in contrast to other GPCRs, which can be recycled back to the plasma membrane once internalized. Thus, greater PAR2 expression indicates continued PAR2 activation and signaling.[214,215] Presently, we show that topical CS significantly limited PAR2 expression during the first three months of treatment in immuno-stained red Duroc HTS. Immunoblots confirmed downregulated PAR2 expression at 2 months post-burn suggesting that global reduction in mast cell degranulation limits PAR2 mitogenic activation, thereby reducing fibroblast proliferation and HTS-associated fibrosis. Additionally, immunoblots revealed that CS treatment reduced protein expression of α-smooth muscle actin and collagen-1 after two and three months, respectively. Histologically, trichrome stained HTS tissue showed less dense dermal collagen after 4 months with CS treatment suggesting that a reduction in PAR2 signaling via mast cell stabilization may reduce fibrosis associated with post-burn HTS.

Vascularity is another important feature of cutaneous wound healing. Angiogenesis results in new blood vessels that allow cellular trafficking and endocrine signaling to and from wound sites as well as nutrient delivery and waste disposal. However, angiogenesis must be balanced with the needs of the healing wound. During burn wound healing, vascularity is subjectively monitored by erythema observations, but dermoscopy can offer a more reliable objective assessment. Importantly, increased wound vascularity is

associated with more detrimental scarring and a poorer prognosis in post-burn HTS.[216,217] Histologically, our study revealed that CS treatment reduced red Duroc HTS after 4 months. Mast cells produce, store, and release vascular endothelial growth factor, which is the major factor that dramatically increases endothelial cell proliferation and vessel formation. Moreover, PAR2 activation results in concomitant activation of the vascular endothelial growth factor receptor, which in turn induces angiogenesis. This suggests that vascularity can be reduced through mast cell stabilization with simultaneous reduction in PAR2 expression and activation via CS, resulting in a reduced scar.

Interestingly, we observed a rebounding effect approximately 6 to 8 weeks after CS treatment (2 to 3 months after initial injury) in several quantitative parameters of post-burn HTS in the red Duroc pig. Many scarring criteria, including volume, roughness, and collagen deposition, displayed marked improvement during acute topical CS treatment. However, after approximately 2 months of treatment, equivalent scarring parameters showed a regression back to split-thickness skin graft alone or CS Vehicle treated HTSs. Myofibroblast phenotype as measured by PAR2, αSMA, and collagen expression were all decreased during initial CS treatment, but expression returned to basal levels as the study progressed. We suspect that mast cells were becoming refractory to treatment, meaning dose escalation or more frequent applications of the current CS concentration should be explored in the future. Importantly however, the physical manifestations of reduced mitogenic stimuli and resultant decrease in fibrotic signaling showed an improved scar at 4 months post-burn, which was the endpoint of this study.

Split-thickness skin graft is the current standard of care following severe full-thickness burn injury for patients with sufficient availability of donor skin. Autologous

grafting is immunologically safe and has been shown to reduce scarring when it is completed in a timely manner, within the first 72 hours following a third-degree burn.[218] Split-thickness meshed skin grafts serve multiple purposes. Grafts promptly revitalize the epidermis to provide a critical intact fluid barrier and may contain intact adnexal structures which have been shown to drastically improve wound healing.[219,220] Importantly, here we demonstrated that topical CS treatment in the post-burn HTS model in the red Duroc pig significantly improved the wound healing capacity and reduced scarring more consistently than STSG standard of care alone. Table 2 provides summary scar observations in red Durocs following CS treatment over time.

	STSG Control	CS Vehicle	CS 4%
Scar Perimeter	Decreased	Decreased	Increased
Scar Surface Area	Increased	Increased	No Change
Scar Volume	Increased	Increased	Decreased
Scar Height	Increased	Increased	Decreased
Scar Roughness	No Change	Increased	Decreased
Epidermal Thickness	No Change	No Change	Decreased
Collagen	Increased	Increased	No Change
Vascularity	Increased	Increased	Decreased

Table 2: Summary observations of scarring parameters over time during administration of tropical cromolyn sodium in the post HTS model of the red Duroc pig.

Topical cromolyn sodium treatment reduces post-burn HTS compared to STSG or vehicle treatment alone. CS treatment flattened the scar and reduced vascularity and collagen deposition over 3 months.

Previous investigations have demonstrated decreased scarring in red Durocs treated with the mast cell stabilizer ketotifen. Systemic treatment lessened contraction and dermal fibrosis after 10 weeks and scar improvement was sustained for several weeks after

treatment cessation.[88] Ketotifen has also been used to successfully treat contractures in a rabbit model of joint fibrosis. Researchers showed that systemic ketotifen administration reduced α-SMA and collagen-1 expression in wounds.[89] Both investigations demonstrated fibrotic improvement, however, systemic mast cell stabilization would not be ideal. Mast cells are sentinel cells and provide critical protection against pathogens. Directly targeting scar tissue through topical application is most likely the best tolerated, will have less detrimental side effects, and minimize confounding variables associated with systemic approaches.

In addition to limiting systemic variables, we chose topical application in the current study because CS shows poor gastrointestinal absorption and demonstrates very little hepatic metabolism when intestinally absorbed. Most CS (up to 99%) is excreted unmodified.[221] CS is small, approximately 500 Daltons, which is easily transported through epidermal layers and dosed directly into dermal tissue making targeted delivery and anti-fibrotic efficacy more likely through topical application.[222] Additionally, CS is FDA approved, easy to emulsify, and inexpensive compared to newer mast cell stabilizers. A recent randomized clinical trial that included 177 subjects concluded topical 4% SC was safe and well tolerated in children for up to 15 months,[207] making it a potential candidate for reducing HTS fibrosis in pediatric burn survivors. Moreover, a majority of pediatric burn survivors with large burns and HTS still report significant itch up to two years following injury.[3] In addition to the anti-fibrotic potential, CS treatment may have the additional benefit to reduce histaminergic itch.

Overall, it is likely that many cell populations create vast and complex molecular signaling mechanisms that contribute to HTS pathogenesis. However, in our current study,

we show that mast cells contribute directly to fibrosis and may provide a viable target to reduce post-burn HTS pathology. Topical mast cell stabilization with cromolyn sodium may be a reliable adjuvant with emergent therapies to improve the function and well-being of burn survivors.

CHAPTER 5: SIGNIFICANCE AND CONCLUSION

Hypertrophic scar (HTS) result from cutaneous full-thickness burn injuries that pose difficult and expensive treatment challenges long-term. Increased systemic catecholamines along with protracted inflammatory stimuli act as detrimental catalysts to increase fibrotic output of burn wound fibroblasts. However, our understanding of the cellular and molecular basis of post-burn HTS is now evolving. Evidence points directly to aberrant signaling and dysfunction in deep dermal fibroblasts within the healing burn wound and shows that they are responsible for excess collagen production and contraction in post-burn HTS. Many investigations have reported the fibrotic influence of macrophages, circulating monocytes, and T lymphocytes; significantly upregulating expression of pro-inflammatory cytokines, which prolongs the inflammatory phase of wound healing and stimulates a myofibroblast phenotypic switch in remaining wound fibroblasts. Despite this knowledge, current therapies are inadequate to completely resolve post-burn HTS, limiting the quality of life for burn survivors. Other cell populations and molecular mechanisms must play a role in post-burn scarring. Mast cells, often found at sites of injury, are regularly understudied in post-burn HTS investigations, yet they are implicated in several fibrotic pathologies. We hypothesized that mast cell infiltration following burn injury initiates and drives HTS pathophysiology.

A major finding in this investigation is that mast cells are found in increasing densities within the post-burn HTS of pediatric burn survivors compared to non-burned skin. This is consistent with other studies linking mast cell infiltration to fibrogenesis. Increased numbers of mast cells are reported in myocardial, renal, and hepatic fibrosis[18,179,180] where mast cells are thought to impact wound healing acutely, during initial

inflammation. Histamine and VEGF, released by mast cells, contribute directly to vasodilation, allowing further influx of lymphoid cells to sites of injury and drive myofibroblast phenotype through paracrine signaling.[48,184] Studies also show increased histamine concentrations acutely following burn injury, which confirms active mast cell degranulation.[20,49] Surprisingly, we found significantly elevated mast cell densities in HTS up to 4 years post-burn. This is the first evidence to report long-term mast cell persistence in burn HTS and validates a crucial link to scar progression. Critically, atopic dermatitis or any other mast cell disorder were not diagnosed for any patient, further highlighting that mast cell presence was important to maintain chronic post-burn HTS.

Additionally, our investigations measured elevated serum tryptase concentrations in patient-matched samples after a severe burn. Elevated tryptase has been reported during progression of pancreatic lesions and idiopathic pulmonary fibrosis, indicating a potential fibrotic association.[60,61] Here, we show that tryptase was significantly increased acutely following injury in pediatric patients with large burns (≥30% total body surface area) compared to healthy uninjured children. Notably, six months after initial injury, tryptase remained significantly elevated. Chronic elevation is surprising, but the data indicates that mast cell degranulation is sustained over time and further corroborates histological data in human samples. A limitation of this study was the paucity of consistently matched patient samples over time. Although significance was achieved with five patient-matched samples, a larger cohort would confirm these results. However, data demonstrated that mast cells are not only found in increasing numbers in burn scars, but also establishes that they are actively degranulating at least up to six months post-burn.

Proteinases such as tryptase contribute to both extracellular matrix remodeling and a fibrotic phenotype through a mast cell-fibroblast paracrine axis, although mechanisms remain poorly understood. This paracrine axis points to a role for proteinase-activated receptors (PAR) in dermal fibroblasts. Physiologically, tryptase is the only mast cell granule known to activate PAR2 and stimulation initiates fibroblast proliferation,[65,213] yet PAR2 expression, activation, and subsequent signaling have yet to be reported in post-burn HTS pathology. Here, we show that PAR2 expression increases over time after tryptase activation in HTS fibroblasts. This data supports earlier studies that show PAR2 must be synthesized *de novo* in order to re-sensitize the cell for continued signaling.[214,223] Interestingly, basal PAR2 expression was significantly increased in untreated HTS fibroblasts compared to non-burned skin fibroblasts, indicating a distinct phenotypic difference between fibroblast populations. This suggests that deep thermal injury primes wound fibroblasts for sustained PAR2 signaling and further supports the hypothesis of a dermal "critical depth",[9,11] below which, myofibroblasts dominate to promote scarring. Future investigations will need to determine what post-burn factors and mechanisms contribute to this phenotypic switch.

The present studies also demonstrate that mast cell tryptase is the major serine protease to elicit proliferation via PAR2 activation in burn wound fibroblasts; chymase induced no proliferation or migration. Furthermore, PAR2 activation significantly upregulated collagen-1 and α-smooth muscle actin production, which are both hallmarks of myofibroblasts – the dominant cell type in post-burn HTS. Many other fibrotic markers including potent growth factors like keratinocyte growth factor and fibroblast growth factor were also significantly elevated following PAR2 activation, which is consistent with

previous studies demonstrating that PAR2 signaling is profoundly mitogenic.[224,225] Consequently, PAR2 blockade with synthetic antagonists or expression knockdown with PAR2 siRNA significantly diminished tryptase-induced proliferation and fibrotic phenotype of HTS fibroblasts. With positive *in vitro* results, we then aimed to explore mast cell stabilization *in vivo* to reduce scarring.

Pharmacologic mast cell stabilization has been utilized for decades to relieve symptoms associated with mast cell activation disorders such as atopic dermatitis. Stabilizing compounds block calcium and chloride flux through mast cell membranes to prevent degranulation of irritating pruritic and vasoactive stimuli. However, their use to minimize mast cell-induced fibrosis is now gaining attention. Previous studies have demonstrated that systemic application of mast cell stabilizers, specifically ketotifen, effectively reduced small cutaneous scars in excisional wound models.[87-89] Cromolyn sodium is a small molecular weight, naturally-derived mast cell stabilizer. Due to its small size, it can easily penetrate epidermal barriers when carried in appropriate vehicles. In the present investigation, we applied a 4% cromolyn sodium emulsification topically to post-burn hypertrophic scars of red Duroc pigs. After 4 months, cromolyn sodium diminished many scarring parameters when compared with standard of care, split-thickness skin grafts alone. Biweekly cromolyn treatment significantly reduced mast cell numbers in the scar over time. Consequently, collagen density, scar height, volume, and roughness were all lessened, and epidermal thickness decreased, further indicating an improved water barrier after four months with topical cromolyn treatment. Importantly, we observed significantly decreased PAR2 expression in HTS treated with cromolyn as well, which further links mast cell presence and degranulation with signaling of this mitogenic receptor. As a result of

126

reduced PAR2 expression, fibrotic signaling and production of collagen and α-smooth muscle actin was reduced up to 4 months post-burn, significantly improving the scar. These investigations have also validated our model of the red Duroc pig as a reliable model to consistently recapitulate HTSs that closely resemble human pathology. Furthermore, to simulate real-life scenarios, full-thickness burns were excised and grafted 24 to 48 hours post-burn, giving this model greater pre-clinical application.

Although results from the current investigations highlight the importance of mast cells in wound healing, HTS pathogenesis and subsequent fibrotic progression is most likely the result of interplay between numerous inflammatory cells and convergent molecular signaling. To inhibit one of these will assuredly limit scar development, but it will be inadequate to completely resolve the entire fibrotic pathophysiology. Returning the scar to a normal wound healing state, and ultimately a "scarless" wound, will likely require combined therapies. These studies now demonstrate that mast cells contribute to the pathogenesis and progression of post-burn HTS. Therefore, it may be possible to minimize or limit some detrimental aspects of scarring through mast cell stabilization. Importantly, stabilization may also provide the added benefit of minimizing histaminergic pruritus. Since mast cells are sentinel cells, required to fight bacterial and parasitic infections, a more focused approach may be necessary to reduce mast cell-induced fibrosis. Ultimately, PAR2 inhibition, targeted directly in post-burn HTS tissue, may provide the greatest anti-fibrotic benefit with fewer side effects than complete mast cell stabilization. Overall, this project established mast cells as moderators of fibrotic progression in HTS and that targeting this vital cell population may be a means to reduce HTS to improve the life and well-being of pediatric burn survivors.

Appendix A

3-Dimensional Quantitative Analysis: Equipment, Software, and Calculations

LifeVizII Imaging System:
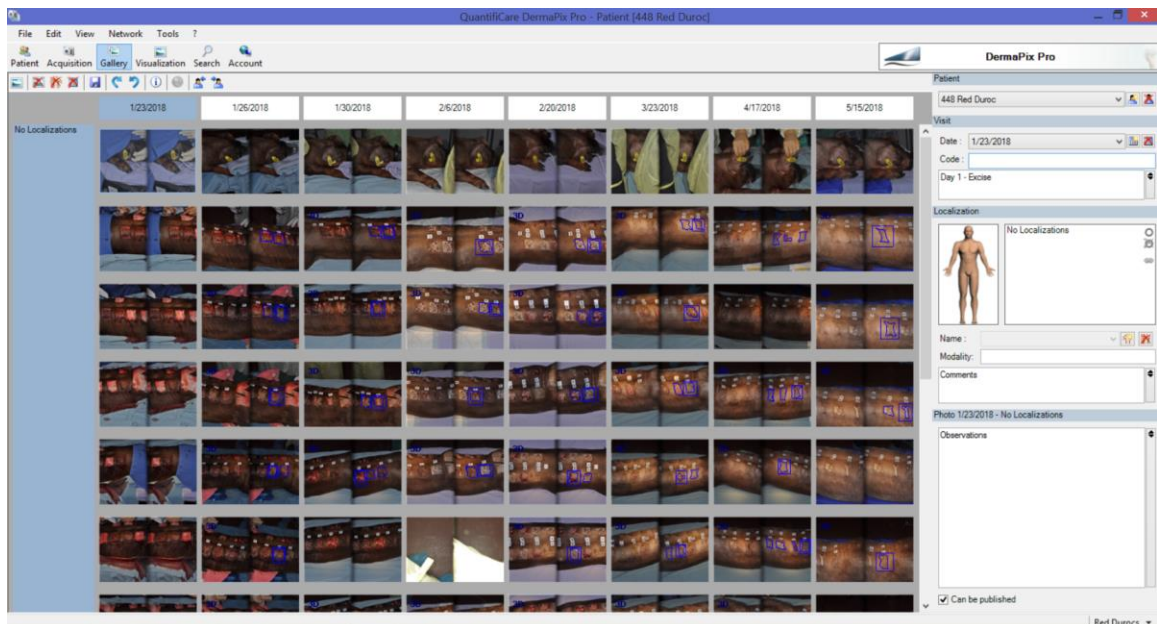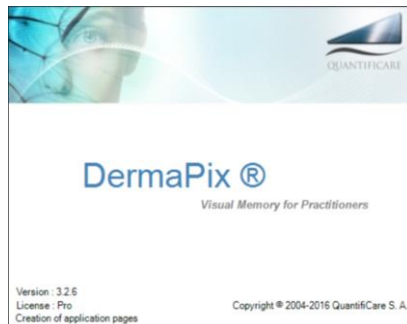
- **Perimeter**: boundary length of the wound (in *mm.*); user defines wound/scar boundary

- **Surface Area**: real 3D surface area of the user defined wound/scar (in *mm²*)

- **Volume**: total volume of the wound/scar based on user defined boundaries (in *mm³*); **Volume = volume > 0 + volume < 0**

Analysed surface

Baseline *
Positive volume
Negative volume

*Baseline is calculated by the software (DermaPix®)

.
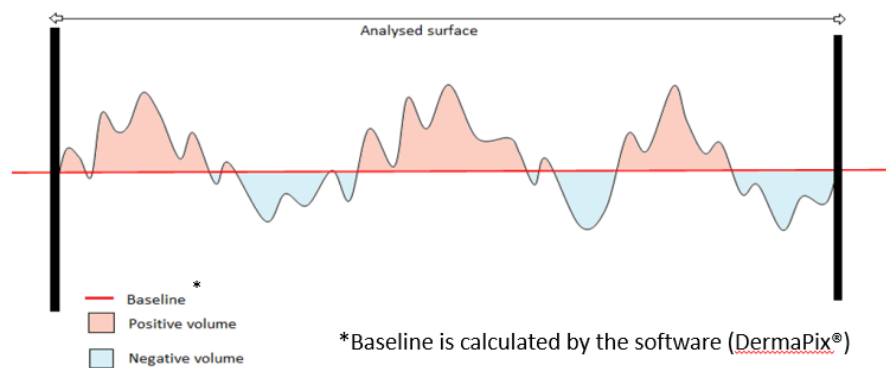
- **Depth**: Average based on the contour of wound/scar; **Avg. Depth (in *mm*) = Negative Volume / Surface Area**

- **Height**: Average based on the contour of wound/scar; **Avg. Height (in *mm*) = Positive Volume / Surface Area**

- **Roughness**: Based on the regularity (or lack thereof) of the skin surface adjacent to user-defined wound/scar; **Avg. Roughness (unit less) = (|Positive Volume| + |Negative Volume|) / Surface Area** It is the average height of the surface variation from normal skin

References

1. *Burns: Prevention and Care.* Geneva, Switzerland: World Health Organization;2018.
2. Capek KD, Sousse LE, Hundeshagen G, et al. Contemporary Burn Survival. *Journal of the American College of Surgeons.* 2018;226(4):453-463.
3. Wurzer P, Forbes AA, Hundeshagen G, et al. Two-year follow-up of outcomes related to scarring and distress in children with severe burns. *Disability and rehabilitation.* 2017;39(16):1639-1643.
4. Finnerty CC, Jeschke MG, Branski LK, Barret JP, Dziewulski P, Herndon DN. Hypertrophic scarring: the greatest unmet challenge after burn injury. *Lancet.* 2016;388(10052):1427-1436.
5. El Ayadi A, Prasai A, Wang Y, Herndon DN, Finnerty CC. beta-Adrenergic Receptor Trafficking, Degradation, and Cell Surface Expression Are Altered in Dermal Fibroblasts from Hypertrophic Scars. *The Journal of investigative dermatology.* 2018;138(7):1645-1655.
6. Sorrell JM, Caplan AI. Fibroblast heterogeneity: more than skin deep. *Journal of cell science.* 2004;117(Pt 5):667-675.
7. Wang J, Dodd C, Shankowsky HA, Scott PG, Tredget EE. Deep dermal fibroblasts contribute to hypertrophic scarring. *Laboratory investigation; a journal of technical methods and pathology.* 2008;88(12):1278-1290.
8. Ali-Bahar M, Bauer B, Tredget EE, Ghahary A. Dermal fibroblasts from different layers of human skin are heterogeneous in expression of collagenase and types I and III procollagen mRNA. *Wound repair and regeneration : official publication of the Wound Healing Society [and] the European Tissue Repair Society.* 2004;12(2):175-182.
9. Dunkin CS, Pleat JM, Gillespie PH, Tyler MP, Roberts AH, McGrouther DA. Scarring occurs at a critical depth of skin injury: precise measurement in a graduated dermal scratch in human volunteers. *Plastic and reconstructive surgery.* 2007;119(6):1722-1732; discussion 1733-1724.
10. Kwon SY, Park SD, Park K. Comparative effect of topical silicone gel and topical tretinoin cream for the prevention of hypertrophic scar and keloid formation and the improvement of scars. *Journal of the European Academy of Dermatology and Venereology : JEADV.* 2014;28(8):1025-1033.
11. Tredget EE, Levi B, Donelan MB. Biology and principles of scar management and burn reconstruction. *The Surgical clinics of North America.* 2014;94(4):793-815.
12. Velnar T, Bailey T, Smrkolj V. The wound healing process: an overview of the cellular and molecular mechanisms. *The Journal of international medical research.* 2009;37(5):1528-1542.
13. Kim MH, Gorouhi F, Ramirez S, et al. Catecholamine stress alters neutrophil trafficking and impairs wound healing by beta2-adrenergic receptor-mediated upregulation of IL-6. *The Journal of investigative dermatology.* 2014;134(3):809-817.

14. Jay J, El Ayadi A, mac D, et al. Mast cell mediated fibrosis via PAR-2 activation in postburn scars. *Wound repair and regeneration : official publication of the Wound Healing Society [and] the European Tissue Repair Society.* 2016;24(5):A13-14.

15. Oskeritzian CA. Mast Cells and Wound Healing. *Advances in wound care.* 2012;1(1):23-28.

16. Shiota N, Rysa J, Kovanen PT, Ruskoaho H, Kokkonen JO, Lindstedt KA. A role for cardiac mast cells in the pathogenesis of hypertensive heart disease. *Journal of hypertension.* 2003;21(10):1935-1944.

17. Veerappan A, O'Connor NJ, Brazin J, et al. Mast cells: a pivotal role in pulmonary fibrosis. *DNA and cell biology.* 2013;32(4):206-218.

18. Silver RB. Role of mast cells in renal fibrosis. *Kidney international.* 2013;84(1):214.

19. Kischer CW, Bunce H, 3rd, Shetlah MR. Mast cell analyses in hypertrophic scars, hypertrophic scars treated with pressure and mature scars. *The Journal of investigative dermatology.* 1978;70(6):355-357.

20. Tredget EE, Shankowsky HA, Pannu R, et al. Transforming growth factor-beta in thermally injured patients with hypertrophic scars: effects of interferon alpha-2b. *Plastic and reconstructive surgery.* 1998;102(5):1317-1328; discussion 1329-1330.

21. Shiota N, Nishikori Y, Kakizoe E, et al. Pathophysiological role of skin mast cells in wound healing after scald injury: study with mast cell-deficient W/W(V) mice. *International archives of allergy and immunology.* 2010;151(1):80-88.

22. Finnerty CC, Herndon DN, Przkora R, et al. Cytokine expression profile over time in severely burned pediatric patients. *Shock (Augusta, Ga).* 2006;26(1):13-19.

23. Jeschke MG, Chinkes DL, Finnerty CC, et al. Pathophysiologic response to severe burn injury. *Annals of surgery.* 2008;248(3):387-401.

24. Bai G, Yan G, Wang G, Wan P, Zhang R. Anti-hepatic fibrosis effects of a novel turtle shell decoction by inhibiting hepatic stellate cell proliferation and blocking TGF-beta1/Smad signaling pathway in rats. *Oncology reports.* 2016.

25. Lijnen PJ, Petrov VV, Fagard RH. Induction of cardiac fibrosis by transforming growth factor-beta(1). *Molecular genetics and metabolism.* 2000;71(1-2):418-435.

26. Pulichino AM, Wang IM, Caron A, et al. Identification of transforming growth factor beta1-driven genetic programs of acute lung fibrosis. *American journal of respiratory cell and molecular biology.* 2008;39(3):324-336.

27. Shi JH, Guan H, Shi S, et al. Protection against TGF-beta1-induced fibrosis effects of IL-10 on dermal fibroblasts and its potential therapeutics for the reduction of skin scarring. *Archives of dermatological research.* 2013;305(4):341-352.

28. Gruber BL, Marchese MJ, Kew RR. Transforming growth factor-beta 1 mediates mast cell chemotaxis. *Journal of immunology (Baltimore, Md : 1950).* 1994;152(12):5860-5867.

29. Olsson N, Rak S, Nilsson G. Demonstration of mast cell chemotactic activity in bronchoalveolar lavage fluid collected from asthmatic patients before and during pollen season. *The Journal of allergy and clinical immunology.* 2000;105(3):455-461.

30. Frangogiannis NG, Perrard JL, Mendoza LH, et al. Stem cell factor induction is associated with mast cell accumulation after canine myocardial ischemia and reperfusion. *Circulation.* 1998;98(7):687-698.

31. Samayawardhena LA, Pallen CJ. Protein-tyrosine phosphatase alpha regulates stem cell factor-dependent c-Kit activation and migration of mast cells. *The Journal of biological chemistry.* 2008;283(43):29175-29185.

32. Sugihara A, Tsujimura T, Fujita Y, Nakata Y, Terada N. Evaluation of role of mast cells in the development of liver fibrosis using mast cell-deficient rats and mice. *Journal of hepatology.* 1999;30(5):859-867.

33. Yamamoto T, Hartmann K, Eckes B, Krieg T. Role of stem cell factor and monocyte chemoattractant protein-1 in the interaction between fibroblasts and mast cells in fibrosis. *Journal of dermatological science.* 2001;26(2):106-111.

34. Halova I, Draberova L, Draber P. Mast cell chemotaxis - chemoattractants and signaling pathways. *Frontiers in immunology.* 2012;3:119.

35. Gleich GJ, Dunnette SL, Volenec FJ, Mani MM. Quantification of serum IgE in patients with burns. *Clinical allergy.* 1979;9(2):133-139.

36. Polacek V, Jira M, Fara M, Strejcek J, Konigova R. Immunoglobulin E (IgE) in patients with severe burns. *Burns, including thermal injury.* 1987;13(6):458-461.

37. Scott JR, Muangman PR, Tamura RN, et al. Substance P levels and neutral endopeptidase activity in acute burn wounds and hypertrophic scar. *Plastic and reconstructive surgery.* 2005;115(4):1095-1102.

38. Suzuki H, Miura S, Liu YY, Tsuchiya M, Ishii H. Substance P induces degranulation of mast cells and leukocyte adhesion to venular endothelium. *Peptides.* 1995;16(8):1447-1452.

39. van der Kleij HP, Ma D, Redegeld FA, Kraneveld AD, Nijkamp FP, Bienenstock J. Functional expression of neurokinin 1 receptors on mast cells induced by IL-4 and stem cell factor. *Journal of immunology (Baltimore, Md : 1950).* 2003;171(4):2074-2079.

40. Succar J, Douaiher J, Lancerotto L, et al. The role of mouse mast cell proteases in the proliferative phase of wound healing in microdeformational wound therapy. *Plastic and reconstructive surgery.* 2014;134(3):459-467.

41. Prey S, Leaute-Labreze C, Pain C, et al. Mast cells as possible targets of propranolol therapy: an immunohistological study of beta-adrenergic receptors in infantile haemangiomas. *Histopathology.* 2014;65(3):436-439.

42. Boesiger J, Tsai M, Maurer M, et al. Mast cells can secrete vascular permeability factor/ vascular endothelial cell growth factor and exhibit enhanced release after immunoglobulin E-dependent upregulation of fc epsilon receptor I expression. *The Journal of experimental medicine.* 1998;188(6):1135-1145.

43. Grutzkau A, Kruger-Krasagakes S, Baumeister H, et al. Synthesis, storage, and release of vascular endothelial growth factor/vascular permeability factor (VEGF/VPF) by human mast cells: implications for the biological significance of VEGF206. *Molecular biology of the cell.* 1998;9(4):875-884.

44. Horie M, Saito A, Yamauchi Y, et al. Histamine induces human lung fibroblast-mediated collagen gel contraction via histamine H1 receptor. *Experimental lung research.* 2014;40(5):222-236.

45. Ikawa Y, Shiba K, Ohki E, et al. Comparative study of histamine H4 receptor expression in human dermal fibroblasts. *The Journal of toxicological sciences.* 2008;33(4):503-508.

46. Uddin Ahmed AF, Ohtani H, Nio M, et al. Intrahepatic mast cell population correlates with clinical outcome in biliary atresia. *Journal of pediatric surgery.* 2000;35(12):1762-1765.

47. Zhou K, Xie G, Wen J, et al. Histamine is correlated with liver fibrosis in biliary atresia. *Digestive and liver disease : official journal of the Italian Society of Gastroenterology and the Italian Association for the Study of the Liver.* 2016;48(8):921-926.

48. Kupietzky A, Levi-Schaffer F. The role of mast cell-derived histamine in the closure of an in vitro wound. *Inflammation research : official journal of the European Histamine Research Society [et al].* 1996;45(4):176-180.

49. Johansson J, Backryd E, Granerus G, Sjoberg F. Urinary excretion of histamine and methylhistamine after burns. *Burns : journal of the International Society for Burn Injuries.* 2012;38(7):1005-1009.

50. McEuen AR, Walls AF. Purification and characterization of mast cell tryptase and chymase from human tissues. *Methods in molecular medicine.* 2008;138:299-317.

51. Pejler G, Karlstrom A. Thrombin is inactivated by mast cell secretory granule chymase. *The Journal of biological chemistry.* 1993;268(16):11817-11822.

52. Dong X, Zhang C, Ma S, Wen H. High concentrations of mast cell chymase facilitate the transduction of the transforming growth factor-beta1/Smads signaling pathway in skin fibroblasts. *Experimental and therapeutic medicine.* 2015;9(3):955-960.

53. Kofford MW, Schwartz LB, Schechter NM, Yager DR, Diegelmann RF, Graham MF. Cleavage of type I procollagen by human mast cell chymase initiates collagen fibril formation and generates a unique carboxyl-terminal propeptide. *The Journal of biological chemistry.* 1997;272(11):7127-7131.

54. Dong X, Chen J, Zhang Y, Cen Y. Mast cell chymase promotes cell proliferation and expression of certain cytokines in a dose-dependent manner. *Molecular medicine reports.* 2012;5(6):1487-1490.

55. Dong X, Geng Z, Zhao Y, Chen J, Cen Y. Involvement of mast cell chymase in burn wound healing in hamsters. *Experimental and therapeutic medicine.* 2013;5(2):643-647.

56. Nishikori Y, Kakizoe E, Kobayashi Y, Shimoura K, Okunishi H, Dekio S. Skin mast cell promotion of matrix remodeling in burn wound healing in mice: relevance of chymase. *Archives of dermatological research.* 1998;290(10):553-560.

57. Caughey GH. Mast cell proteases as protective and inflammatory mediators. *Advances in experimental medicine and biology.* 2011;716:212-234.

58. Lohi J, Harvima I, Keski-Oja J. Pericellular substrates of human mast cell tryptase: 72,000 dalton gelatinase and fibronectin. *Journal of cellular biochemistry.* 1992;50(4):337-349.

59. He S, Gaca MD, Walls AF. A role for tryptase in the activation of human mast cells: modulation of histamine release by tryptase and inhibitors of tryptase. *The Journal of pharmacology and experimental therapeutics.* 1998;286(1):289-297.

60. Klion AD, Noel P, Akin C, et al. Elevated serum tryptase levels identify a subset of patients with a myeloproliferative variant of idiopathic hypereosinophilic syndrome associated with tissue fibrosis, poor prognosis, and imatinib responsiveness. *Blood.* 2003;101(12):4660-4666.

61. Mentula P, Kylanpaa ML, Kemppainen E, et al. Serum levels of mast cell tryptase, vascular endothelial growth factor and basic fibroblast growth factor in patients with acute pancreatitis. *Pancreas.* 2003;27(2):e29-33.

62. Blair RJ, Meng H, Marchese MJ, et al. Human mast cells stimulate vascular tube formation. Tryptase is a novel, potent angiogenic factor. *The Journal of clinical investigation.* 1997;99(11):2691-2700.

63. Masuko K, Murata M, Xiang Y, et al. Tryptase enhances release of vascular endothelial growth factor from human osteoarthritic chondrocytes. *Clinical and experimental rheumatology.* 2007;25(6):860-865.

64. Frungieri MB, Albrecht M, Raemsch R, Mayerhofer A. The action of the mast cell product tryptase on cyclooxygenase-2 (COX2) and subsequent fibroblast proliferation involves activation of the extracellular signal-regulated kinase isoforms 1 and 2 (erk1/2). *Cellular signalling.* 2005;17(4):525-533.

65. Bagher M, Larsson-Callerfelt AK, Rosmark O, Hallgren O, Bjermer L, Westergren-Thorsson G. Mast cells and mast cell tryptase enhance migration of human lung fibroblasts through protease-activated receptor 2. *Cell communication and signaling : CCS.* 2018;16(1):59.

66. Masamune A, Kikuta K, Satoh M, Suzuki N, Shimosegawa T. Protease-activated receptor-2-mediated proliferation and collagen production of rat pancreatic stellate cells. *The Journal of pharmacology and experimental therapeutics.* 2005;312(2):651-658.

67. Wang Z, Li Q, Xiang M, et al. Astragaloside Alleviates Hepatic Fibrosis Function via PAR2 Signaling Pathway in Diabetic Rats. *Cellular physiology and biochemistry : international journal of experimental cellular physiology, biochemistry, and pharmacology.* 2017;41(3):1156-1166.

68. Gilfillan AM, Austin SJ, Metcalfe DD. Mast cell biology: introduction and overview. *Advances in experimental medicine and biology.* 2011;716:2-12.

69. Lewis RA, Soter NA, Diamond PT, Austen KF, Oates JA, Roberts LJ, 2nd. Prostaglandin D2 generation after activation of rat and human mast cells with anti-IgE. *Journal of immunology (Baltimore, Md : 1950).* 1982;129(4):1627-1631.

70. Arturson G. Prostaglandins in human burn-wound secretion. *Burns, including thermal injury.* 1977;3(2):112-118.

71. Ozaki-Okayama Y, Matsumura K, Ibuki T, et al. Burn injury enhances brain prostaglandin E2 production through induction of cyclooxygenase-2 and microsomal prostaglandin E synthase in cerebral vascular endothelial cells in rats. *Critical care medicine.* 2004;32(3):795-800.

72. Abe M, Kurosawa M, Ishikawa O, Miyachi Y. Effect of mast cell-derived mediators and mast cell-related neutral proteases on human dermal fibroblast proliferation and type I collagen production. *The Journal of allergy and clinical immunology.* 2000;106(1 Pt 2):S78-84.

73.   Kohyama T, Wyatt TA, Liu X, et al. PGD(2) modulates fibroblast-mediated native collagen gel contraction. *American journal of respiratory cell and molecular biology.* 2002;27(3):375-381.

74.   Dobke MK, Hayes EC, Baxter CR. Leukotrienes LTB4 and LTC4 in thermally injured patients' plasma and burn blister fluid. *The Journal of burn care & rehabilitation.* 1987;8(3):189-191.

75.   Perng DW, Wu YC, Chang KT, et al. Leukotriene C4 induces TGF-beta1 production in airway epithelium via p38 kinase pathway. *American journal of respiratory cell and molecular biology.* 2006;34(1):101-107.

76.   Yoshisue H, Kirkham-Brown J, Healy E, Holgate ST, Sampson AP, Davies DE. Cysteinyl leukotrienes synergize with growth factors to induce proliferation of human bronchial fibroblasts. *The Journal of allergy and clinical immunology.* 2007;119(1):132-140.

77.   Heinke S, Szucs G, Norris A, Droogmans G, Nilius B. Inhibition of volume-activated chloride currents in endothelial cells by chromones. *British journal of pharmacology.* 1995;115(8):1393-1398.

78.   Jaggi AS, Kaur G, Bali A, Singh N. Pharmacological investigations on mast cell stabilizer and histamine receptor antagonists in vincristine-induced neuropathic pain. *Naunyn-Schmiedeberg's archives of pharmacology.* 2017;390(11):1087-1096.

79.   Chin GN. Treatment of vernal keratoconjunctivitis with topical cromolyn sodium. *Journal of pediatric ophthalmology and strabismus.* 1978;15(5):326-329.

80.   Confino J, Brown SI. Treatment of superior limbic keratoconjunctivitis with topical cromolyn sodium. *Annals of ophthalmology.* 1987;19(4):129-131.

81.   Allan RN. Sodium cromoglycate in proctitis and ulcerative colitis. *British medical journal (Clinical research ed).* 1982;284(6309):70-71.

82.   Horan RF, Sheffer AL, Austen KF. Cromolyn sodium in the management of systemic mastocytosis. *The Journal of allergy and clinical immunology.* 1990;85(5):852-855.

83.   Stevens MT, Edwards AM. The effect of 4% sodium cromoglicate cutaneous emulsion compared to vehicle in atopic dermatitis in children--A meta-analysis of total SCORAD scores. *The Journal of dermatological treatment.* 2015;26(3):284-290.

84.   Vieira Dos Santos R, Magerl M, Martus P, et al. Topical sodium cromoglicate relieves allergen- and histamine-induced dermal pruritus. *The British journal of dermatology.* 2010;162(3):674-676.

85.   Choi JS, Kim JK, Yang YJ, et al. Identification of cromolyn sodium as an anti-fibrotic agent targeting both hepatocytes and hepatic stellate cells. *Pharmacological research.* 2015;102:176-183.

86.   Chen L, Schrementi ME, Ranzer MJ, Wilgus TA, DiPietro LA. Blockade of mast cell activation reduces cutaneous scar formation. *PloS one.* 2014;9(1):e85226.

87.   Walker M, Harley R, LeRoy EC. Ketotifen prevents skin fibrosis in the tight skin mouse. *The Journal of rheumatology.* 1990;17(1):57-59.

88.   Gallant-Behm CL, Hildebrand KA, Hart DA. The mast cell stabilizer ketotifen prevents development of excessive skin wound contraction and fibrosis in red

Duroc pigs. *Wound repair and regeneration : official publication of the Wound Healing Society [and] the European Tissue Repair Society.* 2008;16(2):226-233.

89. Monument MJ, Hart DA, Befus AD, Salo PT, Zhang M, Hildebrand KA. The mast cell stabilizer ketotifen fumarate lessens contracture severity and myofibroblast hyperplasia: a study of a rabbit model of posttraumatic joint contractures. *The Journal of bone and joint surgery American volume.* 2010;92(6):1468-1477.

90. Tremaine WJ, Brzezinski A, Katz JA, et al. Treatment of mildly to moderately active ulcerative colitis with a tryptase inhibitor (APC 2059): an open-label pilot study. *Alimentary pharmacology & therapeutics.* 2002;16(3):407-413.

91. Yoshida N, Yoshikawa T. Basic and translational research on proteinase-activated receptors: implication of proteinase/proteinase-activated receptor in gastrointestinal inflammation. *Journal of pharmacological sciences.* 2008;108(4):415-421.

92. Sendo T, Itoh Y, Goromaru T, et al. A potent tryptase inhibitor nafamostat mesilate dramatically suppressed pulmonary dysfunction induced in rats by a radiographic contrast medium. *British journal of pharmacology.* 2003;138(5):959-967.

93. Barr TP, Garzia C, Guha S, et al. PAR2 Pepducin-Based Suppression of Inflammation and Itch in Atopic Dermatitis Models. *The Journal of investigative dermatology.* 2018.

94. Michael ES, Kuliopulos A, Covic L, Steer ML, Perides G. Pharmacological inhibition of PAR2 with the pepducin P2pal-18S protects mice against acute experimental biliary pancreatitis. *American journal of physiology Gastrointestinal and liver physiology.* 2013;304(5):G516-526.

95. Shearer AM, Rana R, Austin K, et al. Targeting Liver Fibrosis with a Cell-penetrating Protease-activated Receptor-2 (PAR2) Pepducin. *The Journal of biological chemistry.* 2016;291(44):23188-23198.

96. Association AB. National Burn Repository: Report of Data from 2008-2017. 2017;13.

97. Bombaro KM, Engrav LH, Carrougher GJ, et al. What is the prevalence of hypertrophic scarring following burns? *Burns : journal of the International Society for Burn Injuries.* 2003;29(4):299-302.

98. Lawrence JW, Mason ST, Schomer K, Klein MB. Epidemiology and impact of scarring after burn injury: a systematic review of the literature. *Journal of burn care & research : official publication of the American Burn Association.* 2012;33(1):136-146.

99. Engrav LH, Heimbach DM, Rivara FP, et al. 12-Year within-wound study of the effectiveness of custom pressure garment therapy. *Burns : journal of the International Society for Burn Injuries.* 2010;36(7):975-983.

100. Kim JY, Willard JJ, Supp DM, et al. Burn Scar Biomechanics after Pressure Garment Therapy. *Plastic and reconstructive surgery.* 2015;136(3):572-581.

101. DeBruler DM, Zbinden JC, Baumann ME, et al. Early cessation of pressure garment therapy results in scar contraction and thickening. *PloS one.* 2018;13(6):e0197558.

102. Haedersdal M, Moreau KE, Beyer DM, Nymann P, Alsbjorn B. Fractional nonablative 1540 nm laser resurfacing for thermal burn scars: a randomized controlled trial. *Lasers in surgery and medicine.* 2009;41(3):189-195.

103. Taudorf EH, Danielsen PL, Paulsen IF, et al. Non-ablative fractional laser provides long-term improvement of mature burn scars--a randomized controlled trial with histological assessment. *Lasers in surgery and medicine.* 2015;47(2):141-147.

104. Waibel J, Wulkan AJ, Lupo M, Beer K, Anderson RR. Treatment of burn scars with the 1,550 nm nonablative fractional Erbium Laser. *Lasers in surgery and medicine.* 2012;44(6):441-446.

105. Scott K, Bradding P. Human mast cell chemokines receptors: implications for mast cell tissue localization in asthma. *Clinical and experimental allergy : journal of the British Society for Allergy and Clinical Immunology.* 2005;35(6):693-697.

106. Miyazawa S, Hotta O, Doi N, Natori Y, Nishikawa K, Natori Y. Role of mast cells in the development of renal fibrosis: use of mast cell-deficient rats. *Kidney international.* 2004;65(6):2228-2237.

107. Bozyk PD, Moore BB. Prostaglandin E2 and the pathogenesis of pulmonary fibrosis. *American journal of respiratory cell and molecular biology.* 2011;45(3):445-452.

108. Keane MP, Strieter RM, Belperio JA. Mechanisms and mediators of pulmonary fibrosis. *Critical reviews in immunology.* 2005;25(6):429-463.

109. Xue M, Chan YK, Shen K, et al. Protease-activated receptor 2, rather than protease-activated receptor 1, contributes to the aggressive properties of synovial fibroblasts in rheumatoid arthritis. *Arthritis and rheumatism.* 2012;64(1):88-98.

110. Klinger M, Caviggioli F, Klinger FM, et al. Autologous fat graft in scar treatment. *The Journal of craniofacial surgery.* 2013;24(5):1610-1615.

111. Piccolo NS, Piccolo MS, Piccolo MT. Fat grafting for treatment of burns, burn scars, and other difficult wounds. *Clinics in plastic surgery.* 2015;42(2):263-283.

112. Herndon D, Capek KD, Ross E, et al. Reduced Postburn Hypertrophic Scarring and Improved Physical Recovery With Yearlong Administration of Oxandrolone and Propranolol. *Annals of surgery.* 2018;268(3):431-441.

113. Popescu FC, Mogosanu GD, Busuioc CJ, Parvanescu H, Lascar I, Mogoanta L. Macrophage response in experimental third-degree skin burns treated with allograft. Histological and immunohistochemical study. *Romanian journal of morphology and embryology = Revue roumaine de morphologie et embryologie.* 2012;53(4):1027-1036.

114. Rani M, Zhang Q, Scherer MR, Cap AP, Schwacha MG. Activated skin gammadelta T-cells regulate T-cell infiltration of the wound site after burn. *Innate immunity.* 2015;21(2):140-150.

115. Rani M, Zhang Q, Schwacha MG. Burn wound gammadelta T-cells support a Th2 and Th17 immune response. *Journal of burn care & research : official publication of the American Burn Association.* 2014;35(1):46-53.

116. He L, Marneros AG. Macrophages are essential for the early wound healing response and the formation of a fibrovascular scar. *The American journal of pathology.* 2013;182(6):2407-2417.

117. Hesketh M, Sahin KB, West ZE, Murray RZ. Macrophage Phenotypes Regulate Scar Formation and Chronic Wound Healing. *International journal of molecular sciences.* 2017;18(7).

118. Zhu Z, Ding J, Ma Z, Iwashina T, Tredget EE. Systemic depletion of macrophages in the subacute phase of wound healing reduces hypertrophic scar formation.

Wound repair and regeneration : official publication of the Wound Healing Society [and] the European Tissue Repair Society. 2016;24(4):644-656.

119. Amiot L, Vu N, Rauch M, et al. Expression of HLA-G by mast cells is associated with hepatitis C virus-induced liver fibrosis. *Journal of hepatology.* 2014;60(2):245-252.

120. Hirai S, Ohyane C, Kim YI, et al. Involvement of mast cells in adipose tissue fibrosis. *American journal of physiology Endocrinology and metabolism.* 2014;306(3):E247-255.

121. Levick SP, Widiapradja A. Mast Cells: Key Contributors to Cardiac Fibrosis. *International journal of molecular sciences.* 2018;19(1).

122. Tredget EE, Iwashina T, Scott PG, Ghahary A. Determination of plasma Ntau-methylhistamine in vivo by isotope dilution using benchtop gas chromatography-mass spectrometry. *J Chromatogr B Biomed Sci Appl.* 1997;694(1):1-9.

123. Sawamukai N, Yukawa S, Saito K, Nakayamada S, Kambayashi T, Tanaka Y. Mast cell-derived tryptase inhibits apoptosis of human rheumatoid synovial fibroblasts via rho-mediated signaling. *Arthritis and rheumatism.* 2010;62(4):952-959.

124. Gruber BL, Kew RR, Jelaska A, et al. Human mast cells activate fibroblasts: tryptase is a fibrogenic factor stimulating collagen messenger ribonucleic acid synthesis and fibroblast chemotaxis. *Journal of immunology (Baltimore, Md : 1950).* 1997;158(5):2310-2317.

125. Chen H, Xu Y, Yang G, et al. Mast cell chymase promotes hypertrophic scar fibroblast proliferation and collagen synthesis by activating TGF-beta1/Smads signaling pathway. *Experimental and therapeutic medicine.* 2017;14(5):4438-4442.

126. Jiang Y, Wu Y, Hardie WJ, Zhou X. Mast cell chymase affects the proliferation and metastasis of lung carcinoma cells in vitro. *Oncology letters.* 2017;14(3):3193-3198.

127. Lazaar AL, Plotnick MI, Kucich U, et al. Mast cell chymase modifies cell-matrix interactions and inhibits mitogen-induced proliferation of human airway smooth muscle cells. *Journal of immunology (Baltimore, Md : 1950).* 2002;169(2):1014-1020.

128. Schneider JC, Nadler DL, Herndon DN, et al. Pruritus in pediatric burn survivors: defining the clinical course. *Journal of burn care & research : official publication of the American Burn Association.* 2015;36(1):151-158.

129. Carrougher GJ, Martinez EM, McMullen KS, et al. Pruritus in adult burn survivors: postburn prevalence and risk factors associated with increased intensity. *Journal of burn care & research : official publication of the American Burn Association.* 2013;34(1):94-101.

130. Finnerty CC, Capek KD, Voigt C, et al. The P50 Research Center in Perioperative Sciences: How the investment by the National Institute of General Medical Sciences in team science has reduced postburn mortality. *The journal of trauma and acute care surgery.* 2017;83(3):532-542.

131. Tompkins RG. Survival from burns in the new millennium: 70 years' experience from a single institution. *Annals of surgery.* 2015;261(2):263-268.

132. Thakurdas SM, Melicoff E, Sansores-Garcia L, et al. The mast cell-restricted tryptase mMCP-6 has a critical immunoprotective role in bacterial infections. *The Journal of biological chemistry.* 2007;282(29):20809-20815.

133. Salib RJ, Kumar S, Wilson SJ, Howarth PH. Nasal mucosal immunoexpression of the mast cell chemoattractants TGF-beta, eotaxin, and stem cell factor and their receptors in allergic rhinitis. *The Journal of allergy and clinical immunology.* 2004;114(4):799-806.

134. Jay J, Prasai A, El Ayadi A, Wetzel M, Herndon D, Finnerty CC. Mast cell tryptase induction of postburn fibrosis via protease-activated receptor-2. *Wound repair and regeneration : official publication of the Wound Healing Society [and] the European Tissue Repair Society.* 2017;25(5):A7-8.

135. Wilgus TA, Ferreira AM, Oberyszyn TM, Bergdall VK, Dipietro LA. Regulation of scar formation by vascular endothelial growth factor. *Laboratory investigation; a journal of technical methods and pathology.* 2008;88(6):579-590.

136. Au SR, Au K, Saggers GC, Karne N, Ehrlich HP. Rat mast cells communicate with fibroblasts via gap junction intercellular communications. *Journal of cellular biochemistry.* 2007;100(5):1170-1177.

137. Foley TT, Saggers GC, Moyer KE, Ehrlich HP. Rat mast cells enhance fibroblast proliferation and fibroblast-populated collagen lattice contraction through gap junctional intercellular communications. *Plastic and reconstructive surgery.* 2011;127(4):1478-1486.

138. Villar J, Cabrera-Benitez NE, Valladares F, et al. Tryptase is involved in the development of early ventilator-induced pulmonary fibrosis in sepsis-induced lung injury. *Critical care (London, England).* 2015;19:138.

139. Nguyen TD, Moody MW, Steinhoff M, Okolo C, Koh DS, Bunnett NW. Trypsin activates pancreatic duct epithelial cell ion channels through proteinase-activated receptor-2. *The Journal of clinical investigation.* 1999;103(2):261-269.

140. Sobey CG, Moffatt JD, Cocks TM. Evidence for selective effects of chronic hypertension on cerebral artery vasodilatation to protease-activated receptor-2 activation. *Stroke.* 1999;30(9):1933-1940; discussion 1941.

141. Macfarlane SR, Seatter MJ, Kanke T, Hunter GD, Plevin R. Proteinase-activated receptors. *Pharmacological reviews.* 2001;53(2):245-282.

142. Nystedt S, Emilsson K, Larsson AK, Strombeck B, Sundelin J. Molecular cloning and functional expression of the gene encoding the human proteinase-activated receptor 2. *European journal of biochemistry / FEBS.* 1995;232(1):84-89.

143. Cottrell GS, Amadesi S, Schmidlin F, Bunnett N. Protease-activated receptor 2: activation, signalling and function. *Biochemical Society transactions.* 2003;31(Pt 6):1191-1197.

144. DeFea KA, Zalevsky J, Thoma MS, Dery O, Mullins RD, Bunnett NW. beta-arrestin-dependent endocytosis of proteinase-activated receptor 2 is required for intracellular targeting of activated ERK1/2. *The Journal of cell biology.* 2000;148(6):1267-1281.

145. Blackhart BD, Emilsson K, Nguyen D, et al. Ligand cross-reactivity within the protease-activated receptor family. *The Journal of biological chemistry.* 1996;271(28):16466-16471.

146. Soh UJ, Dores MR, Chen B, Trejo J. Signal transduction by protease-activated receptors. *British journal of pharmacology.* 2010;160(2):191-203.

147. Akers IA, Parsons M, Hill MR, et al. Mast cell tryptase stimulates human lung fibroblast proliferation via protease-activated receptor-2. *American journal of physiology Lung cellular and molecular physiology.* 2000;278(1):L193-201.

148. Chung H, Ramachandran R, Hollenberg MD, Muruve DA. Proteinase-activated receptor-2 transactivation of epidermal growth factor receptor and transforming growth factor-beta receptor signaling pathways contributes to renal fibrosis. *The Journal of biological chemistry.* 2013;288(52):37319-37331.

149. McCloy RA, Rogers S, Caldon CE, Lorca T, Castro A, Burgess A. Partial inhibition of Cdk1 in G 2 phase overrides the SAC and decouples mitotic events. *Cell cycle (Georgetown, Tex).* 2014;13(9):1400-1412.

150. Geback T, Schulz MM, Koumoutsakos P, Detmar M. TScratch: a novel and simple software tool for automated analysis of monolayer wound healing assays. *BioTechniques.* 2009;46(4):265-274.

151. Rothschild AM. Mechanisms of histamine release by compound 48-80. *British journal of pharmacology.* 1970;38(1):253-262.

152. Barry GD, Suen JY, Le GT, Cotterell A, Reid RC, Fairlie DP. Novel agonists and antagonists for human protease activated receptor 2. *Journal of medicinal chemistry.* 2010;53(20):7428-7440.

153. Kanke T, Ishiwata H, Kabeya M, et al. Binding of a highly potent protease-activated receptor-2 (PAR2) activating peptide, [3H]2-furoyl-LIGRL-NH2, to human PAR2. *British journal of pharmacology.* 2005;145(2):255-263.

154. Bloemen MC, van der Veer WM, Ulrich MM, van Zuijlen PP, Niessen FB, Middelkoop E. Prevention and curative management of hypertrophic scar formation. *Burns : journal of the International Society for Burn Injuries.* 2009;35(4):463-475.

155. Oosterwijk AM, Mouton LJ, Schouten H, Disseldorp LM, van der Schans CP, Nieuwenhuis MK. Prevalence of scar contractures after burn: A systematic review. *Burns : journal of the International Society for Burn Injuries.* 2017;43(1):41-49.

156. Rabello FB, Souza CD, Farina Junior JA. Update on hypertrophic scar treatment. *Clinics (Sao Paulo, Brazil).* 2014;69(8):565-573.

157. Akhzari S, Rezvan H, Zolhavarieh SM. Expression of pro-inflammatory genes in lesions, spleens and blood neutrophils after burn injuries in mice treated with silver sulfodiazine. *Iranian journal of basic medical sciences.* 2017;20(7):769-775.

158. Kwan PO, Tredget EE. Biological Principles of Scar and Contracture. *Hand clinics.* 2017;33(2):277-292.

159. White MJ, Galvis-Carvajal E, Gomer RH. A brief exposure to tryptase or thrombin potentiates fibrocyte differentiation in the presence of serum or serum amyloid p. *Journal of immunology (Baltimore, Md : 1950).* 2015;194(1):142-150.

160. Zhang Z, Finnerty CC, He J, Herndon DN. Smad ubiquitination regulatory factor 2 expression is enhanced in hypertrophic scar fibroblasts from burned children. *Burns : journal of the International Society for Burn Injuries.* 2012;38(2):236-246.

161. Garner WL, Karmiol S, Rodriguez JL, Smith DJ, Jr., Phan SH. Phenotypic differences in cytokine responsiveness of hypertrophic scar versus normal dermal fibroblasts. *The Journal of investigative dermatology.* 1993;101(6):875-879.

162. Song R, Bian HN, Lai W, Chen HD, Zhao KS. Normal skin and hypertrophic scar fibroblasts differentially regulate collagen and fibronectin expression as well as mitochondrial membrane potential in response to basic fibroblast growth factor. *Brazilian journal of medical and biological research = Revista brasileira de pesquisas medicas e biologicas.* 2011;44(5):402-410.

163. Joo YA, Chung H, Yoon S, et al. Skin Barrier Recovery by Protease-Activated Receptor-2 Antagonist Lobaric Acid. *Biomolecules & therapeutics.* 2016;24(5):529-535.

164. Xue M, Lin H, Zhao R, Liang HP, Jackson C. The differential expression of protease activated receptors contributes to functional differences between dark and fair keratinocytes. *Journal of dermatological science.* 2017;85(3):178-185.

165. Groschwitz KR, Wu D, Osterfeld H, Ahrens R, Hogan SP. Chymase-mediated intestinal epithelial permeability is regulated by a protease-activating receptor/matrix metalloproteinase-2-dependent mechanism. *American journal of physiology Gastrointestinal and liver physiology.* 2013;304(5):G479-489.

166. Schechter NM, Brass LF, Lavker RM, Jensen PJ. Reaction of mast cell proteases tryptase and chymase with protease activated receptors (PARs) on keratinocytes and fibroblasts. *Journal of cellular physiology.* 1998;176(2):365-373.

167. Zhu Z, Ding J, Tredget EE. The molecular basis of hypertrophic scars. *Burns & trauma.* 2016;4:2.

168. Canady J, Arndt S, Karrer S, Bosserhoff AK. Increased KGF expression promotes fibroblast activation in a double paracrine manner resulting in cutaneous fibrosis. *The Journal of investigative dermatology.* 2013;133(3):647-657.

169. Giannouli CC, Kletsas D. TGF-beta regulates differentially the proliferation of fetal and adult human skin fibroblasts via the activation of PKA and the autocrine action of FGF-2. *Cellular signalling.* 2006;18(9):1417-1429.

170. Shin D, Minn KW. The effect of myofibroblast on contracture of hypertrophic scar. *Plastic and reconstructive surgery.* 2004;113(2):633-640.

171. Vouret-Craviari V, Grall D, Van Obberghen-Schilling E. Modulation of Rho GTPase activity in endothelial cells by selective proteinase-activated receptor (PAR) agonists. *Journal of thrombosis and haemostasis : JTH.* 2003;1(5):1103-1111.

172. Chiang RS, Borovikova AA, King K, et al. Current concepts related to hypertrophic scarring in burn injuries. *Wound repair and regeneration : official publication of the Wound Healing Society [and] the European Tissue Repair Society.* 2016;24(3):466-477.

173. Goel A, Shrivastava P. Post-burn scars and scar contractures. *Indian journal of plastic surgery : official publication of the Association of Plastic Surgeons of India.* 2010;43(Suppl):S63-71.

174. Kotwal GJ, Chien S. Macrophage Differentiation in Normal and Accelerated Wound Healing. *Results and problems in cell differentiation.* 2017;62:353-364.

175. Wahl SM, McCartney-Francis N, Allen JB, Dougherty EB, Dougherty SF. Macrophage production of TGF-beta and regulation by TGF-beta. *Annals of the New York Academy of Sciences.* 1990;593:188-196.

176. Gharib SA, Johnston LK, Huizar I, et al. MMP28 promotes macrophage polarization toward M2 cells and augments pulmonary fibrosis. *Journal of leukocyte biology.* 2014;95(1):9-18.

177. Tran TH, Rastogi R, Shelke J, Amiji MM. Modulation of Macrophage Functional Polarity towards Anti-Inflammatory Phenotype with Plasmid DNA Delivery in CD44 Targeting Hyaluronic Acid Nanoparticles. *Scientific reports.* 2015;5:16632.

178. Piliponsky AM, Chen CC, Grimbaldeston MA, et al. Mast cell-derived TNF can exacerbate mortality during severe bacterial infections in C57BL/6-KitW-sh/W-sh mice. *The American journal of pathology.* 2010;176(2):926-938.

179. He Z, Li Y, Ma S, et al. Degranulation of Gastrointestinal Mast Cells Contributes to Hepatic Ischemia-Reperfusion Injury in Mice. *Clinical science (London, England : 1979).* 2018.

180. Batlle M, Perez-Villa F, Lazaro A, et al. Correlation between mast cell density and myocardial fibrosis in congestive heart failure patients. *Transplantation proceedings.* 2007;39(7):2347-2349.

181. Welsh TJ, Green RH, Richardson D, Waller DA, O'Byrne KJ, Bradding P. Macrophage and mast-cell invasion of tumor cell islets confers a marked survival advantage in non-small-cell lung cancer. *Journal of clinical oncology : official journal of the American Society of Clinical Oncology.* 2005;23(35):8959-8967.

182. Kondo S, Kagami S, Kido H, Strutz F, Muller GA, Kuroda Y. Role of mast cell tryptase in renal interstitial fibrosis. *Journal of the American Society of Nephrology : JASN.* 2001;12(8):1668-1676.

183. Garbuzenko E, Nagler A, Pickholtz D, et al. Human mast cells stimulate fibroblast proliferation, collagen synthesis and lattice contraction: a direct role for mast cells in skin fibrosis. *Clinical and experimental allergy : journal of the British Society for Allergy and Clinical Immunology.* 2002;32(2):237-246.

184. Jordana M, Befus AD, Newhouse MT, Bienenstock J, Gauldie J. Effect of histamine on proliferation of normal human adult lung fibroblasts. *Thorax.* 1988;43(7):552-558.

185. Taipale J, Lohi J, Saarinen J, Kovanen PT, Keski-Oja J. Human mast cell chymase and leukocyte elastase release latent transforming growth factor-beta 1 from the extracellular matrix of cultured human epithelial and endothelial cells. *The Journal of biological chemistry.* 1995;270(9):4689-4696.

186. Irani AM, Schwartz LB. Human mast cell heterogeneity. *Allergy proceedings : the official journal of regional and state allergy societies.* 1994;15(6):303-308.

187. Gailit J, Marchese MJ, Kew RR, Gruber BL. The differentiation and function of myofibroblasts is regulated by mast cell mediators. *The Journal of investigative dermatology.* 2001;117(5):1113-1119.

188. Jay J, Prasai A, El Ayadi A, Wetzel M, Herndon D, Finnerty CC. Mast cell tryptase induction of postburn fibrosis via protease-activated receptor-2. *Wound repair and regeneration : official publication of the Wound Healing Society [and] the European Tissue Repair Society.* 2017;25(5):A7-8.

189. Wygrecka M, Kwapiszewska G, Jablonska E, et al. Role of protease-activated receptor-2 in idiopathic pulmonary fibrosis. *American journal of respiratory and critical care medicine.* 2011;183(12):1703-1714.

190. Kilpatrick LE, Jakabovics E, McCawley LJ, Kane LH, Korchak HM. Cromolyn inhibits assembly of the NADPH oxidase and superoxide anion generation by human neutrophils. *Journal of immunology (Baltimore, Md : 1950).* 1995;154(7):3429-3436.

191. Murphy S, Kelly HW. Cromolyn sodium: a review of mechanisms and clinical use in asthma. *Drug intelligence & clinical pharmacy.* 1987;21(1 Pt 1):22-35.

192. Berth-Jones J, Pollock I, Hearn RM, et al. A randomised, controlled trial of a 4% cutaneous emulsion of sodium cromoglicate in treatment of atopic dermatitis in children. *The Journal of dermatological treatment.* 2015;26(3):291-296.

193. Haider SA. Treatment of atopic eczema in children: clinical trial of 10% sodium cromoglycate ointment. *British medical journal.* 1977;1(6076):1570-1572.

194. Blackstone BN, Kim JY, McFarland KL, et al. Scar formation following excisional and burn injuries in a red Duroc pig model. *Wound repair and regeneration : official publication of the Wound Healing Society [and] the European Tissue Repair Society.* 2017;25(4):618-631.

195. Zhu KQ, Engrav LH, Tamura RN, et al. Further similarities between cutaneous scarring in the female, red Duroc pig and human hypertrophic scarring. *Burns : journal of the International Society for Burn Injuries.* 2004;30(6):518-530.

196. Kim JY, Dunham DM, Supp DM, Sen CK, Powell HM. Novel burn device for rapid, reproducible burn wound generation. *Burns : journal of the International Society for Burn Injuries.* 2016;42(2):384-391.

197. Hartig SM. Basic image analysis and manipulation in ImageJ. *Current protocols in molecular biology.* 2013;Chapter 14:Unit14.15.

198. Shu J, Dolman GE, Duan J, Qiu G, Ilyas M. Statistical colour models: an automated digital image analysis method for quantification of histological biomarkers. *Biomedical engineering online.* 2016;15:46.

199. Gee Kee EL, Kimble RM, Stockton KA. 3D photography is a reliable burn wound area assessment tool compared to digital planimetry in very young children. *Burns : journal of the International Society for Burn Injuries.* 2015;41(6):1286-1290.

200. Tandara AA, Mustoe TA. The role of the epidermis in the control of scarring: evidence for mechanism of action for silicone gel. *Journal of plastic, reconstructive & aesthetic surgery : JPRAS.* 2008;61(10):1219-1225.

201. Brey EM, Lalani Z, Johnston C, et al. Automated selection of DAB-labeled tissue for immunohistochemical quantification. *The journal of histochemistry and cytochemistry : official journal of the Histochemistry Society.* 2003;51(5):575-584.

202. Armendariz-Borunda J, Lyra-Gonzalez I, Medina-Preciado D, et al. A controlled clinical trial with pirfenidone in the treatment of pathological skin scarring caused by burns in pediatric patients. *Annals of plastic surgery.* 2012;68(1):22-28.

203. Shi J, Li J, Guan H, et al. Anti-fibrotic actions of interleukin-10 against hypertrophic scarring by activation of PI3K/AKT and STAT3 signaling pathways in scar-forming fibroblasts. *PloS one.* 2014;9(5):e98228.

204. Taheri A, Mansoori P, Al-Dabagh A, Feldman SR. Are corticosteroids effective for prevention of scar formation after second-degree skin burn? *The Journal of dermatological treatment.* 2014;25(4):360-362.

205. Jay J, Prasai A, El Ayadi A, Herndon D, Finnerty CC. Protease-activated Receptor-2 Knockdown Attenuates the Fibrotic Phenotype In Postburn Hypertrophic Scar

Fibroblasts. *Wound repair and regeneration : official publication of the Wound Healing Society [and] the European Tissue Repair Society.* 2018;26(5):A15-16.

206. Wygrecka M, Dahal BK, Kosanovic D, et al. Mast cells and fibroblasts work in concert to aggravate pulmonary fibrosis: role of transmembrane SCF and the PAR-2/PKC-alpha/Raf-1/p44/42 signaling pathway. *The American journal of pathology.* 2013;182(6):2094-2108.

207. Edwards AM, Bibawy D, Matthews S, et al. Long-term use of a 4% sodium cromoglicate cutaneous emulsion in the treatment of moderate to severe atopic dermatitis in children. *The Journal of dermatological treatment.* 2015;26(6):541-547.

208. Edwards AM, Stevens MT, Church MK. The effects of topical sodium cromoglicate on itch and flare in human skin induced by intradermal histamine: a randomised double-blind vehicle controlled intra-subject design trial. *BMC research notes.* 2011;4:47.

209. Liu YL, Hu FR, Wang IJ, Chen WL, Hou YC. A double-masked study to compare the efficacy and safety of topical cromolyn for the treatment of allergic conjunctivitis. *Journal of the Formosan Medical Association = Taiwan yi zhi.* 2011;110(11):690-694.

210. Jiang L, Fang P, Septer S, Apte U, Pritchard MT. Inhibition of Mast Cell Degranulation With Cromolyn Sodium Exhibits Organ-Specific Effects in Polycystic Kidney (PCK) Rats. *International journal of toxicology.* 2018;37(4):308-326.

211. Busch KH, Aliu A, Walezko N, Aust M. Medical Needling: Effect on Moisture and Transepidermal Water Loss of Mature Hypertrophic Burn Scars. *Cureus.* 2018;10(3):e2365.

212. Durcanska V, Jedlickova H, Vasku V. Measurement of transepidermal water loss in localized scleroderma. *Dermatologic therapy.* 2016;29(3):177-180.

213. Frungieri MB, Weidinger S, Meineke V, Kohn FM, Mayerhofer A. Proliferative action of mast-cell tryptase is mediated by PAR2, COX2, prostaglandins, and PPARgamma : Possible relevance to human fibrotic disorders. *Proceedings of the National Academy of Sciences of the United States of America.* 2002;99(23):15072-15077.

214. Bohm SK, Khitin LM, Grady EF, Aponte G, Payan DG, Bunnett NW. Mechanisms of desensitization and resensitization of proteinase-activated receptor-2. *The Journal of biological chemistry.* 1996;271(36):22003-22016.

215. Roosterman D, Schmidlin F, Bunnett NW. Rab5a and rab11a mediate agonist-induced trafficking of protease-activated receptor 2. *American journal of physiology Cell physiology.* 2003;284(5):C1319-1329.

216. Oliveira GV, Chinkes D, Mitchell C, Oliveras G, Hawkins HK, Herndon DN. Objective assessment of burn scar vascularity, erythema, pliability, thickness, and planimetry. *Dermatologic surgery : official publication for American Society for Dermatologic Surgery [et al].* 2005;31(1):48-58.

217. Wei Y, Li-Tsang CWP, Luk DCK, Tan T, Zhang W, Chiu TW. A validation study of scar vascularity and pigmentation assessment using dermoscopy. *Burns : journal of the International Society for Burn Injuries.* 2015;41(8):1717-1723.

218. Herndon D. *Total Burn Care.* 5 ed: Elsevier; 2018.

219. Rettinger CL, Fletcher JL, Carlsson AH, Chan RK. Accelerated epithelialization and improved wound healing metrics in porcine full-thickness wounds transplanted with full-thickness skin micrografts. *Wound repair and regeneration : official publication of the Wound Healing Society [and] the European Tissue Repair Society.* 2017;25(5):816-827.

220. Sood R, Roggy DE, Zieger MJ, Nazim M, Hartman BC, Gibbs JT. A comparative study of spray keratinocytes and autologous meshed split-thickness skin graft in the treatment of acute burn injuries. *Wounds : a compendium of clinical research and practice.* 2015;27(2):31-40.

221. Association AM. AMA Drug Evaluations: Cromolyn Disodium. In: Drugs Co, ed. Chicago, IL: American Medical Association; 1994:527.

222. Bos JD, Meinardi MM. The 500 Dalton rule for the skin penetration of chemical compounds and drugs. *Experimental dermatology.* 2000;9(3):165-169.

223. Gruber BL, Marchese MJ, Santiago-Schwarz F, Martin CA, Zhang J, Kew RR. Protease-activated receptor-2 (PAR-2) expression in human fibroblasts is regulated by growth factors and extracellular matrix. *The Journal of investigative dermatology.* 2004;123(5):832-839.

224. Jiang R, Zatta A, Kin H, et al. PAR-2 activation at the time of reperfusion salvages myocardium via an ERK1/2 pathway in in vivo rat hearts. *American journal of physiology Heart and circulatory physiology.* 2007;293(5):H2845-2852.

225. Steinhoff M, Corvera CU, Thoma MS, et al. Proteinase-activated receptor-2 in human skin: tissue distribution and activation of keratinocytes by mast cell tryptase. *Experimental dermatology.* 1999;8(4):282-294.

Vita

Jayson Walter Jay was born on May 5, 1978 in Galveston, Texas to Joan B. Jay. He has been married to Jessica L. Lee for 10 years and they have one son, Andrew L. Jay, who is four years old. They currently reside in Houston, Texas and are expecting a daughter in December 2018. Jayson graduated from O'Connell High School in Galveston and began his undergraduate career in 1996 at the University of Notre Dame in South Bend, Indiana. Jayson completed his BS degree at the University of Houston and earned an MS in biological sciences at the University of Houston-Clear Lake in 2013. Throughout his academic career, Jayson has individually mentored, trained and taught over 30 high school, undergraduate, graduate and post-graduate students and fellows, which continues to be his passion today.

EDUCATION

2013 – Present **Ph.D. Doctoral Candidate**, expected graduation 2018
University of Texas Medical Branch, Human Pathophysiology &
Translational Medicine, Department of Surgery, Galveston, Texas

2011 – 2013 **M.S., Biological Sciences**, Summa Cum Laude
University of Houston at Clear Lake, Houston, Texas

2007 – 2011 **B.S., Biology**, Cum Laude
University of Houston – Downtown, Houston, Texas

HONORS

2013 Outstanding Honors Graduate, University of Houston at Clear Lake

2012 – 2013 Endowed Scholarship, University of Houston at Clear Lake

2007 – 2011 Dean's List Scholar, University of Houston – Downtown

PROFESSIONAL EXPERIENCE

2013 – Present Graduate Research Assistant, Institute for Translational Sciences,
University of Texas Medical Branch, Galveston, Texas

Shriners Hospitals for Children – Galveston, Galveston, Texas
(Mentors: Celeste Finnerty, Ph.D. and David N. Herndon, MD)

2011 – 2013   Graduate Research Assistant, Department of Science and Computer
Engineering, University of Houston at Clear Lake, Houston, Texas
(Mentors: Richard Puzdrowski, Ph.D., Leonard Giblin III, M.D., Ph.D.)

2007 – 2013   Quality Assurance & Quality Control Manager
Entech Engineering, Inc., Houston, Texas

CERTIFICATIONS

Biomedical Safety Levels 1 & 2
Animal Biomedical Safety Levels 1 & 2, Qualified for SQ and IP injections, RO blood collection, inhalation anesthesia, euthanasia, necropsy tissue collection

MEMBERSHIP IN SCIENTIFIC SOCIETIES

Wound Healing Society

MANUSCRIPTS & BOOK CHAPTERS

Hawkins HK, **Jay JW**, Finnerty CC. *Pathophysiology of the Burn Scar*, In: Total Burn Care, 5th ed., Elsevier, 466-475, 2018.

Herndon D, Capek KD, Ross E, **Jay JW**, Prasai A, Ayadi AE, Foncerrada-Ortega G, Blears E, Sommerhalder C, McMullen K, Amtmann D, Cox R, Hundeshagen G, Jennings K, Sousse LE, Suman OE, Meyer WJ 3rd, Finnerty CC. Reduced Post-burn Hypertrophic Scarring and Improved Physical Recovery With Yearlong Administration of Oxandrolone and Propranolol. Ann Surg. 2018 Jul 24. doi: 10.1097/SLA.0000000000002926. PubMed PMID: 30048322.

Bohanon FJ, Lopez ON, Herndon DN, Wang X, Bhattarai N, Ayadi AE, Prasai A, **Jay JW**, Rojas-Khalil Y, Toliver-Kinsky TE, Finnerty CC, Radhakrishnan RS, Porter C. Burn Trauma Acutely Increases the Respiratory Capacity and Function of Liver Mitochondria. Shock. 2017. Epub 2017/07/07. doi: 10.1097/shk.0000000000000935. PubMed PMID: 28682939.

Wetzel MD, **Jay JW**, El Ayadi A, Prasai A, Herndon DN, Finnerty CC. Metformin alters fibroblast epithelial-mesenchymal transition (EMT) in burn induced hypertrophic scar by targeting SMAD3. 2017 (Burns, In Review)

Mascarenhas DD, Ayadi AE, Wetzel M, Prasai A, Mifflin R, **Jay JW**, Herndon DN, Finnerty CC. Effects of the nephrilin peptide on post-burn glycemic control, renal function, fat and lean body mass, and wound healing. International journal of burns

and trauma. 2016;6(3):44-50. Epub 2017/01/13. PubMed PMID: 28078180; PMCID: PMC5218868.

Ijaz T, Jamaluddin M, Zhao Y, Zhang Y, **Jay JW**, Finnerty CC, Herndon DN, Tilton RG, Brasier AR. Coordinate activities of BRD4 and CDK9 in the transcriptional elongation complex are required for TGFbeta-induced Nox4 expression and myofibroblast transdifferentiation. Cell death & disease. 2017;8(2):e2606. Epub 2017/02/10. doi: 10.1038/cddis.2016.434. PubMed PMID: 28182006; PMCID: PMC5386453.

A Guillory, RP Clayton, A Prasai, **Jay JW**, M Wetzel, CD Voigt, CR Anderson, A El Ayadi, DN Herndon, CC Finnerty. 2017. Buprenorphine SR alters hemodynamic parameters in a rat burn model. Journal of Surgical Research.

Prasai, M Wetzel, **Jay JW**, Y Wand, CC Finnerty. 2017. Effects of oxandrolone and exercise on diaphragm muscle proteolysis post burn. A El Ayadi, A (J of Physiology, In Review)

ABSTRACTS & INVITED PRESENTATIONS

Hundeshagen G, **Jay JW**, Prasai A, Foncerrada G, Smith JM, Nguyen AV, Cambiaso-Daniel J, Popp D, Tapking C, Herndon DN, Enkhbaatar P, Finnerty CC, and Branski LK. 2018. First *in vitro* and *in vivo* experiences with a new synthetic dermal substitute with dual microporous structure. American Burn Association annual conference. Chicago, IL. Oral presentation.

Vu MA, **Jay JW**, Mac D, Prasai A, El Ayadi A, Wang Y, Wilkerson M, Herndon DN, Finnerty CC. 2018. Rose Bengal dye reduces collagen expression in post-burn hypertrophic scar fibroblasts *in vitro*. American Academy of Dermatology annual conference. San Diego, CA. Oral Presentation.

Jay JW, Prasai A, El Ayadi A, Finnerty CC. 2017. Evidence for Mast Cell Tryptase Induction of Post-Burn Fibrosis via Protease-Activated Receptor-2 (PAR2). Translational Research Seminar Series, University of Texas Medical Branch, Galveston, TX. Oral Presentation.

George Z, Siddiqui R, Munson C, El Ayadi A, Prasai A, **Jay JW**, Suman O, Anderson O, Herndon DN, Finnerty CC. 2017. Effects of beta-blocker and androgen therapy on catecholamines and cortisol levels post burn. Poster. Biomedical Research Training Summer Program, University of Texas Medical Branch, Galveston, TX. Poster.

Jay JW, A Prasai, A El Ayadi, M Wetzel, DN Herndon, CC Finnerty. 2017. Mast Cell Tryptase Induction of Post-Burn Fibrosis via Protease-Activated Receptor-2 (PAR2). Wound Healing Society, San Diego, CA. Oral Presentation.

Siddiqui R, Munson C, Wang Y, Ayadi AE, Jain A, **Jay JW,** Herndon DN, and Finnerty CC. 2016. The effects of propranolol on collagen deposition in post-burn scars. Biomedical Research Training Summer Program, University of Texas Medical Branch, Galveston, TX. Poster.

Munson C, Wang Y, Ayadi AE, Jain A, **Jay JW,** Wetzel MD, Herndon DN, and Finnerty CC. 2016. The effect of oxandrolone on post-burn rat muscle catabolism and anabolism. Biomedical Research Training Summer Program, University of Texas Medical Branch, Galveston, TX. Poster.

Jay JW, El Ayadi A, Clayton RP, Herndon DN, and Finnerty CC. 2016. Mast cell presence may promote hypertrophic scar progression following burn injury. Clinical and Translational Science Research Forum, University of Texas Medical Branch, Galveston, TX. Poster.

Jay JW, DN Herndon, CC Finnerty. 2016. Characterizing the mast cell-fibroblast paracrine axis in hypertrophic scar following burn injury. Translational Research Seminar Series, Dept. of Surgery, University of Texas Medical Branch, Galveston, TX. Oral Presentation.

Jay JW, El Ayadi A, Prasai A, Wetzel MD, Mac D, Clayton RP, Herndon DN, and Finnerty CC. 2016. Mast cell mediated fibrosis via PAR-2 activation in post-burn scars, Wound Healing Society, Atlanta, GA. Oral Presentation.

Jay JW, Herndon DN, Finnerty CC, Anderson C, and Klein G. 2016. Pamidronate may prevent muscle protein breakdown in burn by indirectly affecting inflammatory cytokines. European Calcified Tissue Society, Rome, Italy. Oral Presentation.

Jay JW, El Ayadi A, Herndon DN, Finnerty CC. 2015. Hypertrophic Scar Modulation Through β-adrenergic Blockade with Propranolol. Clinical and Translational Research Forum, University of Texas Medical Branch, Galveston, TX. Oral Presentation.

El Ayadi A, Wang Y, Prasai A, **Jay JW**, Herndon DN, and Finnerty CC. 2015. Effects of Propranolol on Skin Angiogenesis Following Burn Injury, Wound Healing Society, San Antonio, TX. (Poster and Oral Presentation)

Jay JW. 2012. Porcine Bone Marrow Extracellular Matrix Enhances HEK293 Proliferation *In vitro*. American Society for Cell Biology, New Orleans, LA. Oral Presentation.

Permanent address: 3826 Bandera Reserve Lane, Houston, Texas 77059

This dissertation was typed by Jayson Walter Jay.